AN ABSTRACT OF THE THESIS OF

Hyung-keun Chung for the degree of Doctor of Philosophy in Chemistry presented on December 13, 1989

TITLE: Microcomputer-Based Fluorometric Kinetic Determination of Ascorbic Acid and Flow Injection Analysis Methods for Interference Correction and Kinetic Determinations Based on the Peak Profile

Redacted for privacy

Abstract approved: _____

James D. Ingle, Jr.

A microcomputer-based data acquisition and control system for dynamic fluorometric measurements was developed. This system was first used for a rapid kinetic determination of total ascorbic acid. The ℓ-ascorbic acid is oxidized by mercuric chloride to dehydro-ℓ-ascorbic acid which then forms a fluorescent quinoxaline with o-phenylenediamine in a conventional sample cell. The initial rate of formation was estimated with a fixed-time computational method. With optimized conditions, the detection limit with a 20-s measurement time is 0.02 μg/mL with the linear dynamic range extending to 10 μg/mL.

The data acquisition system was also applied to flow injection analysis (FIA) in which the operation of the FIA components was computer controlled. In the single-line manifold, the peak shape due to physical dispersion of a sample is characterized by injecting a reference solution, quinine sulfate (QS) solution. The distortion of

the peak profile due to multiplicative interferences is indicated by the ratio of the sample to reference signals varying across the profile. An empirical function that normalizes for different analyte concentrations is described and used to prepare correction plots with known amounts of interferents. For the determination of QS, errors due to attenuation of the QS fluorescence by $K_2Cr_2O_7$ (absorber) and KI (quencher) as small as 0.5% can be detected and errors larger than 30% can be reduced to less than 2%.

A new FIA kinetic procedure is described. The FIA profile of the reaction product formed after injection of the sample into a flowing carrier stream (reagent solution) is detected and normalized by the relative dispersion coefficients established with a non-reacting reference solution. With suitable reaction and FIA conditions, the normalized signal due to the product increases from the center to the leading edge of the sample zone due to increased reaction time, and kinetic information can be extracted with the fixed-time rate computational method. The proposed procedure yielded a detection limit of 13 ng/mL for the kinetic determination of Al^{3+} based on formation of a fluorescent complex with 2,4,2′-trihydroxy-azobenzene-5′-sulfonic acid. This method provides discrimination against the interference from a non-reacting fluorescent species (riboflavin) because the normalized signals are time-independent.

MICROCOMPUTER-BASED FLUOROMETRIC KINETIC DETERMINATION OF ASCORBIC ACID AND FLOW INJECTION ANALYSIS METHODS FOR INTERFERENCE CORRECTION AND KINETIC DETERMINATIONS BASED ON THE PEAK PROFILE

by

Hyung-Keun Chung

A THESIS

submitted to

Oregon State University

in partial fulfillment of
the requirements for the
degree of

Doctor of Philosophy

Completed December 13, 1989

Commencement June 1990

APPROVED:

Redacted for privacy

Professor of Chemistry in charge of major

Redacted for privacy

Chairman of Department of Chemistry

Redacted for privacy

Dean of Graduate School

Date thesis is presented December 13, 1989

Typed by Hynug-Keun Chung for Hyung-Keun Chung

To my father and mother

ACKNOWLEDGMENTS

I would like to thank my major professor, James D. Ingle, Jr. for his guidance and assistance in all aspects of this work. Without his help, this thesis cannot be completed. Special recognition goes to Dr. Schuyler for teaching me computers and computer interfacing. Many professors including Dr. Piepmeier and Dr. Krueger should be thanked for their valuable guidance to develop me as a chemist. I would also like to acknowledge the influence of Dr. Dai-Woon Lee, my research advisor at Yonsei University in Korea. Most importantly, I thank my family, Hyeon-Soog, Sorah, and Sohyun, and my parents for their support and patience.

TABLE OF CONTENTS

LIST OF FIGURES

LIST OF TABLES

MICROCOMPUTER-BASED FLUOROMETRIC KINETIC DETERMINATION OF ASCORBIC ACID AND FLOW INJECTION ANALYSIS METHODS FOR INTERFERENCE CORRECTION AND KINETIC DETERMINATIONS BASED ON THE PEAK PROFILE

CHAPTER I

INTRODUCTION

Kinetics-based analysis is based on monitoring the rate of a chemical reaction and analytical information is obtained before the reaction reaches completion. With a suitable reaction monitoring system and data processing method for time-varying signals, kinetic methods often provide greater selectivity and speed over equilibrium-based methods involving the same reaction [1]. These advantages result because kinetic measurements involve measuring a change in a signal rather than an absolute signal and acquiring data in the initial portion of the reaction. Kinetic methods have primarily been applied to the catalytic reactions involving inorganic catalysts or enzymes because a catalyst only affects the rate of the reaction and such reactions often provide a high degree of specificity and sensitivity [2,3].

Kinetic methods have some limitations because the rate of a chemical reaction is always more dependent on experimental conditions such as temperature, pH, etc. and the signal to noise ratio (S/N) is usually lower than that in equilibrium-based methods. These limitations mean that a kinetic method is often the unfavorable

technique for noncatalytic reactions unless no alternative method is available [4]. However, for many noncatalytic reactions, the sample throughput and discrimination against interferences provided by kinetic measurements can make them superior to the corresponding equilibrium-based method.

Fluorescence monitoring for kinetic methods can provide better selectivity and detection limits over absorption monitoring which is the detection method most used commonly. A large linear dynamic range can often be obtained because in dilute solutions the fluorescence signal is linearly proportional to fluorophore concentration. The inherent sensitivity of fluorescence measurements allows small changes in concentration to be measured and can provide excellent detection limits for kinetic analysis. To utilize these advantages, conditions must be arranged to minimize or compensate for interference effects that generally affect fluorescence measurements such as inner-filter and quenching effects.

Computer-controlled kinetic instruments and automatic data-processing approaches have been developed to broaden the scope and to simplify the routine use of kinetic methods which emphasize the inherent advantages over equilibrium methods. Recently, Pardue [5] presented a complete discussion of kinetic methods which includes a thorough classification of methods in terms of data-processing approaches.

The initial studies presented in this thesis are concerned with the development of a rapid fluorometric kinetic method for the determination of total ascorbic acid. A personal computer (PC) was interfaced to a spectrofluorometer for data acquisition of

time-varing signals and control of the instrument which replaced the previous ratemeter system based on a 8-bit microcomputer developed in our laboratory [6,7]. The new PC-based data acquisition system, which has greatly enhanced capabilities, is simpler, more powerful, and more flexible. Because this system stores data over a large portion of the reaction rate curve, rate information can be extracted after the experiment with different rate computational approaches and parameters.

Flow injection analysis (FIA) is a rapidly growing technique based on injection of a sample into a flowing carrier stream (often containing a reagent), controlled dispersion (dilution) of the injected plug of sample in the carrier stream, and detection [8,9]. Typically a reproducible peak-shaped signal is observed as it passes through the detection flow cell due to the reproducible concentration profile of the dispersed sample zone. FIA has been established as a fast and precise technique for routine analysis which minimizes solution handling. Although the peak height is most commonly used as the analytical signal, the signals at other points in the profile or the width of the profile have proven to be useful [8,9].

Many different types of detection techniques have been used with FIA [10]. As for kinetic measurements previously discussed, fluorescence detection can provide enhanced selectivity and detectability. In this research, a single-line FIA manifold with fluorescence detection was constructed, and a PC was interfaced to the FIA system for automatic control of the FIA components. The PC-based FIA system acquires and stores signal versus time data during an FIA run and characterizes the peak by calculating and

reporting the peak height, the peak area, the time for the peak maximum, and the peak width.

This system was used in two unique applications. Both are based on using well-defined concentration profiles that are produced in an FIA system under laminar flow. The first study involves the detection of quenching and inner-filter effects through changes in the peak shape. It is also shown that the effect of the multiplicative interference can be compensated by quantitatively characterizing the degree of peak distortion.

Second, a new method for extracting rate information from the peak profile with a single-line FIA manifold was developed. Sample profiles were normalized for the effect of physical dispersion with dispersion coefficients characterized with a non-reacting sample. This allows the physical and chemical contributions on the peak profile to be differentiated. Rate information was extracted from the normalized profile. This technique was applied for the determination of Al^{3+} with the complexation reagent acid alizarin garnet R. It is shown that the interference from a non-reacting fluorescent species is discriminated.

REFERENCES

1. H. A. Malmstadt, C. J. Delaney, and E. A. Cordos, CRC Crit. Rev. Anal. Chem. 1972, 559.

2. G. G. Guilbault, CRC Crit. Rev. Anal. Chem. 1970, 377.

3. H. A. Mottola, CRC Crit. Rev. Anal. Chem. 1975, 229.

4. H. A. Mottola and H. B. Mark, Jr., Anal. Chem. 1986, **58**, 264R.

5. H. L. Pardue, Anal. Chim. Acta 1989, **216**, 69.

6. R. L. Wilson and J. D. Ingle, Jr., Anal. Chem. 1977, **49**, 1060.

7. M. A. Ryan and J. D. Ingle, Jr., Talanta 1981, **28**, 539.

8. J. Ruzicka and E. H. Hansen, "Flow Injection Analysis", 2nd ed., Wiley, New York, 1988

9. M. Valcarcel and M. D. Luque de Castro, "Flow Injection Analysis: Principles and Applications", Ellis Horwood Limited, U. K., 1987.

10. J. Ruzicka and E. H. Hansen, Anal. Chim. Acta 1986, **179**, 1.

CHAPTER II

HISTORICAL

Kinetics-Based Analysis

Overview

In early development of analytical kinetic methods, the time for completion of the reaction after initiation was measured and related to the concentration of the sought-for species. The earliest paper, published by Roberts in 1881 [1], described a kinetic procedure for the determination of amylase activity and proteolytic activity of pancreatic extracts. This method involves measuring the amount of starch that can be hydrolyzed completely with a fixed amount of enzyme in a fixed time interval. In 1930, Baines [2] described a stop-watch method for the determination of iodide concentration in which the time required from the initiation to the completion of the reaction was measured. These kinetic methods were considered as tedious and time consuming because the reaction was not monitored continuously with a suitable detection device and timing was based on stop watches and visual observation of color changes. It appears that early kinetic methods did not provide significant advantages over equilibrium methods in cases where both methods could be applied.

In the 1960's, significant improvements in kinetic methods were made by taking advantage of new developments in electronics and other

instrumental components. The major emphasis during this period was the development of automated instrumentation in which the reaction was monitored as it proceeded and of rate computation methods. Over a period of time, several primary rate computational approaches were developed for first- or pseudo-first order reactions. Today these are known as: (1) the initial slope method (method of tangents) in which the derivative or slope of the initial portion of the reaction monitor signal vs. time curve is measured, (2) the fixed-time method in which the change in the monitored signal over a predetermined time interval is calculated, and (3) the variable-time method (the fixed-concentration method) in which the time interval required for a predetermined fixed change in the reaction monitor signal is measured and related to the concentration of the analyte. Initially, these methods were used to extract rate information from recorder tracings. Next the rate computational approaches were implemented with dedicated hardware (analog and digital) often denoted as ratemeters. These advances reduced the tedium of rate measurements, increased precision, and eliminated the need to extract manually rate information from recorder tracings. The availability of minicomputers in the 1970's and finally microcomputers in the 1980's brought further advances in kinetic instrumentation. The enhanced control and sophisticated data manipulation provided by software control were used to advantage.

Kinetic methods are now recognized as a powerful tool for the quantitative analysis. Recently, kinetic methods in analytical chemistry have been exclusively reviewed by Pardue [3].

Development of Reaction-Rate Computation System

In the great majority of kinetic methods involving noncatalytic reactions, the reaction is first-order in the analyte, or conditions are arranged so that the reaction is pseudo-first order in the analyte over the time period that data are acquired. In 1966, the first monograph devoted to kinetic methods by Yatsimirskii [4] appeared and the initial slope, fixed-time, and variable-time methods were presented. Of these, the method of tangents, also known as the initial rate method, was preferred for its accuracy; however, it is a tedious and time-consuming technique with manual data processing. These computational techniques found broader application with the development of automatic data processing systems.

In 1958, Blaedel and Petitijean described one of the first instruments that continuously recorded the reaction-monitor signal during the early stages of the reaction [5]. A frequency meter, which was connected to a chart recorder, was used to monitor the frequency changes due to the changes in solution conductance as a reaction proceeded. They also developed the variable-time computational method in which the time for a predetermined change in frequency was measured. Even though the time measurements were obtained from the recorded chart, the reproducibility was excellent (better than 1% RSD) for the determination of ethyl acetate.

In 1960, Malmstadt and Hicks described an automatic variable-time system that measured the time for the reaction monitor signal to pass between two preselected signal levels. It was applied for the determination of glucose in blood serum [6]. A voltage

interval circuit was developed to initiate and stop a timer and the reciprocal of the timer reading was related to the concentration of glucose. In subsequent work, this instrumentation was modified and applied to develop other analytical procedures based on various enzymatic reactions [7-10].

Since automatic rate computational systems proved to be more reliable and faster than manual procedures, a significant amount of research was devoted to improve computational procedures [11,12]. Blaedel and Hicks developed a continuous flow system to measure the initial reaction rate based on the fixed-time method [13]. In their approach, the time delay between the two photometer cells was determined by the length of a reaction tubing between the cells. With a constant flow rate, the absorbance difference was taken as proportional to the initial rate which was related to the concentration of the analyte. This system provided high sample throughput for assays based on enzymatic reactions.

Electromechanical components were used to construct early rate computational circuits. They provide satisfactory results for slow reaction kinetics, but are limited by relatively long response times and the oscillation of the servo balancing system. Eventually, these limitations were minimized by the development of all-electronic rate computational systems. Crouch and Malmstadt described a variable-time ratemeter system based on an operational-amplifier comparator circuit [14]. This system was used for the enzymatic determination of glucose with a total measurement time of 40-50 s per sample. Another all-electronic variable-time ratemeter which measured the time interval and computed the derivative of the logarithm of the

time interval was developed by Stehl et al. [15].

Advances in electronics also made possible to integrate the reaction monitor signal over a given time interval. The fixed-time method can be implemented by taking the difference between integrals acquired over two different time periods. One of the earliest uses of this approach is described in a paper by Cordos et al. [16]. They used an integration and subtraction circuit based on two operational amplifier integrators with a digital voltmeter to provide a number proportional to the rate during a preselected time interval during the course of the reaction.

During the late 1960's, totally digital rate computation circuitry was introduced [17-19]. Parker et al. described a variable-time ratemeter based on all digital circuitry to generate a frequency which is directly proportional to the concentration of analyte [19]. Ingle and Crouch presented a digital counting system that computes the voltage change over a fixed-time interval [20]. The output voltage from the reaction monitor is converted to a frequency by a voltage to frequency (V/F) converter. With precise timing and gating circuits, the difference in the integrals for two equal and adjacent time periods was calculated by counting the V/F pulses with an up-down counter. In a subsequent work, fixed- and variable-time techniques were compared with respect to accuracy and precision for different types of chemical kinetics [21]. They showed that the fixed-time method is superior for pseudo-first order reactions, while the variable-time method is superior for reactions involving nonlinear response curves. By taking advantages of modern technology, more powerful and flexible systems have been reported

[22,23].

One of the first applications of computers is found in an article by James and Pardue [18]. They utilized a digital computer equipped with 8 K of core memory to acquire and store a signal-time profile in computer memory. The analog reaction-monitor signal was converted to a digital signal by an analog-to-digital converter (ADC) and the output of the computer was taken from a teletype to perform either the fixed- or the variable-time approaches. Use of a computer offers greater versatility because the rate computation method can be easily changed depending on the chemical system used for the analysis. With the availability of inexpensive microcomputers, the use of dedicated ratemeters has noticeably decreased. This is mainly because a large number of data points can be easily obtained as a function of time and the rate computational method can be easily varied by software.

Along with these innovations, theoretical aspects for the kinetic methods have been emphasized. Compared to the equilibrium analysis, kinetic determinations are subject to greater uncertainties due to variations in chemical parameters such as pH, ionic strength, and temperature. The effect of the run-to-run variation in the rate constant due to these random errors has been investigated in several papers [24-27]. It has been shown that the precision of rate measurements can be improved by adjusting measurement parameters such as the measurement time for the fixed-time method [27]. Ingle et al. evaluated the effect of noise on the run-to-run precision of rate measurements for different rate computational techniques [28]. Recently, Wentzell and Crouch introduced the two-rate method to

minimize the errors arising from the run-to-run variations in the rate constant [29]. This method is based on obtaining the rate at two points during the reaction. In a subsequent work, most common rate computational methods were classified and compared to evaluate the theoretical and experimental performance of each method [30].

Fluorometric Kinetic Methods

Fluorometric monitoring of reactions can provide better sensitivity and selectivity than does spectrophotometric monitoring. In the early development of fluorometric kinetic methods, enzymatic reactions were primarily studied. In 1954, Theorell and Nygaard [31] first used a fluorometer for the kinetic study of flavin mononucleotide and its apoenzyme and to determine rate constants with improved sensitivity. In 1957, Lowry and co-workers [32] emphasized fluorometric methods as a more sensitive technique over colorimetric methods for the determination of enzyme activity. Fluorometric kinetic methods involving enzymatic reactions for the determination of enzyme activity, substrates, activators, inhibitors has been extensively described by several workers [33,34]. Kinetic fluorometric methods for metal ions based on their inhibition of the activities of enzymes have also been developed [35-37].

With the development of more sophisticated fluorescence instrumentation, fluorometric kinetic methods have been applied to non-enzymatic reactions to take advantage of the greater sensitivity and selectivity. Various inorganic ions have been determined based on their catalytic effect on chemical reactions [38,39] or formation

of fluorescent metal complexes [40,41]. Valcarcel and Grases [42] have classified and reviewed fluorometric reaction-rate methods in inorganic analysis involving enzymatic and non-enzymatic reactions.

The instrumentation for and applications of fluorometric kinetic methods have been described by Ingle et al. [23,43,44].

Flow Injection Analysis

Overview

Continuous flow analysis has been refined over the last few decades to minimize sample manipulation, increase sample throughput, and to improve precision and accuracy. In 1957, Skeggs [45] introduced a new concept of continuous flow analysis. This method involves sequential aspiration of samples and mixing with reagents in a flow stream, dividing the flowing stream into segments by air bubbles to minimize sample overlap, and continuous monitoring of the signal. Based on this air-segmented continuous flow approach, the AutoAnalyzer was developed commercially and became extensively used in the fields of clinical and water chemistry throughout the 1960's.

Many workers have been contributed to unsegmented (i.e., no air bubbles) continuous flow analysis. In 1962, Blaedel and Hicks [13] described a unsegmented flow system for the kinetic determination of glucose. In 1970, Nagy and co-workers [46] described sample injection into a flowing stream of electrolyte. In 1972, Bergmeyer and Hagen [47] reported an enzymatic determination involving sample injection into a recirculating unsegmented flow system.

The new concept of flow injection analysis (FIA), which is based on unsegmented continuous-flow analysis, was established in mid-1970's by two research groups. In 1975, Ruzicka and Hansen [48] modified a segmented flow system for the direct injection of samples. In their method, a peristaltic pump was used to propel the carrier stream and samples were injected with a syringe through the wall of the reaction tube or through a simple injection block. In 1976, Stewart et al. [49] reported a new approach to inject a sample with a multiport sampling valve into a continuously flowing carrier stream. The initial work was based on the use of high-performance liquid chromatography components.

FIA has been compared with other techniques for automated analysis such as segmented flow analysis (SFA) and became recognized as a fast, efficient analytical technique for increasing the speed of routine analysis [50-53]. Initially, FIA was primarily used to automate wet chemical analysis [50-53]. Later, the unique features of FIA which include sample injection, controlled sample dispersion, and reproducible timing have been emphasized and FIA has been recognized as a powerful, versatile, and diagnostic tool [54,55].

Development of FIA

Several workers [51,55-57] have reviewed the early developments of FIA in which the advantages of FIA over conventional analysis are emphasized. Based on injection of a sample into a continuously flowing carrier stream, a reproducible signal response from measurement to measurement has been a main concern. To characterize

the sample dispersion throughout the detection time, the dispersion coefficient (D) was introduced in 1977 by Ruzicka et al. [58]. It provides a direct measure of the sample dilution and is defined as the ratio of the analyte concentration before injection to the concentration at some point in the dispersed sample zone after transport through a given FIA manifold.

In 1978, the merging zone principle was developed by Bergamin et al. [59] to minimize reagent consumption. This method involves the simultaneous injection of the sample and the reagent into two separate carrier streams which later merge at a confluence point. The merging zone technique has been used by Ruzicka and Hansen [60] for stopped-flow measurements to determine reaction rates. Since then, various manifold designs have been designed and applied to different chemical systems [61,62]. In 1982, Olsen et al. [63] demonstrated the gradient technique which is based on using the signal at different specified portions of the dispersed sample zone. This suggested that useful information can be obtained from any portion of the dispersed sample zone with a suitable detection system.

Many workers have investigated dispersion phenomena theoretically. In 1977, Ruzicka et al. [58] reported that the transport of sample through the tubing can be described by laminar flow. In the following year, Ruzicka et al. [64] described the dispersion and concentration profiles based on a tanks-in-series model. Under the laminar flow conditions, the peak profile is known to be affected by convective transport (in the early stage) and diffusion transport (in the later stage) [61,62]. Based on the

convection-diffusion equation, Vanderslice et al. [65] and Mottola et al. [66] derived numerical equations to predict theoretical peak profiles. Tyson [67] derived an equation that relates the peak width to the concentration of injected sample for single-line and merging zone manifold. Kolev and Pungor [68] described mathematical models for single-line FIA systems which account for the individual contributions of the injection device, reactor, and measurement cell to the overall dispersion.

The theoretical models discussed above have been derived to investigate the effect of experimental parameters on the dispersion for a given system and to characterize the peak profile in terms of dispersion. Recently, Dorsey et al. [69] used moment analysis to describe the dispersion based on the peak profile in which the second moment (variance) of the peak is calculated from the FIA response curve and related to the flow rate. For a system involving purely physical dispersion, the second moment is a linearly related to the flow rate. This approach allows the individual contributions of the variances due to injection, transport, and chemical reaction to the total peak variance of different FIA manifold to be obtained and compared.

Microcomputers have been added to FIA systems for control of FIA components and data collection. In 1980, Stewart et al. [70] reported a microcomputer-based FIA system for implementing multiple injections and performing data reduction. In 1985 and 1986, Thijssen et al. [71,72] described a microcomputer-controlled FIA system with software in which on-line control and data reduction are emphasized. Recently, Christian et al. [73] reviewed microcomputer applications

in FIA and described a more complete microcomputer-based FIA system which can be used as a developmental tool.

Applications of FIA to Kinetics-Based Analysis

FIA kinetic measurements based on single-point or two-point detection were first discussed by Ruzicka et al. [74] in 1977. For a two-point detection system, two flow-cells are placed in series and the travel time between the cells defines the reaction time. They demonstrated that the two-point assay eliminates interference due to species that produce a detector signal but do not react with the analytical reagent.

To monitor a chemical reaction as a function of time, the stopped-flow technique was developed [64], which allows multi-point kinetic determinations. A computer-controlled FIA system is commonly employed [75] to stop with precise timing the flow when the center of sample zone is in the detection flow cell. This technique has been widely used for both enzymatic and non-enzymatic assays. Valcarcel et al. [76] compared this technique with the conventional single-point assay for a catalytic-fluorometric determination of copper. They reported that the stopped-flow kinetic method can discriminate against interfering species such as Al^{3+}, Cr^{3+}, and Sn^{2+}.

FIA has also been used to develop differential kinetic methods for simultaneous determination of two or more species in the sample based on the different rates of their reactions. A wide variety of FIA manifolds which involve splitting the sample, multi-injection, or multi-detectors have been designed for kinetic determinations.

Valcarcel et al. [77] have published a good review for simultaneous determinations which involve various FIA manifolds.

REFERENCES

1. W. Roberts, Proc. Roy, Soc. London 1881, 32, 145.
2. H. A. Baines, J. Soc. Chem. Ind. 1930, 49 PT, 481T
3. H. L. Pardue, Anal. Chim. Acta 1989, 216, 69.
4. K. B. Yatsimirskii, "Kinetic Methods of Analysis", Pergamon Press, Oxford, 1966.
5. W. J. Blaedel and D. L. Petitijean, Anal. Chem. 1958, 30, 1958.
6. H. V. Malmstadt and G. P. Hicks, Anal. Chem. 1960, 32, 394.
7. H. V. Malmstadt and H. L. Pardue, Anal. Chem. 1961, 33, 1040.
8. H. V. Malmstadt and T. P. Hadjiioannou, Anal. Chem. 1962, 34, 452.
9. H. V. Malmstadt and T. P. Hadjiioannou, Anal. Chem. 1962, 34, 455.
10. H. V. Malmstadt and T. P. Hadjiioannou, Anal. Chem. 1963, 35, 14.
11. H. L. Pardue, C. S. Frings, and C. J. Delaney, Anal. Chem. 1965, 37, 1426.
12. R. H. Stehl, D. W. Margerum, and J. J. Latterell, Anal. Chem. 1967, 39, 1346.
13. W. J. Blaedel and G. P. Hicks, Anal. Chem. 1962, 34, 388.
14. H. V. Malmstadt and S. R. Crouch, J. Chem. Educ. 1966, 43, 340.
15. R. H. Stehl, D. W. Dahl, and J. J. Latterell, Anal. Chem. 1967, 39, 1426.
16. E. Cordos, S. R. Crouch, and H. V. Malmstadt, Anal. Chem. 1968, 40, 1812.
17. S. R. Crouch, Anal. Chem. 1969, 41, 880
18. G. E. James and H. L. Pardue, Anal. Chem. 1969, 41, 1618.
19. R. A. Parker and H. L. Pardue, Anal. Chem. 1970, 42, 56.
20. J. D. Ingle, Jr. and S. R. Crouch, Anal. Chem. 1970, 42, 1055.
21. J. D. Ingle, Jr. and S. R. Crouch, Anal. Chem. 1971, 43, 697.

45. R. L. Wilson and J. D. Ingle, Jr., Anal. Chem. 1977, 49, 1060.

22. R. L. Wilson and J. D. Ingle, Jr., Anal. Chim. Acta 1976, 83, 203.

23. M.A. Ryan and J. D. Ingle, Jr., Talanta 1981, 28, 539.

24. J. B. Landis, M. Rebec, and H. L. Pardue, Anal. Chem. 1977, 49, 785.

25. P. W. Carr, Anal. Chem. 1978, 50, 1602.

26. G. E. Mieling and H. L. Pardue, Anal. Chem. 1978, 50, 1611.

27. J. E. Davis and B. Renoe, Anal. Chem. 1979, 51, 529.

28. J. D. Ingle, Jr., M. J. White, and E. D. Salin, Anal. Chem. 1982, 54, 56.

29. P. D. Wentzell and S. R. Crouch, Anal. Chem. 1986, 58, 2851.

30. P. D. Wentzell and S. R. Crouch, Anal. Chem. 1986, 58, 2855.

31. H. Theorell and A. Nygaard, Acta. Chem. Scand. 1954, 8, 877.

32. O. H. Lowry, N. R. Roberts, and J. I. Kapphahn, J. Biol. Chem. 1957, 224, 1047.

33. G. G. Guilbault, CRC Crit. Rev. Anal. Chem. 1970, 377.

34. H. V. Malmstadt, C. J. Delaney, and E. A. Cordos, CRC Crit. Rev. Anal. Chem. 1972, 559.

35. G. G. Guilbault, P. Brignac, Jr., and M. Zimmer, Anal. Chem. 1968, 40, 190.

36. A. Townshend and A. Vaughan, Talanta 1969, 16, 929.

37. A. Townshend and A. Vaughan, Talanta 1970, 17, 299.

38. J. Ottaway, J. Fuller, and J. Allan, Analyst 1969, 94, 522.

39. T. Janjic, G. Milovanovic, and M. Celap, Anal. Chem. 1970, 42, 27.

40. L. Hargis, Anal. Chem. 1969, 41, 597.

41. R. L. Wilson and J. D. Ingle, Jr., Anal. Chim. Acta 1977, 92, 417.

42. M. Valcarcel and F. Grases, Talanta 1983, 30, 139.

43. R. L. Wilson and J. D. Ingle, Jr., Anal. Chem. 1977, 49, 1060.

44. J. D. Ingle, Jr. and M. A. Ryan, "Reaction Rate Methods in Fluorescence Analysis" in "Modern Fluorescence Spectroscopy", E. L. Wehry, ed., Plenum Press, New York, 1981, Vol. 3, Chap. 3, pp 95-141.

45. L. T. Skeggs Jr., Am. J. Pathol. 1957, **28**, 311.

46. G. Nagy, Z. Feher, and E. Pungor, Anal. Chim. Acta 1970, **52**, 47.

47. H. U. Bergmeyer, A. Hagen, Fresenius Z. Anal. Chem. 1972, **261**, 333.

48. J. Ruzicka and E. H. Hansen, Anal. Chim. Acta 1975, **78**, 145.

49. K. K. Stewart, G. R. Beecher, and P. E. Hare, Anal. Biochem. 1976, **70**, 167.

50. J. Ruzicka and E. H. Hansen, Anal. Chim. Acta 1978, **98**, 1.

51. L. R. Snyder, Anal. Chim. Acta 1980, **114**, 3.

52. C. B. Ranger, Anal. Chem. 1981, **53**, 21A.

53. B. Rocks and C. Riley, Clin. Chem. 1982, **28**, 409.

54. J. Ruzicka, Anal. Chem. 1983, **55**, 1040A.

55. J. Ruzicka and E. H. Hansen, Anal. Chim. Acta 1986, **179**, 1.

56. D. Betteridge, Anal. Chem. 1978, **50**, 832A.

57. H. A. Mottola, Anal. Chem. 1981, **53**, 1312A.

58. J. Ruzicka, E. H. Hansen, and E. A. Zagatto, Anal. Chim. Acta 1977, **88**, 1.

59. H. Bergamin, E. A. G. Zagatto, F. J. Krug, and B. F. Reis, Anal. Chim. Acta 1978, **101**, 17.

60. J. Ruzicka and E. H. Hansen, Anal. Chim. Acta 1979, **106**, 207.

61. J. Ruzicka and E. H. Hansen, "Flow Injection Analysis", 2nd ed., Wiley, New York, 1988.

62. M. Valcarcel and M. D. Luque de Castro, "Flow Injection Analysis: Principles and Applications", Ellis Horwood, U. K., 1987.

63. S. Olsen, J. Ruzicka, and E. H. Hansen, Anal. Chim. Acta 1982, **136**, 101.

64. J. Ruzicka and E. H. Hansen, Anal. Chim. Acta 1978, **99**, 37.

65. J. T. Vanderslice, K. K. Stewart, A G. Rosenfeld, and D. J. Higgs, Talanta 1981, **28**, 11.

66. C. C. Painton and H. A. Mottola, Anal. Chim. Acta 1984, **158**, 67.

67. J. F. Tyson, Anal. Chim. Acta 1986, **179**, 131.

68. S. D. Kolev and E. Pungor, Anal. Chem. 1988, **60**, 1700.

69. S. H. Brolks, D. V. Leff, M. A. Hernandez Torres, and J. D. Dorsey, Anal. Chem. 1988, **60**, 1737.

70. K. K. Stewart, J. F. Brown, and B. M. Golden, Anal. Chim. Acta 1980, **114**, 119.

71. L. T. M. Prop , P. C. Thijssen, and L. G. G. Van Dongen, Talanta 1985, **32**, 230.

72. F. T. M. Dohmen and P. C. Thijssen, Talanta 1986, **33**, 107.

73. G. D. Clark, G. D. Christian, J. Ruzicka, G. F. Anderson, and J. A. van Zee, Anal. Instr. 1989, **18**, 1.

74. E. H. Hansen, J. Ruzicka, and R. Rietz, Anal. Chim. Acta 1977, **89**, 241.

75. H. Kagenow and A. Jensen, Anal. Chim. Acta 1983, **145**, 125.

76. F. Lazaro, M. D. Luque de Castro, and M. Valcarcel, Anal. Chim. Acta 1984, **165**, 177.

77. M. D. Luque de Castro, and M. Valcarcel, Analyst 1984, **109**, 413.

CHAPTER III

INSTRUMENTATION AND DATA ACQUISITION

Overview

Molecular fluorescence spectrometry was used as the monitoring technique for kinetics-based analysis and for FIA to characterize the profile of the sample zone. In this research, a PC data collection system based on a voltage-to-frequency (V/F) converter and counter was developed. It serves not only as a powerful and flexible reaction-rate data acquisition and computation system for the kinetics-based analysis, but as a high resolution recording device for low-level and widely varying signals in FIA measurements. Signal versus time data are acquired for on-line calculation of results and stored on a floppy diskette for further data reduction.

The basic fluorometer and data acquisition system are discussed first. The section concludes with a more detailed description of the reaction-rate and FIA measurements systems.

Fluorometer Components

A block diagram of the fluorescence spectrometer and data acquisition system is shown in Figure III.1. For reaction-rate measurements, a 1-cm pathlength fused silica cell is used. A magnetic stirrer below the sample cell and a magnetic stirring bar in the cell provide efficient mixing. The last reagent is injected with

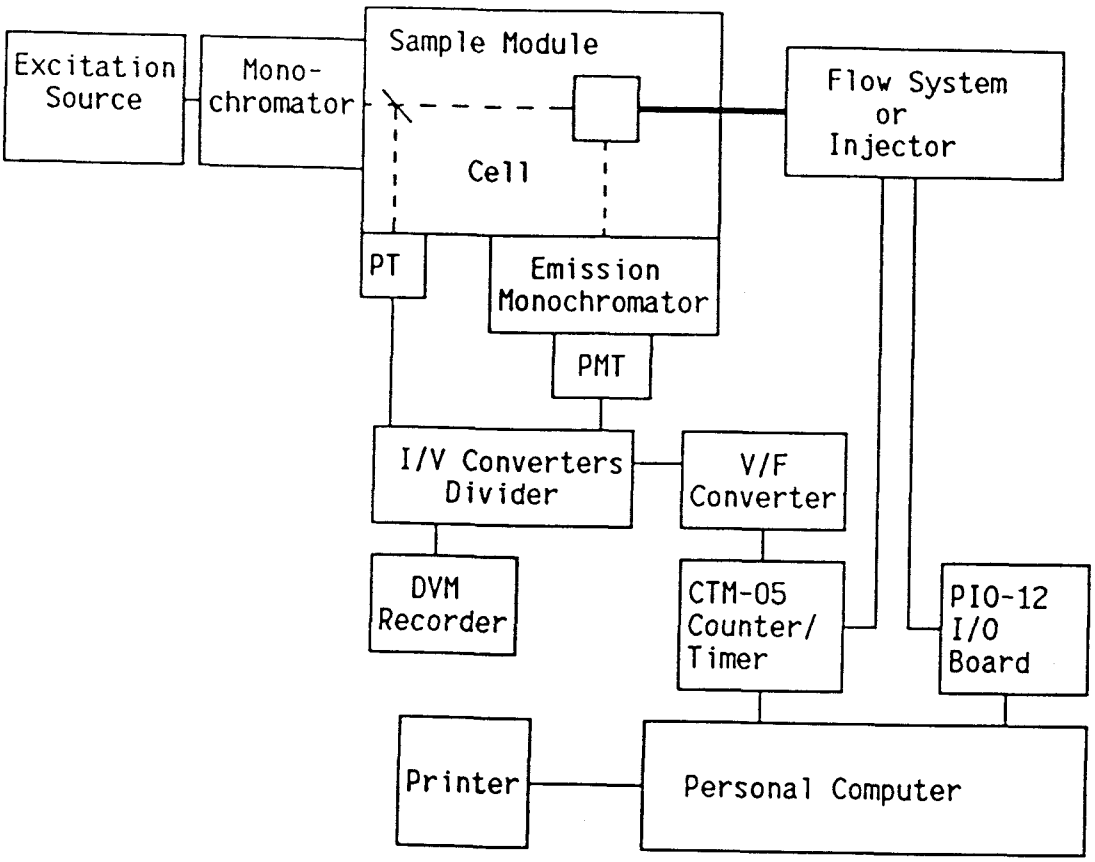

Figure III.1. Fluorescence spectrometer for reaction-rate or FIA measurements with a data acquisition system based on a PC, V/F converter, and a counter board.

an automatic syringe under computer control.

For FIA measurement, a 1-mm pathlength cell is inserted into the sample holder. The sample injection valve and pumps that are used to deliver sample solutions to the flow cell are microcomputer controlled and are discussed in more detail later.

Fluorescence measurements were made with a spectrofluorometer built by Wilson [1]. This fluorometer consists of a 200-W Xe-Hg arc lamp excitation source, an excitation monochromator, a thermostated sample cell holder, an emission filter or monochromator, and a photomultiplier tube (PMT) detector (1P28). The excitation beam is split by a beam splitter and the reflected beam is monitored by a reference vacuum phototube (PT). The PT and PMT photoanodic currents are converted to voltages with operational amplifiers configured as current-to-voltage converters. An analog divider computes the ratio of the fluorescence signal to the reference PT signal in order to obtain a voltage signal compensated for the source fluctuations. The compensated output signal from the divider is input to a V/F converter in order to produce a TTL compatible output pulse train proportional to the fluorescence signal for further processing and also is monitored by a strip chart recorder.

Data Collection System

The data collection system consists of a V/F converter (Teledyne Philbrick model 7405) and a MetraByte 5-channel counter-timer interface board (Model CTM-05) with a IBM PC compatible (Corona PC400). The computer has 512 K of RAM and two 5¼" floppy disc

drives. A MetraByte PIO-12 I/O board is plugged into the computer buss to provide 24 I/O lines. The V/F converter provides an output of 100 kHz/V up to 10 V with less than 0.02% non-linearity. With 0.1-s integration time, it provides a resolution of 100 μV and a dynamic range of 100 μV to 10^5.

The CTM-05 includes a AMD9513 system timing controller (STC), a 1-MHz internal frequency source with a divider, and an 8-bit latched input port and an 8-bit latched output port. The AMD9513 STC (LSI circuit), which includes five independent 16-bit up/down counters, is designed to accomplish many types of counting, sequencing, and timing applications. Since the frequency measurement system used in this research is based on the several features of AMD9513 STC, the basic functions of STC are described. The STC uses two consecutive locations as a data port and a control port which can be accessed by the PC. The data port is set to a starting address or base address of 300 (Hex) (768 decimal value) and is used to transfer data between the PC and internal registers in a counter logic group or the master mode register. The control port (base address +1 or 301 (Hex)) is used to access a command register and a status register. The command register provides indirect addressing of the above registers by an internal data pointer register and control of the loading and enabling of counters, while the status register provides the output status to the host processor.

Each individual counter has its own counter mode, load, and hold registers. The load register is used to reload the counter to a predefined value. The hold register is used to store accumulated count values for later transfer to the host processor or an IBM PC.

The counter mode register is used to define how the counter will be used. Through this register, the user can select one of 10 sources as the input to an individual counter with active-high or active-low input and output polarities, a variety of gating modes, and up or down counting in either binary or BCD. The master mode register is used to control the overall operation of the STC. Important functions are the control of the fundamental crystal frequency with an appropriate scaler, data bus width, and data pointer sequencing.

The crystal oscillator output is input to a frequency scaler that provides frequencies equal to the crystal frequency (1 MHz) divided by 10, 10^2, 10^3, or 10^4 or 2^4, 2^8, 2^{12}, or 2^{16}. Any of these frequencies can be input to any of the counters.

The same data acquisition software was used for the reaction-rate and FIA measurements. Figure III.2 shows a simplified flow diagram of the data collection program. The data collection program is written in assembly language and is initiated by calling from the main BASIC program. Two counters (1 and 2) are used as the working counters to count the pulses from the V/F converter, and one counter (5) serves as the time-base counter which determines the integration time per data point. The variables for the data collection sequence are the number of the low and high order working and time-base counters, the source input, the starting memory location for the accumulated count values, the integration time per data point, and the total number of data points.

After passing the variable values from the BASIC program, the master mode register is first initialized by the loading data pointer register, through the control port of the command register, to

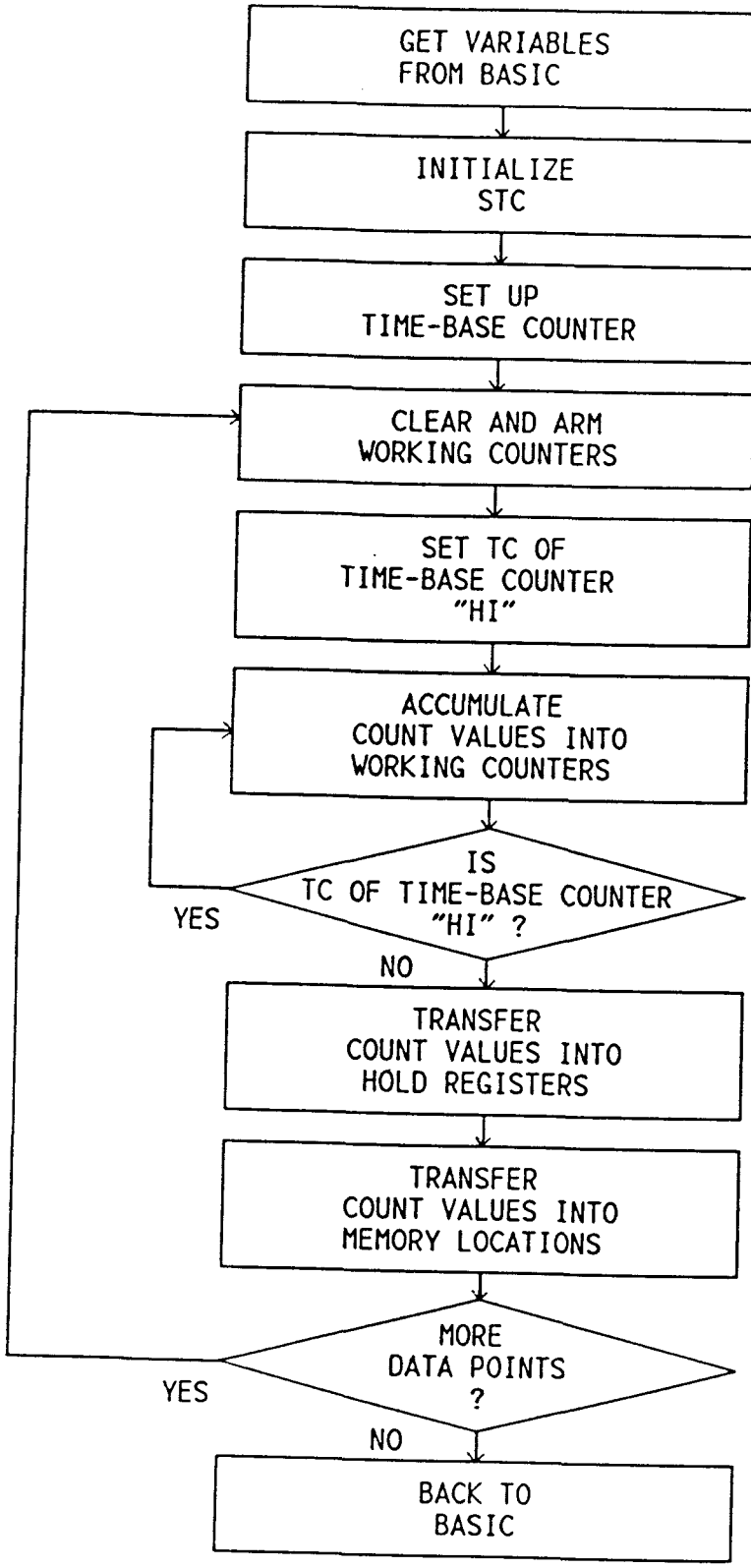

Figure III.2. Simplified flow diagram of data collection program.

control the five working counter groups. In this step, BCD division is selected to provide scaler outputs of 100 kHz, 10 kHz, 1 kHz and 100 Hz. Once the STC is initialized, the time-base counter group is selected and initialized with its own counter mode register. The 1 kHz scaler output is internally gated to the input of the time-base counter. This counter is then set up to countdown on the rising edge of the 1-kHz pulse train and to issue a toggled terminal count (TC) output (logic 0) when the counter value reaches zero. The gate interval or integration time passed from BASIC is loaded into the load register of the time-base counter group (e.g., 1000 for a 1-s integration time). Two adjacent working counter groups are concatenated to obtain 32-bit resolution per data point. These counters are configured to count on the rising edge of the input signal. The input source for the low counter is externally connected to the output of the V/F converter. The low order counter produces a toggled TC output which is internally connected to the count source input of the high order counter.

To initiate the frequency measurement steps, the initial output level (TC) of the time-base counter is set (high) by using the command register. The contents of working counters are cleared and loaded for accumulation of the frequency values. At the same time, the time-base counter is also loaded and armed with the specified integration time. Once all counters are armed with their own mode registers, the counting process continues until the status of toggled TC output of time-base counter goes from high to low. This is accomplished by continually checking the toggled TC output of time-base counter via monitoring the status register through the

control port. The status register OUT bit reflects the state of TC output of corresponding counter.

At the end of the integration time, the counts values accumulated in the working counters are first transferred to hold registers in the corresponding counter groups. These values are then transferred and stored in memory in the PC above those used by BASIC (DEF SEG = 5500 (Hex)). Later these count values are transferred to the BASIC program. Once the measurement procedure for one data point is finished, the program compares the number of data points accumulated to the number desired. If more measurements are required, the program loops through the procedure which performs the actual frequency measurement steps. This avoids repetitive initialization of the counters.

PC-based Reaction-Rate Measurement System

General Considerations

The complete fluorometric reaction-rate measurement system consists of three basic parts:

(a) the spectrofluorometer to monitor the chemical reaction
(b) the data collection system (hardware and software)
(c) the software for computation of the reaction rate which is related to the analyte concentration

In kinetics-based analysis, reproducible mixing between the

analyte and the reagent solutions is necessary so that the reaction curve (signal versus time) is reproducible. The reaction was initiated by injecting a reagent solution into the sample cell containing the analyte solution and other reagents with an automatic filling and dispensing reagent injector (Hamilton model 77000). This injector was previously modified as described by Ryan [2] by addition of pneumatic valves and switching circuitry that is triggered by a +5 V logic pulse. One of output lines on the CTM-05 expansion board was utilized to send a logic high signal at the time reagent addition is desired. This signal remains high for the duration of the measurement period. The computer-controlled automatic liquid dispenser provides reproducible initiation of reaction from measurement to measurement and precise synchronization of the data collection with the start of the reaction.

The advantages of using a microcomputer-based reaction-rate measurement system are extensively described by Ryan [3]. The PC-based reaction-rate data acquisition system developed in this research is simpler and more flexible than previous systems developed in this laboratory which were based on 8-bit microcomputers with only 64 K of RAM. Other than the computer, only a timer-counter board and V/F converter are required in the present system.

Since the integration time per data point can range from 1 ms to 32.757 s and each data point can be composed of a 32 bits in the computer memory, the data collection system provides a wide dynamic range suitable for studies of a wide range of different reaction monitor systems. For example, the voltage resolution is 10 and 100 μV with integration times of 1 and 0.1 s, respectively, and the

maximum input voltage is 10 V (1 MHz output). Even with a 10 V input, the 32-bit counter can count for 4.29×10^3 s (71.6 min) before overflowing. The memory space is sufficient to store a large enough number of data points to characterize completely a reaction-rate curve over the entire reaction period. This allows the user to investigate the whole reaction-rate curve or portions of curve after the experiment and to implement different data reduction techniques. For example, the rate over any desired portion of the reaction rate curve can be computed with the initial rate, fixed-time and variable-time methods. In this research, the fixed-time rate computational method based on the integration over two equal time segments which are sequential is used exclusively to calculate the reaction rate. It would also be possible to fit the acquired data to a model (e.g., exponential) to determine the reaction order.

Software

Menu driven software, written in QuickBASIC (Microsoft version 4.5) with assembly language subroutines, were used for data collection system, reaction-rate calculations and control of the automatic injector. Figure III.3 shows a simplified flow chart of the reaction-rate measurement program. The main program written in QuickBASIC language handles the overall operation of the system, which includes easy input and editing of user parameter values, calling the data collection/injection subroutine, on-line data processing, display of the reaction-rate curve, and saving the raw data for later analysis. The data collection subroutine described in

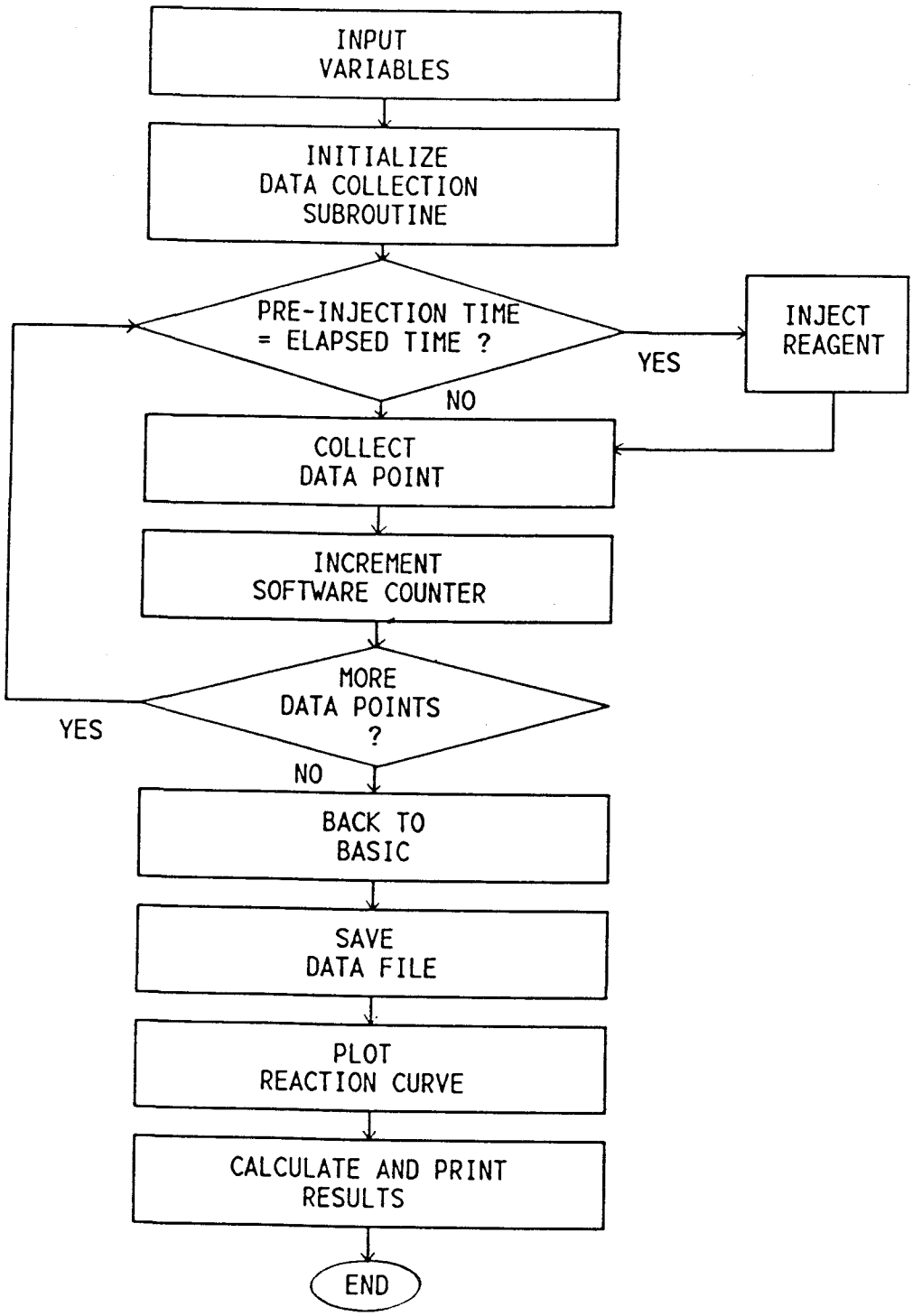

Figure III.3. Simplified flow diagram of reaction-rate measurement program.

the previous section was slightly modified to trigger the addition of the final reagent solution with the liquid dispenser.

When the program is loaded, the main menu is displayed with the following options:

1. Input User Parameters
2. Review and Edit Parameters
3. Do Rate Measurement
4. Rate Calculation
5. Wash Liquid Dispenser
6. Quit

In order to perform different functions stated in the main menu, subprograms within BASIC were written for convenience. This allows the program to be easily read and simple modification without changing the main structure of the program. A sample of the user screen is shown in Figure III.4. For the rate analysis, the operator first inputs the variable values from the keyboard, which govern the measurement of the fluorescence signal, the rate computation, and the name of file to be saved. To acquire data, the integration time per data point, the pre-injection delay time for reagent injection, and the total measurement time are entered. Since the elapsed time is recorded in terms of the number of data points, the pre-injection delay time and the total measurement time are converted into the proper values which are later passed to data collection subroutine. The variables for rate calculation are the post-injection delay time and the time interval for the rate computation. The file name for

1. PARAMETERS FOR DATA ACQUISITION
   -Integration Time Per Data Point (sec) : 0.1
   -Pre-Injection Delay Time (sec) : 3
   -Total Measurement Time (sec) : 30

2. PARAMETERS FOR RATE CALCULATION
   -Post-Injection Delay Time (sec) : 5
   -Computational Time Interval (sec) : 10

3. DATA FILE
   -File Name (Maximum 8 letters) : SAMPLE
   -Index (Numerical Value 1-99) : 1

Figure III.4. A sample of the user screen for rate measurements.

acquired data is also input at this point.

Once all variables are entered, the operator starts the rate measurement by selecting 3 from the main menu. The BASIC program then checks the input variable values, jumps to the assembly subroutine, and passes the valid variable values. Just after called from the BASIC, the assembly subroutine starts to collect the data with the specified integration time per data point. At the end of every integration time, two basic tasks are performed: (1) the accumulated counts are stored in the designated memory location, (2) the number of data points acquired is counted and stored in a software counter. This counter value is checked to determine when to inject the final reagent (after the pre-injection time) and when to stop taking data (at the end of the total measurement time). To activate the liquid dispenser, one of the digital output lines (normally output line 1 or 0) in the CTM-05 is utilized. No rate calculation is carried out during the data collection period.

Based on the measurement algorithm discussed previously, the dead time between data points is negligible. Thus a short integration time (e.g., 0.1 s) can be used without loss of information.

After the data collection sequence is finished, the program returns to the BASIC program which transfers the accumulated counts into a BASIC array and saves the data file on a floppy diskette. Next the raw data are plotted so that reaction curve can be examined qualitatively to allow the operator to make a decision whether the data are good or not before further processing. If a rate calculation is desired, the rate is calculated with the fixed-time

computation method over the time interval defined by the post-injection time and the computational time interval. To do this, the program calculates the difference in the sum of the data points over the second half of the computational period from the corresponding sum over the first half of the computation period. The calculated rate is then printed and the program returns to the main menu. Additional rate calculations over a different time interval also may be obtained by selecting option 4 from the main menu. Option 5 which implements a number of user-specified injections of the liquid dispenser as a convenient way to wash the dispenser. This is independent of rate measurement routine.

PC-based FIA Measurement System

FIA Components

A single-line FIA manifold (Figure III.5) was used in all experiments. The components used in FIA system are listed in Table III.I. An FMI pump driven by a stepper motor with a controller containing a computer interface by IVEK was used as the primary pump. The rotation rate of the stepper motor is governed by the frequency of the pulse train delivered by the pump controller. The pump head module contains a piston and cylinder and employs a unique valveless, variable, and positive-displacement pumping arrangement. Since the accuracy of this type of pump is based on a positive displacement mechanism without valves, a high precision flow rate independent of small pressure fluctuations and fluid viscosity is

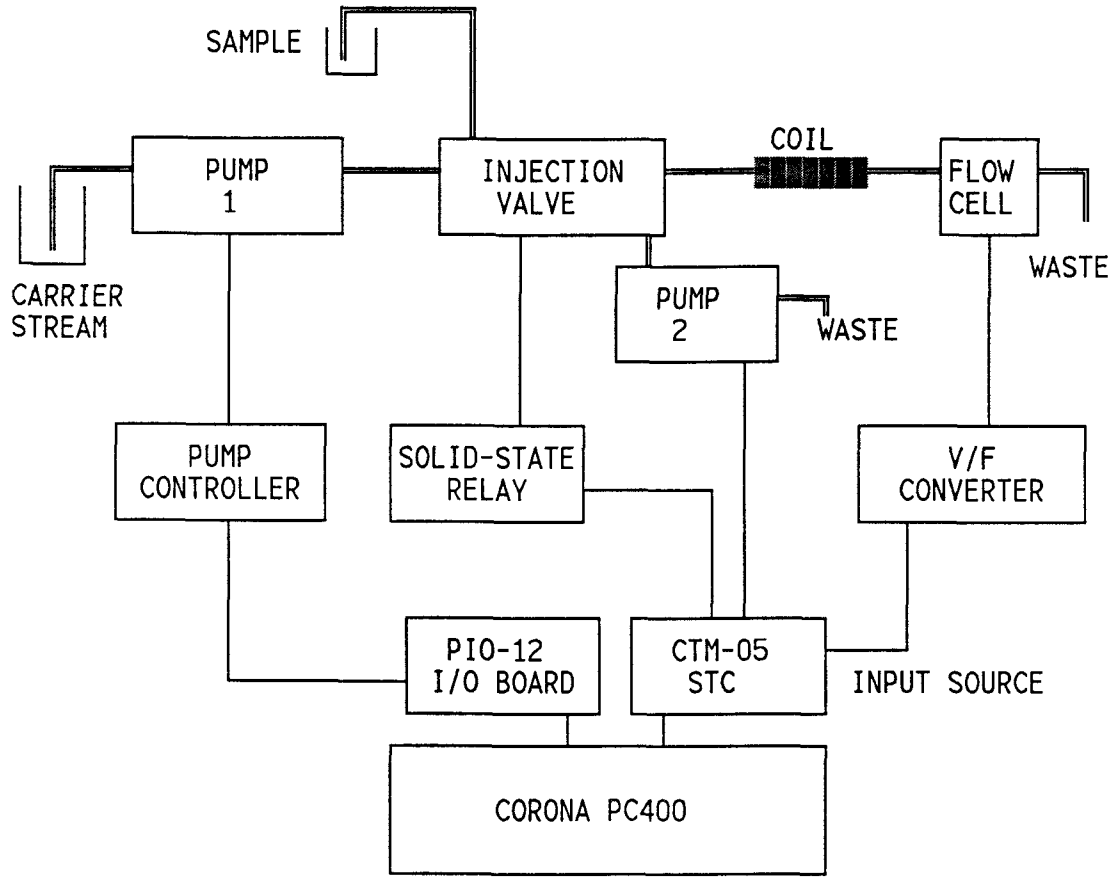

Figure III.5. Block diagram of the flow injection system.

Table III.I. Components of the FIA System

Component	Comments	Source
Main Pump System	Model SO-1 with computer control box, pump is manufactured by Fluid Metering, Inc.	IVEK Corp. Springfield, VT
Sampling Pump	Lab pump Jr., model RHSY	Fluid Metering, Inc.
Injection Valve	4-way slide bar type equipped with pneumatic actuators	Dionex Corp. Cat. No. 030520
Solid State AC Relay	Manufactured by Grayhill Model 70S2-04-B-04-F	Newark Electronics, Inc.
3-Way Solenoid Valve	Model MBD-002, three-way valves switched by AC	Skinner Valve Co. New Britian, CT
Fluorescence Flow Cell	Model #P/N 8830, 20-μL capacity square sample, cavity, 1-mm pathlength	Precision Cells Inc. Hicksville, NY

expected. The sample injection valves are a 4-way double-stack slide bar type valves which are operated by pneumatic activators and require about 60 psi. For pump 2, another positive-displacement pump driven by a synchronous motor is used to pull the sample solutions into the sample loop. This pump is located between the injection valve and the waste bottle.

The flow cell for fluorescence measurements used in this system was initially designed for HPLC detection with stainless steel inlet and outlet tubing equipped with ferrule-type high pressure fittings. In order to use this flow cell for FIA, the stainless steel tubing was replaced by 0.5-mm i.d. Teflon tubing. The flow cell was mounted within the cell compartment of the fluorometer.

The manifold was made from Teflon tubing. Tubing of 1.5-mm i.d. was used before and after the primary pump (60 cm between the carrier stream reservoir and the primary pump and 10 cm after the primary pump) to minimize the pressure drop, and an additional 50 cm of 0.5-mm i.d. tubing is used to connect the outlet line of pump 1 to the injection valve. The tubing for the main flow line including the sample loop (102 cm for 200 μL) was 0.5-mm i.d. The tubing between the injection valve and the flow cell was ≃430 cm including a 400-cm reaction coil in a tight coil, and the length of tubing between the flow cell and waste vessel was 30 cm. Greater details about the manifold components can be found elsewhere [4].

PC-Controlled FIA

The operation of the pumps and the injection valve was automated

by utilizing the I/O lines of the expansion boards in the PC. Two of the 8 CTM-05 output lines are utilized to operate the sampling pump (I/O line 3) and the injection valve (I/O line 1). The 24-bit parallel digital I/O interface board (MetraByte, model PIO-12) was used to control the flow rate of the carrier stream with pump 1. To avoid direct connections between the expansion boards and the FIA components, the I/O lines of the expansion boards are brought out to a connection box. The source input for V/F converter is connected to a BNC plug. The 8 output lines of the CTM-05 board are connected to female banana plugs to allow easy connection to the sampling pump, injection valve, and injector (for rate measurements). The 24 I/O lines from the I/O board are connected to a 37-pin D female connector. The I/O lines from port C are connected to the pump controller with a ribbon cable.

Since the flow rate of the sampling pump does not have to be controlled, an ac solid-state relay was added to activate the synchronous motor by a logic signal (+5 V). The inject or load position of the sample injection valve is selected by applying air pressure to the appropriate side of the valve with one of two 3-way solenoid valves which are controlled by a solid-state relay.

The computer interface board of the carrier stream pump controller accepts 1.4 to 20-V positive BCD logic signals. The I/O line assignments are listed in Table III.II. The flow rate can be controlled in the range from 0 to 9.9 mL/min in steps of 0.1 mL/min. The flow rate is determined by the speed of the stepper motor and the pump displacement volume ($\simeq$10 μL). In the BASIC program, the decimal input value is converted by software into a BCD value which is loaded

Table III.II. Output Bit Assignments of PIO-12 for the Control of the Carrier Stream Flow Rate

I/O bit on PIO-12	Corresponding Pin # on Control Box	Flow Rate (mL/min)
PC0	11	0.1
PC1	12	0.2
PC2	4	0.4
PC3	3	0.8
PC4	13	1.0
PC5	14	2.0
PC6	2	4.0
PC7	1	8.0

into the I/O port C of the PIO-12 board. For example, if a flow rate of 2.5 mL/min is chosen, PC5, PC2 and PC0 are set to logic level 1 and the binary number for this flow rate is 0010 0101.

For some experiments, two injection valves were used. The state of the second injection valve was controlled by I/O line 2 from the CTM-05 board. This injection valve was filled by sending a logic HI signal for a given period of time.

FIA Software

Menu driven FIA software was developed to control the FIA components and to obtain time-dependent fluorescence signal information. The software provides versatility and flexibility in terms of control of experiment and different modes of operation. The precise control of the timing of all operations and data acquisition provided by the automated FIA system is critical for obtaining high reproducibility from run to run for characterization of the peak shape.

The software for the FIA system consists of two basic parts. The main program is written in QuickBASIC along with an assembly subroutine for data acquisition and control of the sample injection valve with the CTM-05. The BASIC program is responsible for main control of FIA system which includes input of variable values from the operator, display of FIA peaks, calculation and printing of FIA peak parameters, and saving of data.

When the program is loaded, it allocates the array of memory space for the data points and resets the variables related to the

status of the measurement and data analysis. At the same time, it resets the injection valves to the filling position and sets the carrier stream pump speed to zero. The main program then displays the main menu containing the following options:

1. Input User Parameters
2. Review and Edit Parameters
3. Start FIA Analysis
4. Data Analysis
5. Quit

Option 1 is always chosen first. If the operator provides all the valid parameter values, these are used as default values for the rest of the measurements. When certain parameter values must be corrected or changed between measurements, option 2 is used as it allows changing selected parameter values (i.e., the user does not have to edit all the parameter values). Option 3 initiates the FIA experiment. Option 4 allows recalculation of peak parameters with a different time segment of the data saved as a file on a floppy diskette. Once a given task (options 1-4) is completed, the main menu is always displayed.

When the option 1 is chosen, the user is asked to input information in five categories as illustrated by the sample input screen shown in Figure III.6. Once the flow rate of the carrier stream pump is input, the pump immediately attains the specified flow rate and rinses out the tubing with the carrier solution while additional inputs are made. Next two data acquisition parameters are

1. FLOW RATE CONTROL (0-9.9 mL/min)
   -Flow Rate of Pump : 2.5

2. FREQUENCY COUNT
   -Time Interval (sec) : 0.1
   -Measurement Time (sec) : 40

3. INJECTION CONTROL DURING DATA COLLECTION
   -Time for First Injection (sec) : 0
   -Repetitive Injections (Y/N) : N

4. DATA FILE
   -File Name (Maximum 8 letters) : SAMPLE
   -Index (Numerical Value 1-99) : 1

5. MEASUREMENT MODE
   -Number of Repetitive Measurements : 1
   -Plot Data (Y/N) : Y
   -Calculate Results (Y/N) : Y
   -Current Measurement Number : 0

Figure III.6. A sample of the input screen for FIA measurements.

entered: the integration time per data point and the total measurement time. The integration time (1 ms - 32.757 s) per data point is typically 0.1-1 s to provide adequate time resolution to characterize the profile shape and position and the magnitude of the peak maximum or peak area. A relatively large integration time can be used to reduce total analysis time and number of data points if only peak area is of interest. The total analysis time is the time for data collection, plotting data, and calculations, while the measurement time is the time for data collection only and is independent of integration time. Normally a relatively long measurement time is initially selected to ensure that the whole FIA peak is recorded.

The injection control variables define the timing of the sample loop filling period and the switching of the sample injection valve. The user can also choose to make a single injection or multiple injections during the specified measurement period. For the single injection mode, the filling time for the sample loop, the pre-injection delay time, and a injection delay time between the start of the measurement period and the time of injection are entered. A sub-menu not shown in Figure III.6 is used to enter values for the first two parameters. If a 10-s sampling time, a 5-s pre-injection delay time, and 3-s injection delay time are chosen, the BASIC program turns the sampling pump on for 10 s, waits 5 s to allow the pressure in the system to equalize, calls the assembly subroutine to start data collection, and injects the sample after a 3-s delay.

The file name for saving the raw data on a diskette can be any

combination of legal characters for DOS from 1 to 8 characters. For convenience, the extension of the file name is used for numbering the sample measured. After every measurement, the extension is increased by 1.

The final group of input parameters determine the number of repetitive measurements to be conducted for one sample, the plotting and calculation of results, and time portion of the data used to determine the baseline and peak parameters. These latter time parameters are chosen in sub-menus not shown in Figure III.6. If more than one measurement is selected, the identical complete sampling, injection, and measurement sequence is repeated for the specified number of repetitions. Each run is stored as a separate file.

Figure III.7 shows a simplified flow chart of the measurement sequence. After the operator initiates the run, the sampling pump with a flow rate of 5 mL/min fills the sample loop with sample. After the sampling step and specified pre-injection delay, the program converts the input variable values into the proper form and passes them from BASIC to the assembly language subroutine and data acquisition commences.

A pointer is used to check the elapsed time by accumulating the number of the toggled TCs of the time-base counter so that the injection delay and the total measurement can be timed. During the measurement, the pointer is compared to the injection delay time in terms of the number of data points. Once this time is reached, the injection valve is switched to the inject position with a output line from the CTM-05 board. After all the measurements are performed for

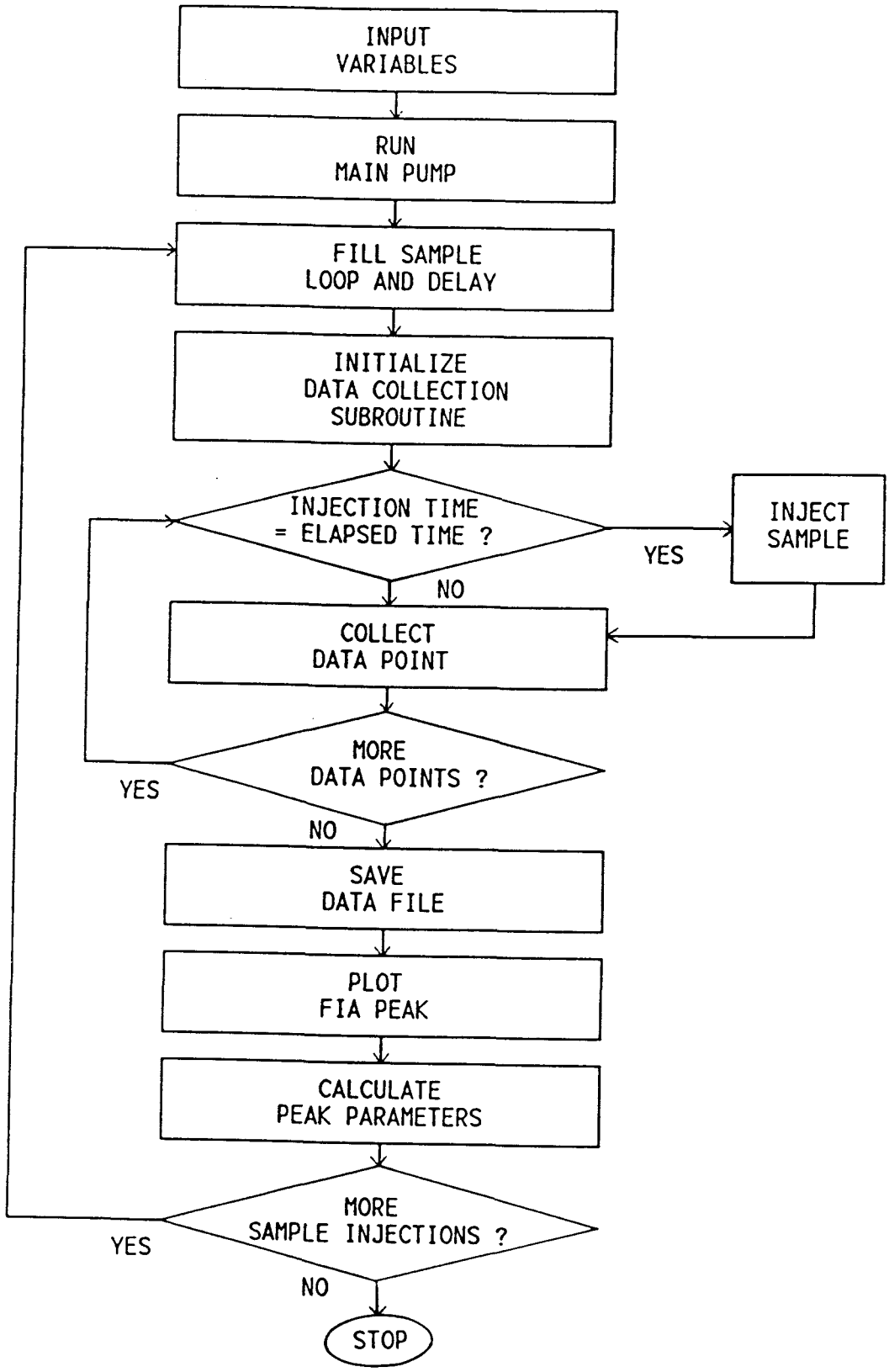

Figure III.7. Simplified flow diagram of the FIA program.

a given measurement time, the injection valve is switched to the by-pass position and the assembly subroutine returns to the main program.

After returning to BASIC program, the stored data values are transferred and stored in a BASIC file (starting address of 5500 (Hex)) with the PEEK command and saved into a floppy diskette with the specified file name. The main program then configures the screen for the graphics mode and plots the collected data on the screen. For convenience and viewing of all the data collected, the x and y scales are automatically adjusted. The plotting subprogram also allows the user to choose to plot the data over a smaller time interval than the measurement time to expand the FIA peaks if desired.

Finally the main program is programmed to calculate the fundamental readouts based on the time parameters given by the operator. Before data processing, every data point is first corrected to obtain net signal by subtracting the baseline. The followings are parameters obtained:

(a) travel time
(b) peak maximum time
(c) end time
(d) baseline value
(e) peak maximum
(f) peak area

The baseline, peak maximum and peak area are given in terms of

counts, while the time parameters are given in terms of seconds. These results can also be printed for later use. After the results are printed, the program returns to the main menu.

From the stored data file (signal vs. time), the baseline signal is first calculated. The data points for a user selected period of time (e.g., 5 s) before the FIA peak are summed and divided by the number of data points summed. This average baseline signal is subtracted from total signal for all data points to obtain the net signals over the entire measurement period. After the baseline correction step, the peak maximum and the peak time are obtained. To obtain the travel time (beginning of the peak), the data points from the injection time are searched until a data point exceeds 1% of the peak maximum. Similarly, the end time is obtained by searching the data points after the peak maximum until the first point is reached that is less than 1% of the peak maximum. The user can also select a value different from 1% to establish the beginning and end of the peak (e.g., 10%) and the time interval over which to examine the data file for peak information. The baseline peak width is taken as the difference between the peak travel time and end time. The data points within the baseline peak width are summed to calculate the peak area.

Multiple Injections

If the option for a single injection during the measurement period is selected, repetitive runs for one sample can be performed by selecting the desired number of repetitive measurements as

discussed previously. Figure III.8a shows the operational sequence when a single injection is involved. For each run, the sampling time and pre-injection delay time are timed with the time-of-day clock of the PC, while the timing for the sample injection delay is performed with the toggled TC of the time-base counter in the STC during the data collection sequence. From the time of sample injection, the sample loop valve remains in the inject position until the measurement period is complete. Since the input variables except the index of the file name are preserved until the operator edits the variables or quits the program, the entire sequence for the analysis can be repeated automatically for multiple runs. The data for each run are saved as a separate file.

Multiple injections during a given measurement period can also be performed to achieve a higher sample throughput rate. To operate in this mode, time parameters such as the time interval between injections, the time for the sample injection period, the delay before injection, and the sample loop filling period must be provided properly. These time parameters are requested only if repetitive injections are desired. The timing sequence is summarized in Figure III.8b. The sample loop filling time (sampling period 1) and pre-injection delay (pre-inj. delay 1) are performed by the system clock of the PC only once before the first injection. After each subsequent sample injection, the injection period, the delay before the sample loop filling (delay 1), and the sample loop filling period (sampling period 2) occur before the next injection while data are collected. Thus, the time interval between injections, which must be greater than the time for the injection period and sample loop

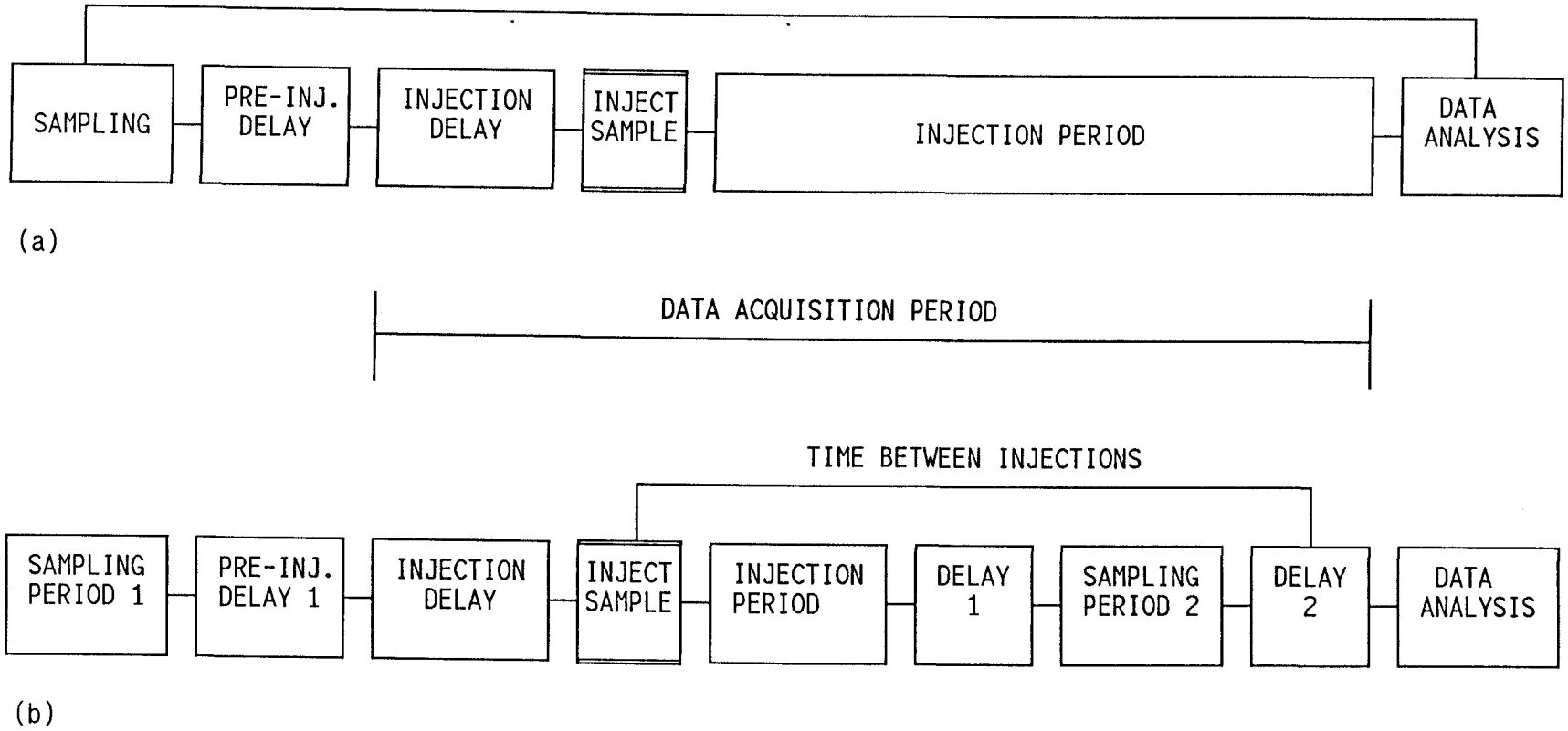

Figure III.8. Time sequences for FIA. (a) single injection; (b) multiple injections. For (b), the program calculates delay 2 by subtracting time for the injection period, delay 1 , and sampling period 2 from the time between injections.

filling period, can be as small as the width of the peak to avoid peak overlap. Figure III.9 shows a typical output for repetitive injections of 1 μg/mL quinine sulfate (QS). Note that 10 FIA peaks are recorded in a total measurement period of 317 s.

The current version of the program calculates the height, area, and time parameters for the first peak. However, the values of the peak parameters for other peaks can be found with option 4 by specifying the time segment which encompasses the desired peak.

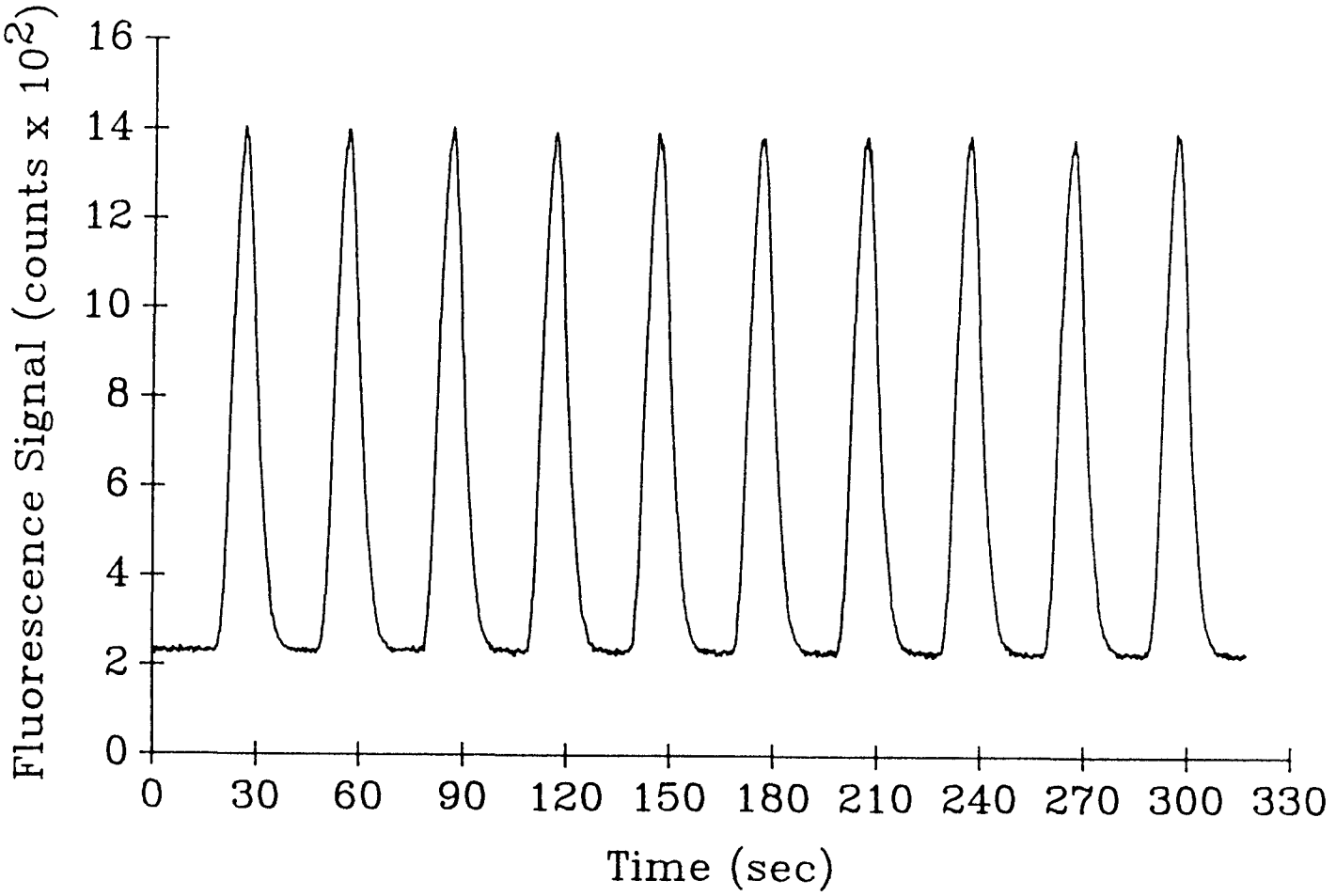

Figure III.9. Ten injections of 1 µg/mL QS over a 317-s measurement period.

REFERENCES

1. R. L. Wilson, Ph.D. thesis, Oregon State University, 1976.

2. M. A. Ryan, Ph.D. thesis, Oregon State University, 1982.

3. M. A. Ryan and J. D. Ingle, Jr., Talanta 1981, **28**, 539.

4. C. B. Elliott, Ph.D. thesis, Oregon State University, 1982.

CHAPTER IV

FLUOROMETRIC KINETIC METHOD FOR THE DETERMINATION OF TOTAL ASCORBIC ACID WITH o-PHENYLENEDIAMINE

H. K. Chung and J. D. Ingle, Jr.*

Department of Chemistry

Oregon State University

Gilbert Hall 153

Corvallis, Oregon 97331-4003

ABSTRACT

A new fluorometric reaction-rate method for the determination of ℓ-ascorbic acid (AA) in aqueous solution is presented. The technique is based on the rapid oxidation of AA by mercuric chloride to dehydro-ℓ-ascorbic acid which then reacts with o-phenylenediamine (OPDA) to form a fluorescent quinoxaline. The formation of the product is monitored fluorometrically with a data acquisition system based on a microcomputer (an IBM PC compatible), a V/F converter, and a timer/counter board. The initial rate is estimated with a fixed-time computational method. With a 20-s measurement time (after a 5-s delay from initiation of the reaction), the detection limit for AA is 0.02 μg/mL with a linear dynamic range extending to 10 μg/mL. For a 10-s measurement time, the detection limit is 0.06 μg/mL and linearity is observed up to 50 μg/mL. The new procedure is applied to the determination of the AA in vitamin pills and juice. The relative standard deviation (RSD) is 1.9% or better.

INTRODUCTION

Methods for determination of ascorbic acid have been reviewed [1-3]. In aqueous solution AA can be easily oxidized to dehydro-ℓ-ascorbic acid by mild oxidants. Determinations of AA in aqueous solution by oxidative titration methods or colorimetric methods based on redox indicators have been widely developed. Common organic oxidants include 2,6-dichloroindophenol [4], N-bromosuccinimide [5,6], and chloramine-T [7]. The drawbacks of these methods include lack of selectivity and instability of the reagents. Inorganic oxidants such as iodine or iodate [8-10], thallium(III) [11] and hexacyanoferrate(III) [12], which are thought to be more stable, have been suggested, but selectivity is still a problem. The determination of AA based on its oxidation in the presence of other reducing species has been found to be less selective compared to chromatographic, spectrometric and enzymatic methods [2].

Methods based on derivatization reactions have been developed to improve the selectivity and detectability for total ascorbic acid (AA and dehydro-ℓ-ascorbic acid) in pharmaceutical and food samples [13-15]. Usually AA is first converted with a suitable oxidizing agent to dehydro-ℓ-ascorbic acid which then is reacted with a selective reagent such as dinitrophenylhydrazine to produce an absorbing product [13] or OPDA to form a fluorescent product [15]. Normally equilibrium-based procedures are used. The stability of derivatization product and the preparation of a suitable blank solution have been the limitations in these approaches. Non-reacting species or instrumental factors can contribute to the total absolute

spectrometric signal observed. Equilibrium methods can be time consuming if separation steps are required to eliminate interferences or the reaction is slow to reach equilibrium.

Several fluorometric techniques for vitamin C have been developed and can offer greater selectivity. Deutsch and Weeks reported a microfluorometric assay for vitamin C [15], which was accepted as an official AOAC method. In their method, AA is oxidized to dehydroascorbic acid with activated charcoal (Norit) and then reacted with OPDA to form a fluorescent condensation product [3-(1,2-dihydroxyethyl)furo[3,4-b]-quinoxaline-1-one]. The reaction is shown in Figure IV.1. Fluorescence measurements are made after equilibrium is reached. Although this method shows good selectivity for the samples containing large amounts of reducing interferents, sugars, or highly colored species, instability of the reagent during the reaction time (35 min to obtain equilibrium) is a major drawback, which may cause poor reproducibility [16]. This method is somewhat tedious and time-consuming because the sample is percolated through a column containing Norit or mixed with Norit and filtered.

Several modifications to the OPDA method have been reported. Roy and co-workers developed an automated continuous flow fluorometric method using an AutoAnalyzer [16]. A solution of N-bromosuccinimide was used as a oxidant instead of the Norit. Egberg and co-workers later developed a semiautomated fluorometric method adapted by the AOAC [7]. This method involves a manual Norit oxidation and extraction step prior to introduction of the sample into an Autoanalyzer to overcome interference problems due to naturally fluorescent compounds or oxidation of sample components to

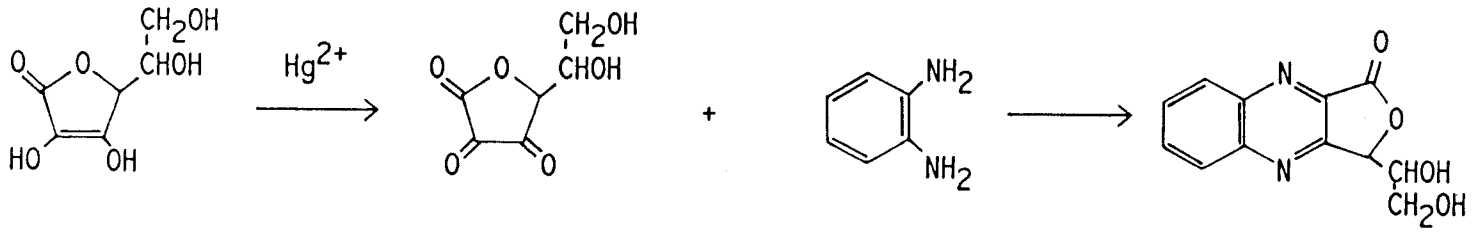

Figure IV.1. Formation of the condensation product.

produce fluorescent species [17].

Only a few reaction-rate methods for determining ascorbic acid have been reported and all involve spectrophotometric monitoring. Karayannis developed a kinetic method based on the reaction between AA and 2,6-dichloroindophenol which has been widely used for equilibrium-based determinations [17]. This initial rate method was shown to be fast, sensitive, and accurate. Kriss and co-workers presented a kinetic method based on the activating effect of a AA on the vanadium(V)-catalyzed oxidation of iodide by chlorate [18]. However, both methods are susceptible to interference from reducing species and total ascorbic acid can not be determined.

In previous work, the kinetics of formation of the quinoxaline from dehyroascorbic acid and OPDA has not been studied because equilibrium methods or continuous flow analyzers have been employed. To increase speed and selectivity for determination of vitamin C, the OPDA fluorometric method was adapted to a kinetic procedure which does not require a prior Norit oxidation step or a continuous flow analyzer (i.e., a conventional spectrofluorometer and fluorescence sample cell are used). $HgCl_2$ is shown to oxidize AA completely and rapidly. This paper also describes the use of a microcomputer (PC compatible) system to obtain the reaction rate information.

EXPERIMENTAL

Instrumentation

Spectrophotometric measurements were made with a HP model 8451A diode array spectrophotometer. Fluorescence measurements were made with a fluorescence spectrometer equipped with a temperature controlled sample cell in which a magnetic stirring bar was placed to provide efficient mixing of the reagents and the sample. The spectro-fluorometer is identical to that previously described [20-21] except that the data acquisition was carried out with a PC compatible microcomputer. The excitation beam is split by a beam splitter to obtain a reference signal. The fluorescence photomultiplier signal (compensated for source fluctuations by ratioing to the reference signal) is input to a voltage to frequency (V/F) converter. The output pulse train from the V/F converter is directed to the input source of a CTM-05 system timer-counter expansion board (MetraByte) which is configured as frequency counter. An automatic syringe injector which is controlled by a logic signal from an I/O line from the expansion board is used to dispense the OPDA reagent solution to initiate the condensation reaction.

Software was developed to control the timer-counter board and the injector, to acquire and store the reaction-rate monitor signal as a function of time, and to calculate the reaction rate. The rate is calculated based on the fixed-time method in which the difference in count values acquired over two equal time increments which are sequential is calculated. This difference is proportional to the

initial reaction rate.

The program was written in QuickBASIC (Microsoft version 4.5) with an assembly subroutine for control of the injector and the data collection. This program is menu driven which allows convenient optimization of the parameter values and offers versatility in the modes of operation. The main menu displays four main options: inputting or editing of variable values for the reaction-rate runs, initiating a reaction-rate run with data acquisition, calculating the reaction rate, and rinsing the liquid dispenser. When the program is first loaded, the operator is responsible for entering values for the pre-injection delay time, the post-injection delay time, the measurement time, the rate computational time, and the integration time interval per data point. The corrected values of these input variables are passed from BASIC to the assembly subroutine.

Once the data collection sequence is selected and started from the main menu, the frequency signal from V/F converter is converted to accumulated counts via two concatenated counters in the expansion board which provides up to 32-bits of resolution. After integration for the selected integration time (typically 0.1-1 s), the counts accumulated are stored as a data point at a memory location specified by the BASIC program. Sequential data points are taken and stored until the specified measurement period is complete. Injection of the last reagent occurs after the selected pre-injection delay time.

After the measurement sequence is completed, BASIC peeks the values from the memory locations, stores the data file on a diskette for hard copy or later data manipulation with commercial software such as Lotus 123, displays the reaction curve on the monitor, and

calculates the reaction rate based on fixed-time method. The rate is calculated from the data taken from the end of the post-injection delay time to this time plus the selected rate computation period. After the data are taken, the rate over different time periods can be calculated by changing the post-injection time and computational time. The automatic syringe is rinsed under control of software if desired.

Solution Preparation

All chemicals used were reagent grade. Double deionized water from a Millipore Milli-Q system was used for solution preparation. Acetate buffer solutions of 0.25 M sodium acetate in the pH range of 3.7 to 5.4 were prepared by dissolving 20.51 g of sodium acetate in water and adjusting to the appropriate pH by adding concentrated acetic acid. Phthalate buffers in the pH range of 3.0 to 3.6 were prepared from potassium hydrogen phthalate and HCl, and phosphate buffers in the pH range of 5.4 to 7.1 were prepared from sodium phosphate and phosphoric acid. Metaphosphoric acid-acetic acid extracting solution was prepared by dissolving 15 g of glacial metaphosphoric acid in 40 mL of glacial acetic acid and 200 mL of water and diluting to 500 mL with water. A stock solution of 1×10^{-2} M $HgCl_2$ was prepared in water. Stock solutions of 1000 µg/mL AA standard and 0.1 M OPDA were prepared in water daily. Solutions with lower concentrations of AA were prepared by dilution of these stock solutions in water and made to contain 1% (v/v) of the extracting solution. Buffer, OPDA, AA, and extracting reagent

solutions were stored in a refrigerator at ≈ 6^{o} C when not in use.

The vitamin C pills (Nature Made Nutritional Products), multivitamin (Nature Made Nutritional Products), and grape juice samples (Ocean Spray) were obtained at a local store. The vitamin tablets tested were ground in a mortar, weighed and diluted to 100 mL with the extracting solution. These solutions were filtered with Whatman No. 2 filter paper and 1 mL of the filtrate was diluted to 100 mL with water before measurement. For the juice samples, 1 mL of sample and 1 mL of the extracting solution were diluted to 100 mL with water.

Procedures

Reaction profiles of fluorescence signal as a function of time were acquired with a PMT bias voltage of 800 V, a feedback resistance (current-to-voltage converter) of 1 MΩ, and a time constant of 0.1 s. In all experiments, 1 mL of buffer solution, 0.75 mL of $HgCl_2$ solution, and 0.75 mL of AA standard or sample were added to the sample cell with Eppendorf automatic pipets. To initiate the condensation reaction, 0.5 mL of the final reagent, OPDA, was injected under the computer control. Between each run the sample cell was rinsed once with 10% (v/v) HNO_3, three times with doubly deionized water, and twice with buffer. Vacuum aspiration was used to remove reaction mixture and rinsing solutions. Reagent and analyte solution bottles were stored and equilibrated in the temperature controlled water bath. All measurements were performed at 27^{o} C.

All rates reported are the means from 3 repetitive runs and are blank corrected. The blank rate is obtained with 0.75 mL of water substituted for the AA solution and was typically a small negative value. For most studies with the fixed-time reaction-rate computation method, a data point integration time of 1 s, a 20-s rate computational time, and a 5-s post-injection delay time were used.

RESULTS AND DISCUSSION

Excitation and Emission Spectra

The condensation product has a strong absorption band centered at about 348 nm, while AA and the reagents show no appreciable absorbance above 310 nm. Figure IV.2 shows uncorrected fluorescence excitation and emission spectra. The excitation spectrum shows two strong excitation bands at 313 and 366 nm; the most intense band at 366 nm corresponds to the strong Hg emission line from the Xe-Hg arc source. The condensation exhibits a bright yellow fluorescence with the emission band centered at a wavelength of 435 nm. For further studies, the excitation monochromator was set at 366 nm with 2-mm slits (17-nm spectral bandpass) and the emission monochromator was adjusted to 435 nm with 2.5-mm slits (21-nm spectral bandpass).

Photodecomposition Studies

Figure IV.3 shows the fluorescence intensity as a function of time from the point of initiating the condensation reaction with the optimized reagent concentrations. When the reaction mixture is continually exposed to the Xe-Hg source radiation, a steady state maximum is not observed (solid curve). When the reaction mixture is exposed only momentarily to the intense radiation during the measurement time, equilibrium is reached after about 6 min. These data suggest that the product photodecomposes when exposed to the intense excitation radiation. It was also confirmed with time-based

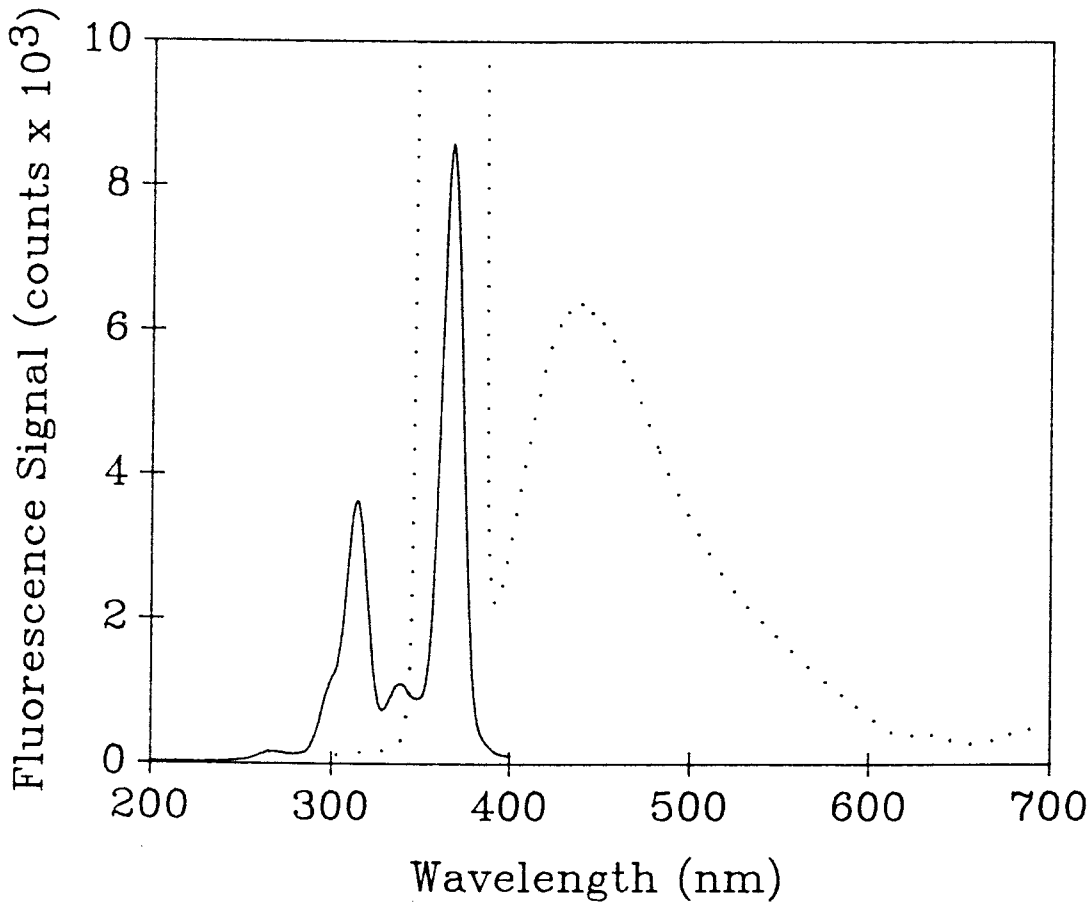

Figure IV.2. Uncorrected fluorescence spectra of the condensation product between AA and OPDA: (a) Excitation spectrum (solid line), emission wavelength, 435 nm; (b) Emission spectrum (dotted line), excitation wavelength, 366 nm. AA conc., 10 µg/mL; OPDA conc., 0.01 M; Hg(II) conc., 1×10^{-3} M; reaction time out of cell, 6 min.

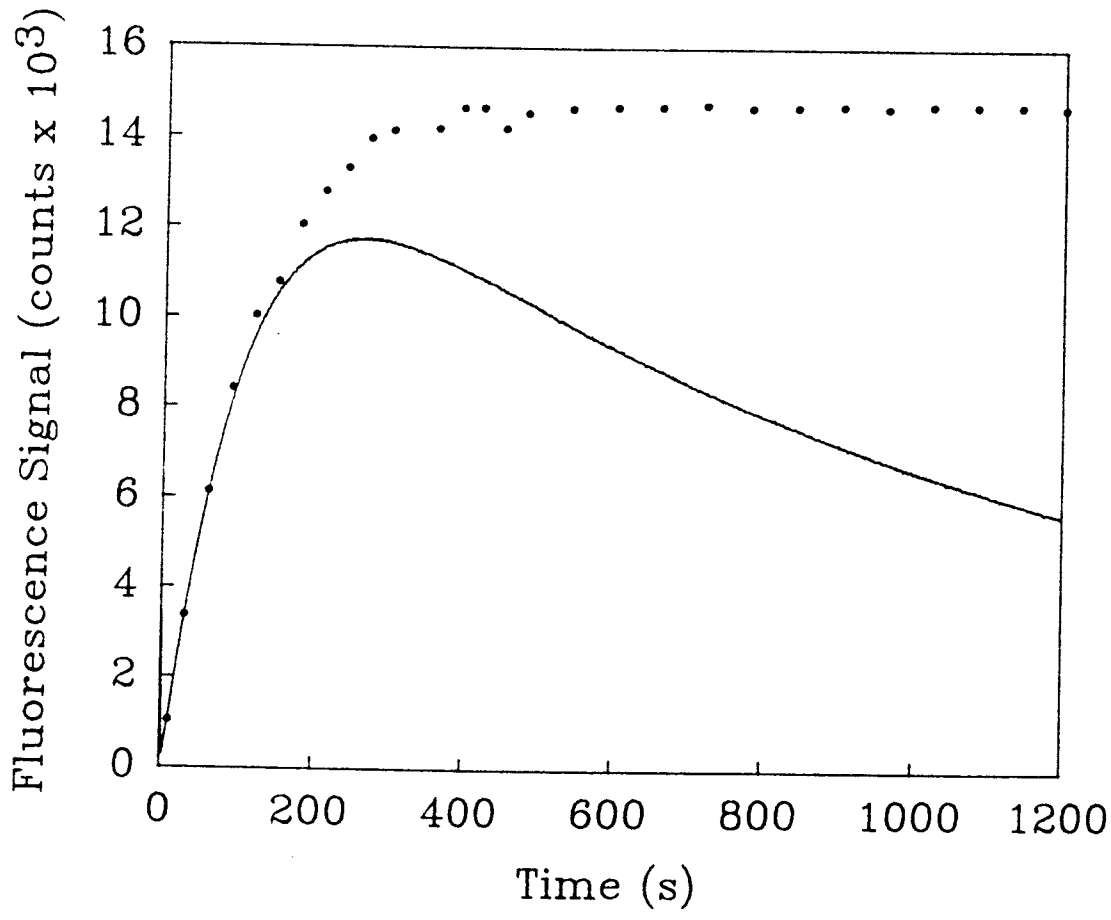

Figure IV.3. Reaction curves for the condensation reaction: Solid line, continuous exposure; filled circle, intermittent exposure; pH 4.2; AA conc., 10 µg/mL; Hg(II) conc., 1 x 10^{-3} M, OPDA conc., 0.01 M.

absorption spectra that the equilibrium absorbance signal of the product monitored at 348 nm is stable for at least 30 min.

Clearly the photodecomposition of the product would affect accuracy and precision of an equilibrium-based method unless the sample was exposed to excitation radiation only after equilibrium is reached. With a kinetics-based method, measurement can be performed within the first few percent of the of reaction before photodecomposition of product becomes significant. In addition, this suggests that kinetics-based method relying on this reaction is superior in terms of speed compared to an equilibrium-based method.

pH Optimization

The effect of pH on the reaction rate was studied in the pH range from 3.0 to 7.1. Initial studies showed that a pH lower than 3.7 (phthalate buffers) is not suitable for a reaction-rate method because the reaction rate is low, the induction period is longer than 3 min, and equilibrium is reached in 15 min or longer. With phosphate buffers in the pH range from 5.4 to 7.1, the reaction rate was greater, but the induction period was longer than 30 s.

With acetate buffers in the pH range from 3.7 to 5.4, the rate was greatest. No induction period was observed such that it is possible to acquire data soon after injecting the OPDA solution for calculation of the reaction rate. Furthermore, AA is most stable in this pH range [22]. As shown in Figure IV.4, the reaction rate at pH 5.4 was 55% of that at pH 4.2. A buffer of pH of 4.2 was selected for further experiments because the reaction rate is highest such

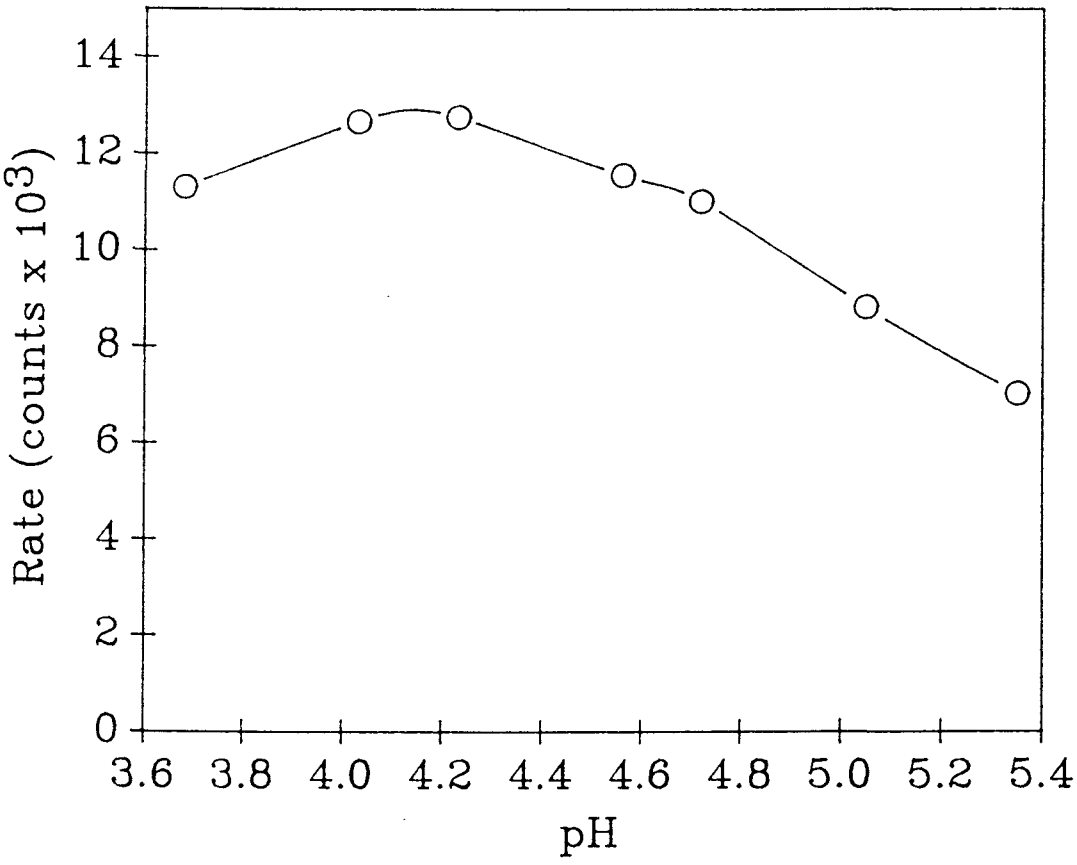

Figure IV.4. Dependence of the rate on pH. AA conc., 10 µg/mL; Hg(II) conc., 1 x 10^{-3} M, OPDA conc., 0.01 M. The RSD was typically 1.4%. Each point is the mean of three measurements

that a short measurement time can be used for rapid analysis, the dependence of the rate on pH is minimal, the buffering capacity of the acetate buffer is high, and the precision is good.

To study the influence of ionic strength on the initial rate, 0.1, 0.25, and 1 M sodium acetate buffer (pH 4.7) solutions were made and the reaction curves were obtained with 1×10^{-3} M $HgCl_2$, 0.01 M OPDA and 10 μg/mL AA. The initial rate of the condensation reaction increases with increasing sodium acetate concentration. The reaction rate with the 1 M buffer was greater by a factor of 1.5 and 2.1 than the rate obtained with 0.25 and 0.1 M buffers, respectively. However, photodecomposition of the fluorescence product becomes significant earlier in the reaction as the buffer concentration increases. For further studies, a 0.25 M sodium acetate buffer was chosen because it provides a large initial rate and pseudo-first order kinetics over measurement times up to 20 s when the analyte concentration is 10 μg/mL or less.

Effect of $HgCl_2$ Concentration

Several oxidizing reagents to convert AA to dehydroascorbic acid, $K_3Fe(CN)_6$, N-bromosuccinimide, and $HgCl_2$, were tested and compared [24]. All these oxidizing reagents oxidized AA effectively. However, when $K_3Fe(CN)_6$ and N-bromosuccinimide are mixed with OPDA in the absence of AA, a new absorption band with a maximum at ca. 450 nm appears which may be due to the oxidation of OPDA. Hence the OPDA and AA compete for a fixed amount of oxidizing agent and a reaction product is produced that absorbs in the

wavelength region that the quinoxaline fluoresces. $HgCl_2$ oxidizes AA completely but no reaction product is observed when $HgCl_2$ is mixed with only OPDA. Moreover, $HgCl_2$ does not absorb at wavelengths longer than 300 nm. For these reasons $HgCl_2$ was selected as the oxidizing agent for further studies of the determination of total AA with the OPDA condensation reaction.

The effect of the time that the AA and $HgCl_2$ are allowed to mix before injection of OPDA with 1×10^{-3} M Hg(II), 0.1 M OPDA, and 10 or 100 μg/mL AA was studied. No difference in reaction rate was observed for oxidation times of 5, 30, and 90 s which indicates that the oxidation is quite rapid. The RSD for all cases was less than 2%. The oxidation of AA by $HgCl_2$ is reported [24] to be initially rapid due to dissociated $HgCl_2$ and then slower with kinetics that are first order in undissociated $HgCl_2$. Since dehydro-ℓ-ascorbic acid could be further oxidized to 2,2-diketo-ℓ-gulonic acid in solution media and react with OPDA to form a fluorescence product [16], a shorter oxidation time is more desirable for fast analysis with good precision. Thus the AA and Hg(II) solution in the sample were normally allowed to mix in the sample cell no longer than 5 s before injection of OPDA.

The effect of the Hg(II) concentration on the rate of formation of the condensation product was studied in the range of 1×10^{-6} to 5×10^{-2} M with 10 μg/mL AA (1.41×10^{-5} M). As shown in Figure IV.5, the reaction rate becomes relatively independent of the $HgCl_2$ concentration above 1×10^{-4} M which is well above the amount of Hg(II) predicted by the stoichiometry of the oxidation. Below 1×10^{-4} M $HgCl_2$, the oxidation of AA may not be quantitative due to

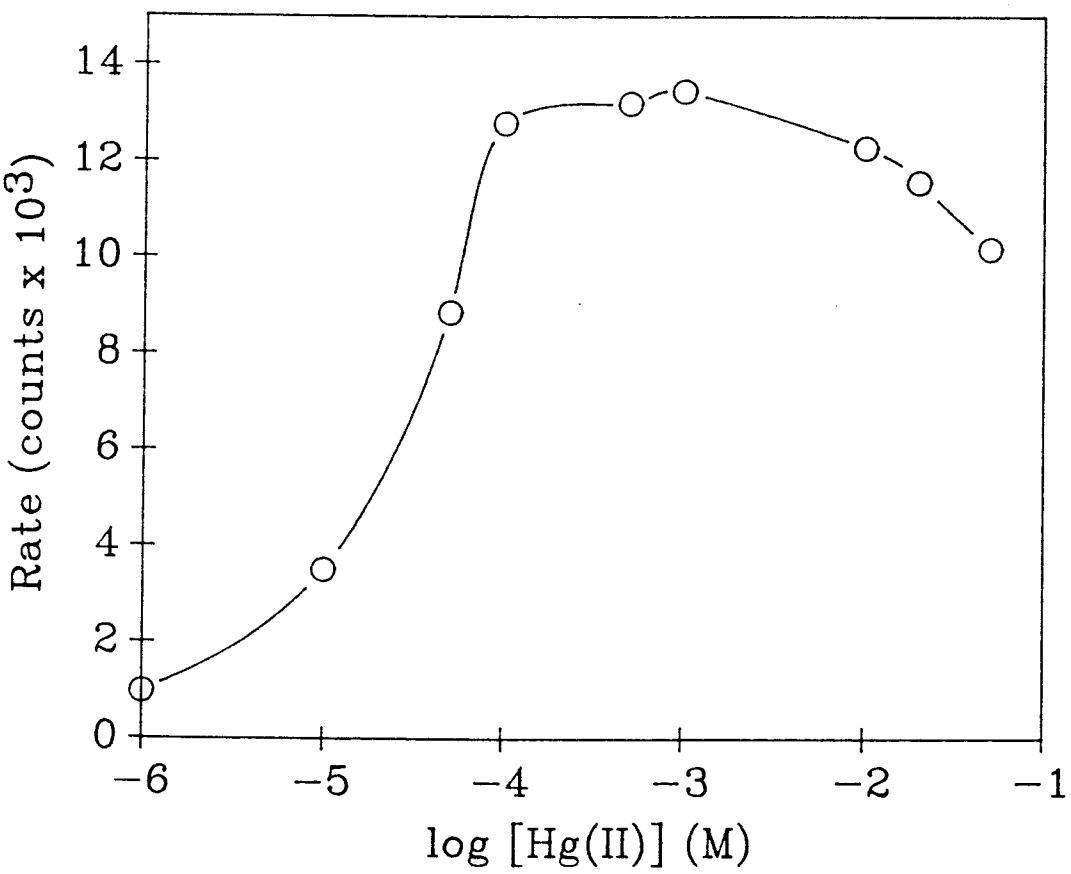

Figure IV.5. Dependence of the rate on $HgCl_2$ concentration. pH 4.2; AA conc., 10 µg/mL, OPDA conc., 0.1 M. The RSD was typically 1.3%. Each point is the mean of three measurements.

incomplete dissociation of $HgCl_2$. Above 1×10^{-3} M $HgCl_2$, the reaction rate decreases slightly, and a white precipitate eventually forms with high concentrations of AA (e.g., 100 µg/mL). Spiking of equilibrated reaction mixtures with more $HgCl_2$ suggest that high concentrations of $HgCl_2$ quench the fluorescent of the product. A concentration of 1×10^{-3} M was chosen for further studies because it provides a rapid and complete oxidation of AA and the maximum rate and the dependence of the rate on Hg(II) concentration is slight.

Effect of o-Phenylenediamine Concentration

Aqueous solutions of OPDA are known to be unstable under the light [15-17]. The effect of the Hg-Xe excitation radiation on OPDA and the condensation product was studied spectrophotometrically. A blank reaction mixture (no AA) was freshly prepared, stored in a volumetric flask for 3 hr, and then the absorption spectrum was taken. No absorption above 350 nm was observed. This reaction mixture was then exposed to the excitation radiation in the spectrofluorometer for 5 min. A absorption band with a maximum absorbance of 0.025 at 450 nm was observed as shown in Figure IV.6, which indicates photodecomposition of OPDA.

A similar study of the decomposition of the condensation reaction product was conducted with a mixture of 10 µg/mL of AA and the reagent mixture for 5 min. When the reaction proceeded for 5 min outside of the spectrofluorometer, no absorption band above 400 nm was observed. When the same reaction mixture was placed in the sample cell for 5 min and exposed continually to the Xe-Hg excitation

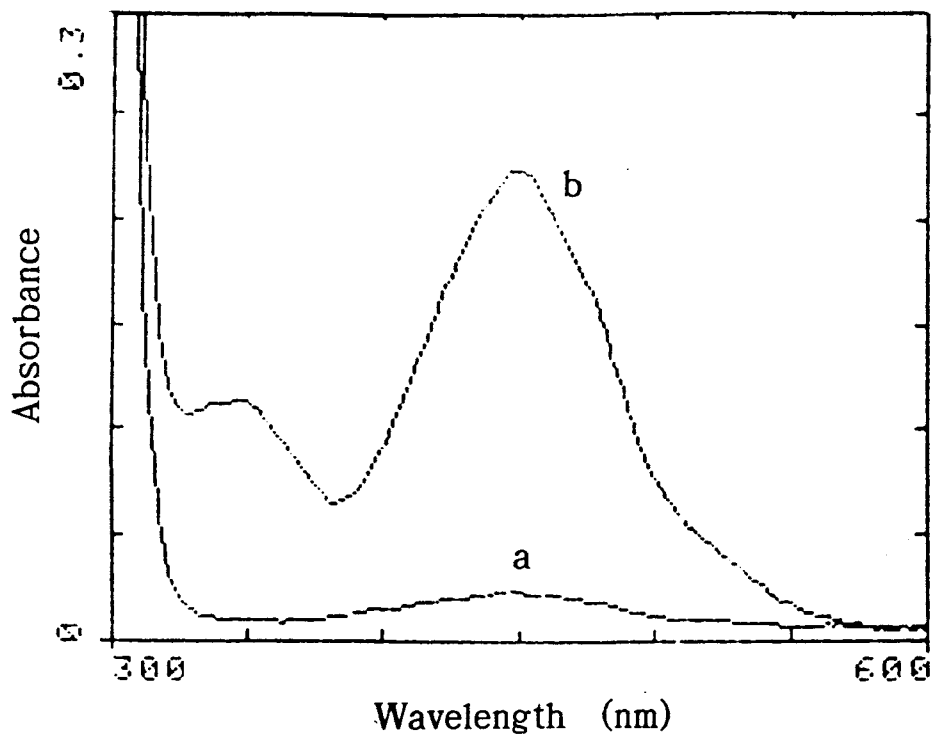

Figure IV.6. Absorption spectra illustrating the decomposition of OPDA and the condensation product by the Xe-Hg excitation radiation. The solutions in the cuvette cell were exposed to the radiation continuously for 5 min; (a) blank; Hg(II) conc., 1×10^{-3} M; OPDA conc., 0.01 M; (b) condensation product; same as (a) except 10 µg/mL of AA added.

radiation, an absorption band with a absorbance of 0.223 at 450 nm was found as shown in Figure IV.6. This photodecomposition product fluoresces with a maximum at 570 nm when excited at 366 nm. The data indicate that photodecompostion of the condensation product is more serious than photodecomposition of OPDA.

Reaction profiles over the first 3 min with various concentrations of OPDA are shown in Figure IV.7. When the OPDA is injected into the sample cell, the fluorescence signal increases momentarily due to turbulent flow. For all cases studied, a stable equilibrium signal was not obtained. As the OPDA concentration increases, the rate of photodecomposition increases. The shape of the reaction curves may also be affected by inner-filter effects due to absorption of the emission radiation by the photodecomposition product. The highest fluorescence signal is observed with a OPDA concentration of 0.05 M. With 0.1 M OPDA, the initial rate due to the formation reaction is greater than that with 0.05 M OPDA, but the photodecomposition reaction becomes significant earlier in the reaction. The maximum transient fluorescence signal is determined by the relative rates of formation and photodecomposition of product.

As shown in Figure IV.8, the reaction rate with a 20-s measurement time increases dramatically up to an OPDA concentration of about 0.05 M and then becomes relatively independent of the OPDA concentration. At 0.1 M OPDA the reaction rate is greatest. For concentrations of OPDA lower than 1×10^{-4} M, no measurable fluorescence signal was observed even though the amount of OPDA was stoichiometrically in excess relative to AA.

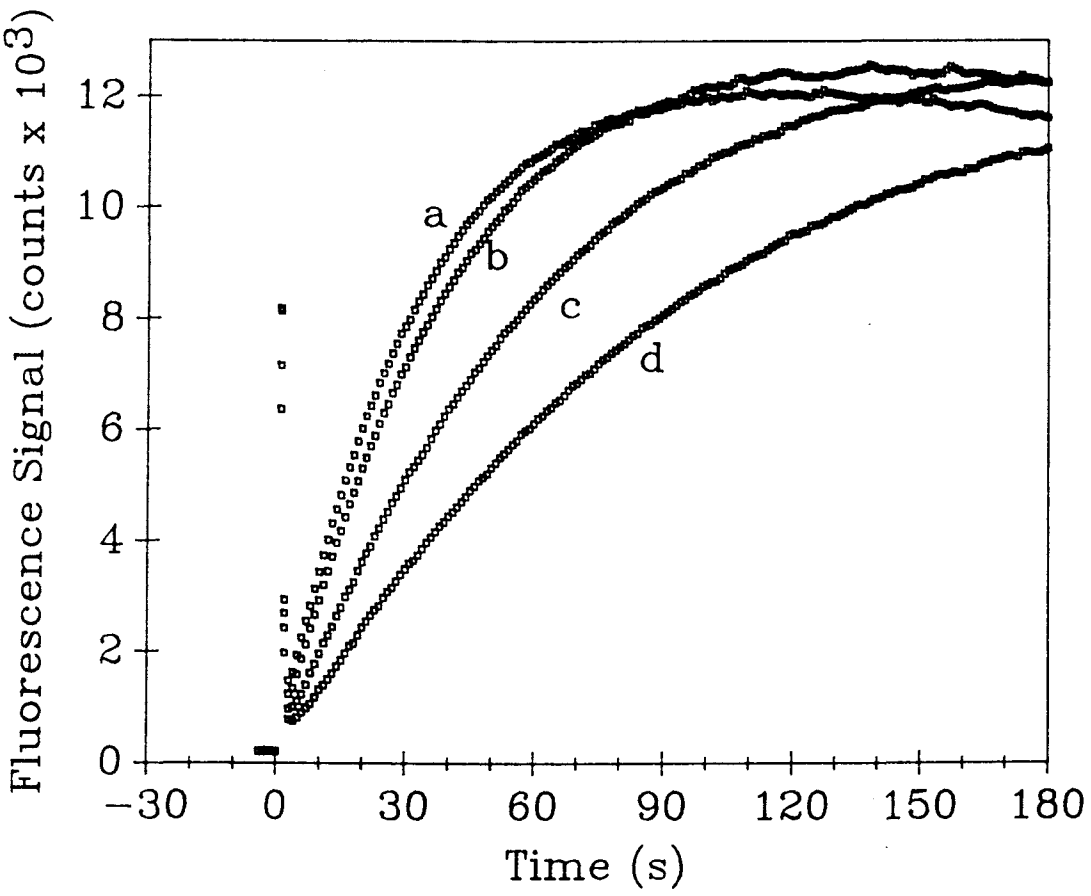

Figure IV.7. Dependence of the reaction curve on o-phenylenediamine concentration. (a) 0.1 M; (b) 0.05 M; (c) 0.02 M; (d) 0.01 M; pH 4.2; AA conc., 10 µg/mL, Hg(II) conc., 1 x 10^{-3} M.

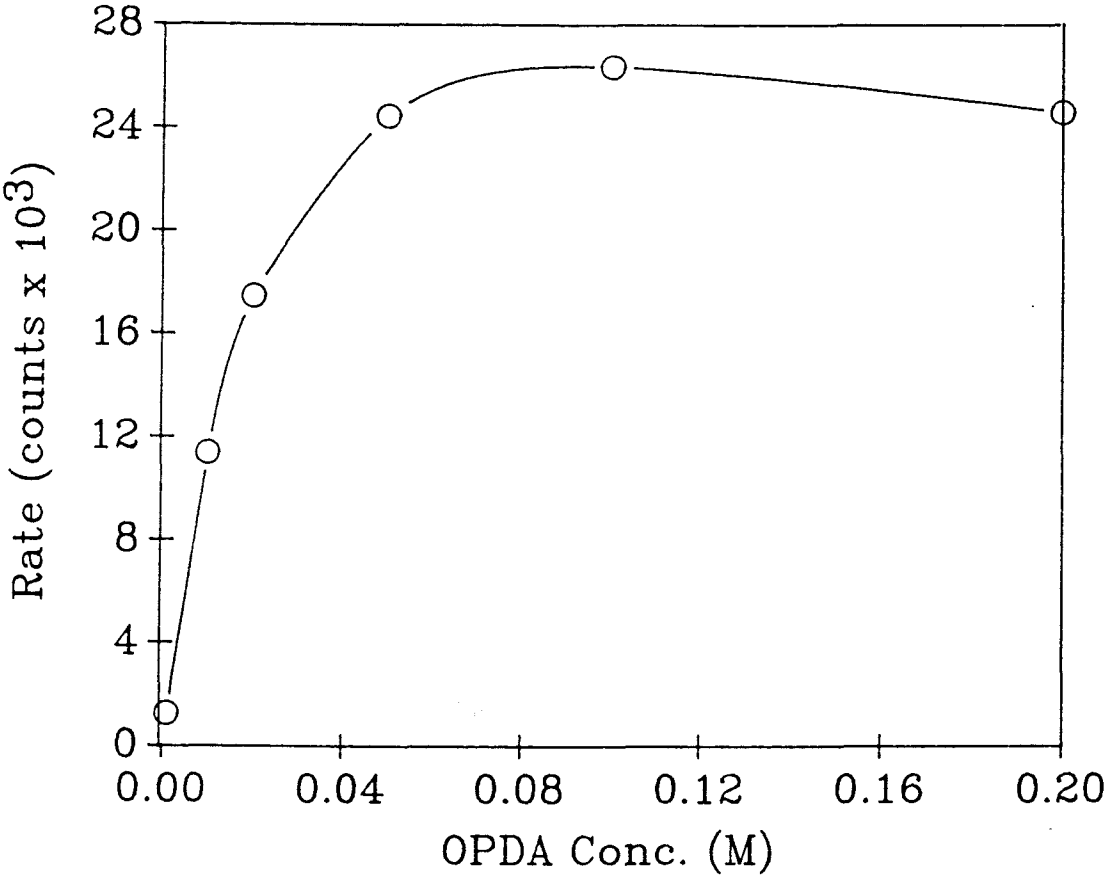

Figure IV.8. Dependence of the rate on o-phenylenediamine concentration. pH 4.2; AA conc., 10 µg/mL; Hg(II) conc., 1×10^{-3} M. The RSD was typically 0.86%. Each point is the mean of three measurements.

Calibration Data

Reaction profiles of fluorescence signal as a function of time were acquired and stored for a wide range of AA concentrations with 1×10^{-3} M Hg(II), 0.25 M pH 4.2 acetate buffer, and OPDA concentrations of 0.1 and 0.01 M. Figures IV.9 and 10 show calibration curves with 10- and 20-s rate computational times, respectively, in which the linear portions are extrapolated. The calibration curves indicate that the upper end of the range of linearity is extended with a smaller OPDA concentration or a shorter computational time. Because the absolute rate of photodecomposition of the product is proportional to the product concentration, the effect of photodecomposition becomes more significant at longer reaction times or under conditions yielding greater rates of formation.

The least squares data for calibration curves with rate computational times of 10 and 20 s and OPDA concentrations of 0.01 and 0.1 M are presented in Table IV.I. Because the rate in counts calculated by the fixed-time method is proportional to the square of measurement time, the slopes and blank standard deviation (SD) values were normalized to signal units of mV/s to allow comparision. With 0.01 M OPDA, the normalized calibration curve slope decreases less than 1.7% when the computational time increases from 10 to 20 s. This indicates that the pseudo-zero order kinetics prevail over computational times of 20 s or less with 0.01 M OPDA. With 0.1 M OPDA, the normalized slope with a 20-s computational time is 13% less than the slope with a 10-s measurement time. This indicates that

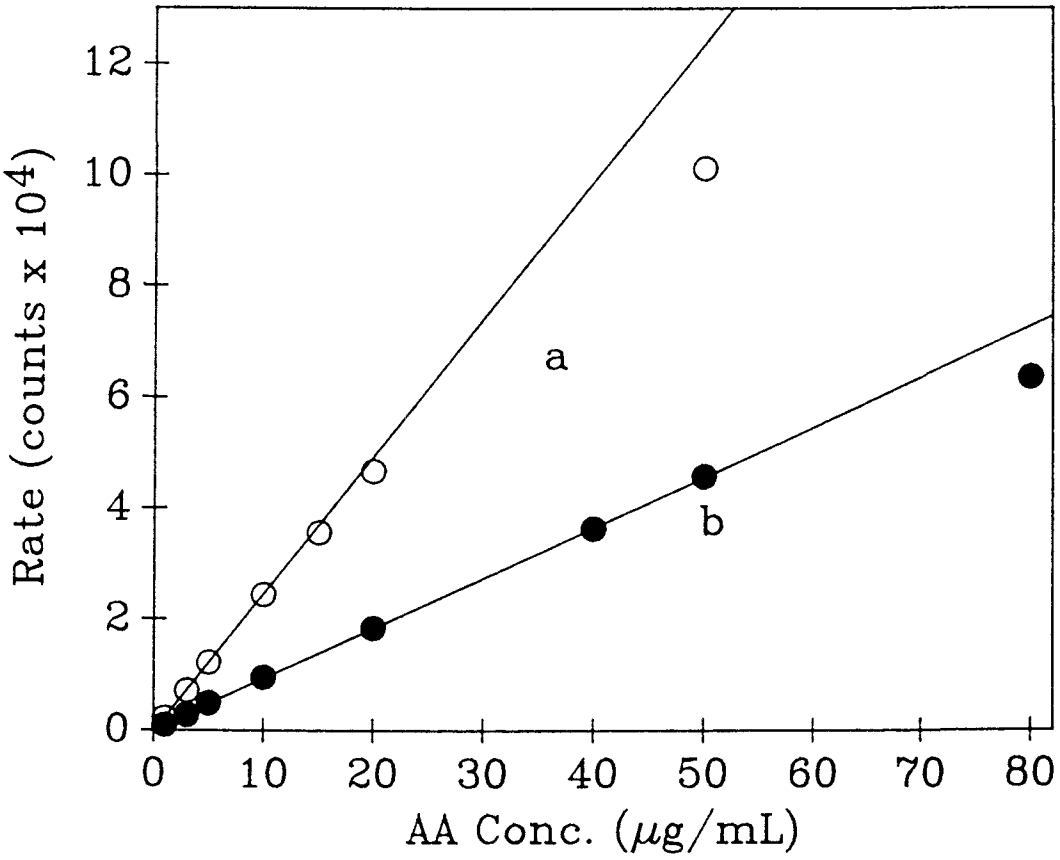

Figure IV.9. Calibration curves for the determination of AA with a 20-s computational time: (a) 0.1 M OPDA; (b) 0.01 M OPDA. pH 4.2; Hg(II) conc., 1×10^{-3} M. For (a), the data for 1-10 µg/mL AA were used for the linear least squares fit, and the rate for 20 µg/mL AA is 6.0% below the rate obtained by extrapolation of the linear portion of the curve. For (b), the data for 1-50 µg/mL AA were used for the linear fit, and the rate observed for 80 µg/mL is 12.7% below that obtained by extrapolation.

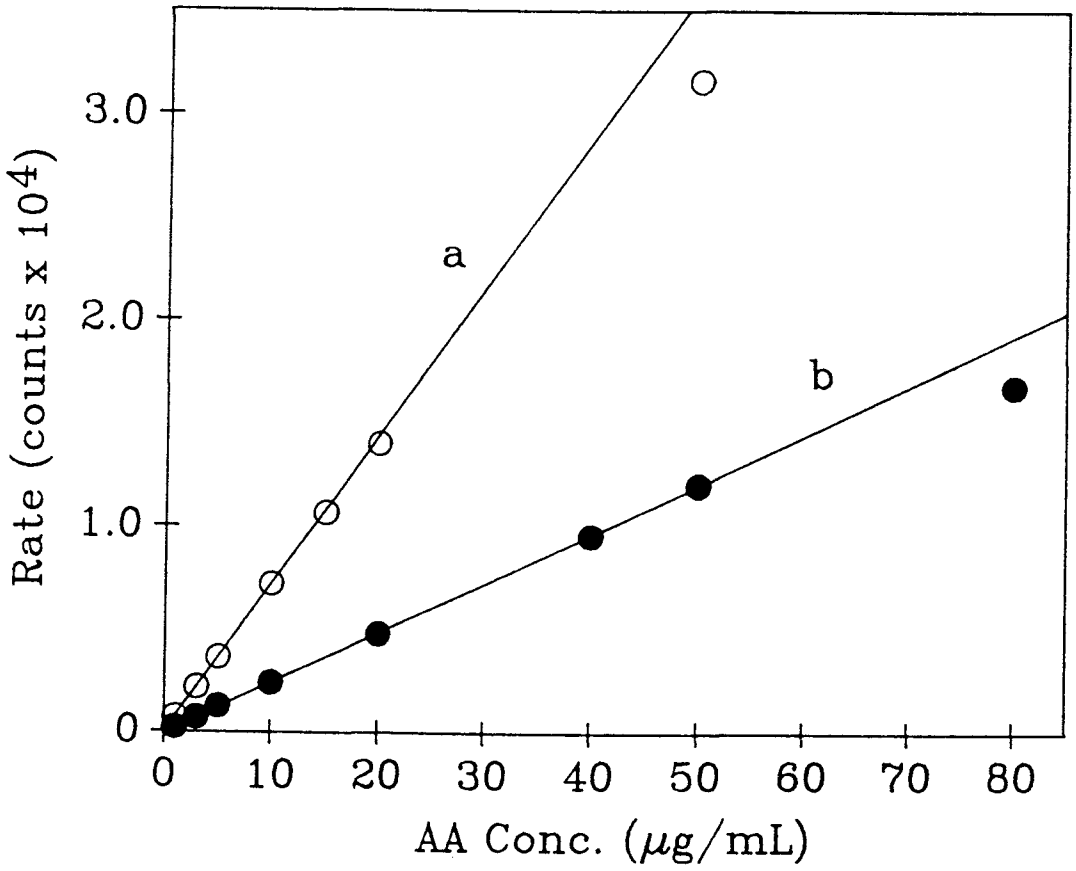

Figure IV.10. Calibration curves for the determination of AA with a 10-s computational time. (a) 0.1 M OPDA; (b) 0.01 M OPDA. pH 4.2; Hg(II) conc., 1×10^{-3} M. For (a), the data for 1-10 µg/mL AA were used for the linear least squares fit, and the rate for 20 µg/mL AA is 2.6% below the rate obtained by extrapolation of the linear portion of the curve. For (b), the data for 1-50 µg/mL AA were used for the linear fit, and the rate observed for 80 µg/mL is 12.6% below that obtained by extrapolation.

Table IV.I. Dependence of Calibration Characteristics on the Measurement Time and OPDA Concentration[a]

OPDA Conc. (M)	Comp. Time (s)	Raw Data			Normalized Data[b]		DL (μg/mL)	Corr. Coeff.
		Slope[c] (counts/μg/mL)	Intercept[c] (counts)	Blank SD[d] (counts)	Slope (mV/s-μg/mL)	Blank SD[d] (10^{-3} mV/s)		
0.01	10	243 (17)	19 (45)	20	0.0972	8	0.17	0.99853
0.01	20	954 (17)	57 (112)	26	0.0954	2.6	0.055	0.99947
0.1	10	717 (5)	28 (33)	24	0.287	9.6	0.067	0.99996
0.1	20	2482 (11)	76 (76)	26	0.248	2.6	0.021	0.99998

[a] $HgCl_2$ conc., 1×10^{-3} M; AA conc., 1 - 10 μg/mL; pH 4.2.

[b] Normalized data obtained by dividing raw data by $k\Delta t^2$, where Δt is the half of the computational time and k is the V/F conversion factor (100 Hz/mV).

[c] SD given in ( ).

[d] From 10 blank measurements.

rate decreases during the computational period. However, the correlation coefficient and calibration curves show that the first-order kinetics prevail over a reasonable AA concentration range. Hence the fixed-time method can be applied for the first 25 s or less of the reaction up to an AA concentrations of at least 10 μg/mL without significant problems due to product decomposition.

Table IV.I also shows that the normalized SD of the blank rate with a 20-s computational time is significantly less than that with a 10-s computational time for both OPDA concentrations. With a 30-s computational time, the SD of the normalized blank rate (2.8×10^{-3} mV/s with 0.1 M OPDA) did not improve. The detection limit (DL) for AA, defined as twice the SD of the blank rate divided by the slope of the calibration curve, is reported for 4 situations in Table IV.I. The best detection limit of 0.021 μg/mL is obtained with 0.1 M OPDA and a 20-s measurement time.

With 0.1 M OPDA, the RSD for the 1 to 5 μg/mL AA range varied from 0.70 to 2.6% for the 20-s computational time and from 1.2 to 4.2% for the 10-s computational time. The RSD values for the concentrations greater than 5 μg/mL AA were less than 0.76% with both computational times.

Determination of Total Ascorbic Acid in Real Samples

Triplicate samples of vitamin C pills, multivitamin pills and a juice were analyzed with the proposed method. Calibration standards of 1, 3, 5, 7, and 10 μg/mL AA were used and the dilution of the samples were adjusted, so that the AA concentrations were in the 1-10

μg/mL range. Table IV.II summarizes the results. For the vitamin C and multivitamin pills, the experimental values agree with the nominal values within 4%, while the experimental value for the juice sample is significantly greater from the nominal value. How close the true amounts must be to the nominal values is not known.

To further test the proposed method, the samples were spiked with a 1 mL of 100 μg/mL AA standard before final dilution to yield a 1 μg/mL increase in AA concentration in the final test solution. To calculate the recoveries, the difference in the rate for samples before and after the spike were compared to the rate for a 1 μg/mL standard. The results presented in Table IV.III show that the percent recovery for both vitamin pills is good. This indicates that other substances in these samples do not significantly affect the slope of the calibration curve and standard-addition techniques are not required. However, the recovery with the juice sample was low and a standard-addition technique is required for best accuracy. Although the juice sample chosen has a very strong color, the absorbances of the diluted juice sample in the cell were 0.01 and 0.005 at excitation and emission wavelengths, respectively. Thus factors other than inner-filter effects must be responsible for the low recovery.

Table IV.II. Determination of Ascorbic Acid in Real Samples

Sample	Nominal Mass (mg)	Conc.[a] (μg/mL)	Mass Found[b] (mg)
Vitamin C pill	500	4.397	512 (0.9)
Multivitamin pill	120	3.830	115 (1.9)
Juice	60	4.080	72 (0.8)

[a]Concentration in sample solution assayed.
[b]% RSD in ().

Table IV.III. Recovery of Ascorbic Acid from Spiked Samples

Sample	Conc. Found[a] (μg/mL)	Recovery (%)
Vitamin C pill	5.423 (1.8)	102.6
Multivitamin pill	4.851 (0.94)	102.1
Juice	5.016 (0.59)	93.6

[a]total concentration after addition of 1 μg/mL of AA; % RSD in ( ).

CONCLUSIONS

The reaction-rate method based on the AA-OPDA condensation reaction provides several advantages including a linear dynamic range of almost three orders of magnitude and good precision. The reaction can be run in a standard fluorometric sample cell without prior heating or column oxidation steps. Because rate data are obtained in less than 30 s, the technique is rapid and minimizes errors due to photdecomposition of the monitored product. As an oxidant, the $HgCl_2$ has been proved to be very effective without spectral and chemical interference. This reaction should also be suitable for flow injection analysis or HPLC post-column derivatization.

The reaction-rate measurement system based on a PC offers versatility for data manipulation. Because the reaction curve data are stored, the reaction rate can be recalculated with different computational parameters to optimize these parameters.

REFERENCES

1. R. B. Roy and A. Conetta, Food Technology 1976, 94.

2. L. A. Pachla, D. L. Reynolds, and P. T. Kissinger, J. Assoc. Off. Anal. Chem. 1985, **68**, 1.

3. L. J. Machlin, "Handbook of Vitamins: Nutritional, Biomedical, and Clinical Aspects", M. Dekker, New York, 1984.

4. O. A. Bessey and C. G. King, J. Biol. Chem. 1933, **103**, 687.

5. M. Z. Barakat, M. F. Abdel-Wahab, and M. M. El-Sadr, Anal. Chem. 1955, **27**, 536.

6. D. F. Evered, Analyst 1960, **85**, 515.

7. K. K. Verma and A. K. Gulati, Anal. Chem. 1980, **52**, 2336.

8. M. Z. Barakat, S. K. Shehab, N. Darwish, and A. El-Zoheiry, Anal. Biochem. 1973, **53**, 245.

9. K. S. Panwar, S. P. Rao, and J. N. kGaur, Anal. Chim. Acta 1961, **25**, 218.

10. C. N. Murtyand N. G. Bapat, Z. Anal. Chem. 1963, **199**, 367.

11. D. Gupta, P. D. Sharma, and Y. K. Gupta, Talanta 1975, **22**, 913.

12. G. S.Sastri and G. G. Rao, Talanta 1972, **19**, 212.

13. J. H. Roe and C. A. Kuether, Anal. Biochem. 1943, **43**, 399.

14. M. Schmall, C. W. Pifer, and E. G. Wollish, Anal. Chem. 1953, **25**, 1486.

15. M. J. Deutsch and C. E. Weeks, J. Assoc. Off. Anal. Chem. 1965, **48**, 1248.

16. R. A. Roy, A. Conneta, and J. Saltpeter, J. Assoc. Off. Anal. Chem. 1976, **59**, 1244.

17. D. C. Egberg, R. H. Potter, and J. C. Heroff, J. Assoc. Off. Anal. Chem. 1977, **60**, 126.

18. M. I. Karayannis, Anal. Chim. Acta 1975, **76**, 121.

19. E. E. Kriss, G. T. Kurbatova, and K. B. Yatsimirskii, Zhurnal Analiticheskoi Khimii 1976, **31**, 598.

20. R. L. Wilson and J. D. Ingle, Jr., Anal. Chem. 1977, **49**, 1060.

21. M. A. Ryan and J. D. Ingle, Jr., Anal. Chem. 1980, 52, 2177.

22. J. Velisek, J. Davidek and G. Janicek, Collection Czechoslov. Chem. Commun. 1972, 37, 1465.

23. A. Tello, Undergraduate Research Project Report, Oregon State University, 1985.

24. S. P. Mushran and M. C. Agrawal, J. Scient. Ind. Res. 1977, 36, 274.

CHAPTER V

DETECTION AND CORRECTION OF INTERFERENCES IN SINGLE-LINE FLOW INJECTION ANALYSIS WITH FLUORESCENCE DETECTION

H. K. Chung and J. D. Ingle, Jr.*

Department of Chemistry

Oregon State University

Gilbert Hall 153

Corvallis, Oregon 97331-4003

ABSTRACT

Quenching and inner-filter interference effects in fluorescence measurements were investigated with a single-line flow injection analysis (FIA) system interfaced to a microcomputer for data collection, control, and data manipulation. A reference peak profile due to physical dilution was obtained by injecting a quinine sulfate (QS) solution and compared with peak profiles of sample solutions to evaluate the effect of concentration-dependent interferences. The distortion of the peak profile due to multiplicative interferences can be detected by a variation in the ratio of the reference to sample signals throughout the sample zone. An empirical function, which involves a normalization for different analyte concentrations, is described and used to generate correction plots based on the distortion of the profile. Application of the method is demonstrated for the determination of QS with $K_2Cr_2O_7$ (absorber) and KI (quencher) as interferents. Errors due to these interferents as small as 0.5% can be detected, and errors larger than 30% can be reduced to less than 2%.

INTRODUCTION

Fluorometric determinations can be in error if the fluorescence signal from the analyte in a sample is affected by other species in the sample. Common multiplicative interferents that decrease the observed fluorescence signal include species that absorb a significant amount of the excitation or emission radiation (inner-filter effect) or that quench the analyte fluorescence (i.e, reduce the fluorescence quantum efficiency).

Several techniques have been developed to evaluate if inner-filter effects are important for a given sample, and in some cases, to correct for the errors that arise [1]. The absorbance of the sample at the excitation and emission wavelengths can be measured with a separate instrument or measured simultaneously along with the fluorescence in specialized instruments [2,3]. As a rule of thumb, the absorbance should be less than about 0.01 A.U. at both wavelengths to keep errors due to absorption effects below 1%. Specialized spectrofluorometers that are configured to implement the cell-shift or cell-rotation methods [2,3] can also be employed. Inner-filter effects are indicated if the fluorescence signals from different equivalent volume elements within the sample cell are not equal. A double-pass method has been proposed in which the fluorescence signal is measured without and with a mirror in place to reflect the excitation beam back through the sample cell [4]. If absorbers are present, the relative increase in fluorescence signal with the mirror in place is less than without the mirror because of the longer pathlength that the reflected excitation beam travels.

The presence of quenchers can be detected by measuring the fluorescence lifetime which decreases if significant quenching occurs [5]. Standard-addition techniques can also be used to detect and compensate for inner-filter effects or quenchers [6] although this technique does not differentiate between the two effects.

When quantitative fluorescence measurements are made, it would be best to check every sample for quenching or inner-filter effect interferences. This is rarely done because specialized instrumentation or additional measurements are required as noted above. Although a literature reference could not be found, another simple method to detect these multiplicative interferences is dilution. The signal attenuation caused by inner-filter or quenching effects depends on the interferent concentration but is independent of the analyte concentration. If the ratio of blank-corrected fluorescence signals from a sample and a 1 to 1 dilution of the sample is not equal to 2, a significant multiplicative interference is indicated. This paper extends the idea of using dilution to detect multiplicative interferences by taking advantage of the fact that FIA techniques automatically provide a large range of dilution of the sample.

In FIA, well-defined concentration profiles due to dispersion are obtained under conditions of laminar flow [7,8]. The overall dispersion of the injected sample, which originates from the injection, transport, and detection processes [9], can be experimentally characterized in terms of the dispersion coefficients throughout the sample zone. These dispersion coefficients define the dilution ratio of a sample at any portion of the sample zone relative

to the analyte concentration in the sample prior to injection.

For analytical FIA measurements the peak height, peak area, or peak width (defined by some detector level above baseline) have been used as the analytical signal. Most commonly the peak maximum has been used because this readout can be easily made [10]. However, the signals at different portions of the profile can be used to construct calibration curves and this technique has been denoted the gradient calibration technique [11]. A microcomputer-controlled system is best suited to obtain signals at precise points in the profile. The peak width has been used most extensively for FIA titrations [12,13] in which case the titrant is used as the carrier stream.

This paper is concerned with using signal information from most of the FIA peak profile to obtain not only analytical information but also information about the accuracy of the determination. It is shown that the shape of an FIA profile with fluorescence detection is distorted by absorbers or quenchers. With a microcomputer controlled FIA and data acquisition system, these multiplicative interferences can be easily detected by comparing the sample peak profile to a reference peak profile. Moreover, a new method for the correction of concentration-dependent interferences in fluorescence measurements is described.

EXPERIMENTAL

Reagents and Solutions

All chemicals were reagent grade. Aqueous stock solutions of QS (1000 μg/mL), potassium dichromate (100 μg/mL), and potassium iodide (100 μg/mL) were used to prepare more dilute solutions. The carrier stream was 0.1 N sulfuric acid. A 10% (v/v) nitric acid solution or ethanol was used to rinse the tubing after the experiment each day. All water used in the preparation of solutions and carrier stream was double deionized water from a Millipore Milli-Q system.

Instrumentation

A single-line FIA system was used for all measurements. It consisted of a carrier stream pump, a sample injection valve, a coiled reactor, and a flow cell in series. The carrier stream pump was a positive-displacement valveless pump (model RH1CKC, Fluid Metering, Inc.) driven by a stepper motor (model Super Lox SO-1, Ivek Corp. Springfield, VT). Eight microcomputer I/O lines were connected to the pump controller interface to allow control of the flow rate with a microcomputer. The sample injection valve was a double-stack slide bar type valve equipped with pneumatic activators (model 30520, Dionex Corp. Sunnyvale, CA). With two 3-way air valves and a solid-state relay, the inject or fill position was selected by the signal on one microcomputer I/O line. The sample loop was filled by aspiration with another positive-displacement pump driven by a

synchronous motor (Lab pump Jr., model RHSY, Fluid Metering, Inc.). The on/off state of this pump was controlled by the microcomputer through one I/O line and a solid-state relay. The Teflon tubing for the main flow line including the sample loop and reaction coil was 0.5-mm i.d. The reaction coil was 4 m of tubing in a tight coil.

The detector was a 20-μL volume, 1 mm-pathlength flow-cell (model P/N 8830, Precision Cells Inc., Hicksville, NY) in a modified spectrofluorometer [14,15]. The fluorescence signal (compensated for source fluctuations) was input to a voltage to frequency (V/F) converter (Teledyne Philbrick, model 7405, 100 kHz/V). The V/F converter produces a pulse train whose frequency is proportional to the fluorescence signal. The V/F converter output was connected to the counter input of a CTM-05 system-timer counter board (Metrabyte Corp., Taunton, MA) installed in a PC 400 Corona microcomputer. Two output lines from this board were used to control the sample valve and filling pump. An additional I/O board (model PIO-12, Metrabyte Corp., Taunton, MA) was installed to obtain 8 more I/O lines to control the primary pump.

The software, written in BASIC with an assembly language subroutine (QuickBASIC version 4.5 and Macroassembler version 4.0 from Microsoft) was developed to control the FIA system and to acquire peak profiles. BASIC language was utilized to operate the main pump, to propel the carrier stream at a user specified flow rate, to fill the sample loop for a given period of time, to store the raw data, to plot the data on the monitor, and to calculate the FIA responses and print the values of FIA peak parameters. The assembly language subroutine was used to control the injection valve

and to acquire the raw data for a user specified period of time (generally from the time of injection to after the dispersed sample had totally passed through the cell). Each data point is the number of V/F counts accumulated in the user-specified integration time.

From the stored data file (signal vs. time), the program first calculates the baseline fluorescence signal. The data points for a given period of time before the FIA peak are summed and divided by the number of data points summed. This average baseline signal is subtracted from total signal for all data points to obtain the net fluorescence signal due to the analyte. After the baseline correction step, the peak maximum and the peak time are first obtained. All times are relative to the start of the measurement time which can be the same or earlier than the sample injection time. The travel time (beginning of peak) is operationally defined as the time at which a data point (starting from the beginning of the data file) first exceeds 1% of the peak maximum signal. The end time of a peak is defined in a similar fashion and the data file is searched from longer to shorter times. The baseline peak width is taken as the difference between the peak travel time and end time. The data points within the baseline peak width are summed to calculate the net peak area.

Procedures

FIA profiles of fluorescence signal were acquired with a PMT bias voltage of 800 V, a feedback resistance (current-to-voltage converter) of 1 MΩ, and a time constant of 0.1 s. The excitation

monochromator was set at 366 nm with 2-mm slits (17-nm spectral bandpass) and the emission monochromator was adjusted to 460 nm with 2.5-mm slits (21-nm spectral bandpass). The carrier stream was pumped at a flow rate of 2.0 mL/min. After loading the 30-µL sample loop for 10 s at a flow rate of 5 mL/min and a 3-s delay time, sample was injected and data acquisition was initiated. Data were collected for 40 s with a 0.2-s integration time per data point and stored on a floppy diskette. After the data acquisition, the baseline signal was calculated from data over 5-s period (from 10 to 15 s). The sample profiles were continuously displayed on a chart recorder during the measurement time.

QS solutions were injected to obtain reference or interference-free peak profiles. To study the effect of interferences on the peak profile, 10 µg/mL QS solutions containing KI or $K_2Cr_2O_7$ were injected into the carrier stream.

From the stored disk files, the signal value at time t for a test solution was compared to the signal at the same time for a reference solution (e.g., 10 µg/mL QS). Different functions for comparing the data were used as discussed later. A spread sheet (Symphony version 1.2) was used to investigate the peak profiles and normalize data. Unless otherwise specified, samples were injected in triplicate, and thus all values reported are the mean from three runs.

METHOD DEVELOPMENT

In FIA, an injected sample undergoes well-defined dispersion as a result of physical mass transport and the shape of the peak profile is a descriptor of a FIA response. If the detector response is proportional to the concentration of a analyte, the concentration profile of a sample zone can be determined as a function of time. Because the concentration profile of the injected sample at the detector is fixed for a given FIA manifold with a constant flow rate of the carrier stream, the peak profile can be used as a unique diagnostic tool to detect the multiplicative interferences in fluorescence measurements. More specifically, an interfering substance experiences the same dispersion as the analyte. If an interferent is present and its effect on the analyte signal is dependent on the interferent concentration but independent of the analyte concentration, the peak profile will be different than a reference peak profile established by injection of an analyte solution containing no interferent. In general, the distortion of the peak profile will be greatest at the normal peak maximum because the interferent concentration is greatest at this point in the sample zone.

With an automated FIA system with microcomputer controlled data acquisition, it is possible to store signal profile data files (signal vs. time) for the reference solution ($S_r(t)$) and the sample solution ($S_s(t)$). If the FIA manifold and conditions are not changed, one reference data file can be used to compare to a subsequent series of sample injections. The stored data files can be

compared in different ways. One way is to calculate the ratio of the signal of the reference to that of the test solution throughout the sample zone [$R(t) = S_r(t)/S_s(t)$]. If R(t) is constant, no concentration-dependent interference is detected. However if the ratio varies across the profile, a concentration-dependent interference is indicated. For a interferent that suppresses the analytical signal, R(t) will usually be greatest at the maximum of the reference profile. Note that the value of R(t) at any point in the sample profile depends on the analyte concentration which is unknown. Thus, the magnitude of R(t) does not provide direct information about the degree of interference that could be used to correct for the interference effect.

In this paper, an empirical function is introduced to determine the effect of the profile distortion more quantitatively and to allow the corrected peak height and area to be obtained. This function (F(t)) is given by

$$F(t) = S_r(t) - R_A \times S_s(t) \qquad (1)$$

where R_A is the ratio of the peak area of the reference profile to that of the sample solution. If there is no concentration-dependent interferent and a chemical reaction is not involved, the signal at any point in the profile of the sample solution is proportional to that of the reference solution. Thus, F(t) is independent of t and zero because the shape of the peak profile is the same for the reference and sample solutions.

A key component of equation 1 is R_A which is the normalization

factor that accounts for different analyte concentrations in the reference and sample solutions. Thus, the value of F(t) at any point in profile is independent of the analyte concentration in the reference or the sample solutions for a given concentration of interferent. If the analyte concentration in the sample is twice as great as in the reference solution and no interferents are present, R_A = 0.5 and all signals in the sample profile are multiplied by 0.5 before they subtracted from the corresponding reference signals.

If a concentration-dependent interferent such as a quencher or absorber is present, the time profile of the function, F(t), exhibits a positive maximum at the peak time of the reference where the interference effect is greatest. However, F(t) will be negative valued at the beginning and ending zones of the peak. This occurs because the area ratio R_A is related to the average attenuation of the analytical signal across the profile. At and near the maximum, $R(t) > R_A$ such that $S_r(t) > R_A S_s(t)$. Near the ends of the profile where the attenuation of the analyte fluorescence signal is least, $R(t) < R_A$ or $S_r(t) < R_A S_s(t)$. Note that the integration of F(t) across the whole profile will always be zero. It is proposed that the maximum positive value of F(t) or the integral of F(t) over the region which it is positive provides a measure of the relative interference effect and can be used to correct for certain interference effects.

RESULTS AND DISCUSSION

Reproducibility of the FIA Profile

The reproducibility of the peak profiles for standard solutions of QS was first examined. Ten repetitive injections of 1 and 10 µg/mL QS solutions were made and the time parameters of the signal profiles are summarized in Table V.I. The data show that the time parameters are very reproducible with a standard deviation (SD) of 0.12 s or less in most cases. For 1 µg/mL QS, the SD for the baseline peak width is 0.68 s. For lower concentrations it is more difficult to establish the beginning and end times because the baseline noise relative to the peak signal is greater. The dispersion coefficient at the peak maximum, determined by comparison to the steady-state signal of a 1 µg/mL QS solution, was 7.60.

The relative standard deviation (RSD) values of the peak height and area for both concentrations of QS were 0.27 and 0.46%, respectively. Thus the FIA system employed in this work provides excellent between-run precision. In further studies, the peak time parameters, peak height and the peak area were calculated and checked to ensure the proper operation of the FIA system.

Evaluation of the Peak Profile

To demonstrate that multiplicative interferences can be detected by their distortion of FIA profiles, it was first necessary to confirm that the profile shape is reproducible and independent of the

Table V.I. Precision of the FIA time parameters

Time Parameter	QS Conc. (µg/mL)	Time (s)	SD (s)
Travel Time	1	15.6	0.1
	10	15.8	< 0.1
Peak Time	1	20.4	0.12
	10	20.5	0.11
Baseline Peak Width	1	16.8	0.68
	10	16.9	0.11

analyte concentration. To do this, signal versus time data files were obtained for injections of 1, 5, and 10 μg/mL QS solutions. The data from ten repetitive injections of 10 μg/mL were averaged and used as the reference profile ($S_r(t)$ vs. t). The averaged data from triplicate injections for the 1 and 5 μg/mL QS solutions were taken as the test sample profiles ($S_s(t)$ vs. t) and compared to the reference profile in two ways.

The first method involves plotting the ratio of the reference signal to the sample signal of test solution (R(t)) as a function of time. As shown in Figure V.1, the ratio is constant over the sample zone and equal to the ratio of the concentration of the sample solution to that of the reference solution. This indicates that the peak profile of the sample solution is same as that of the reference solution. Note the scatter in the data at the leading and ending zones. This occurs because of the larger relative variance in the signals at these portions of the sample zone.

The second method of comparing reference and sample profiles involves using the reference signal rather than time as the independent variable. The plot of R(t) as a function of the reference signal in Figure V.2 also shows that the ratio is independent of the signal response throughout the peak zone. In this case, the uncertainty in the ratio for data points near the baseline of the profile is manifested by the vertical scatter near zero reference signal. Clearly the data from the peak maximum to 5 to 10% of the maximum of the profile is most useful in establishing if the profile shape has changed.

Overall method 2 is a more informative way to present the data

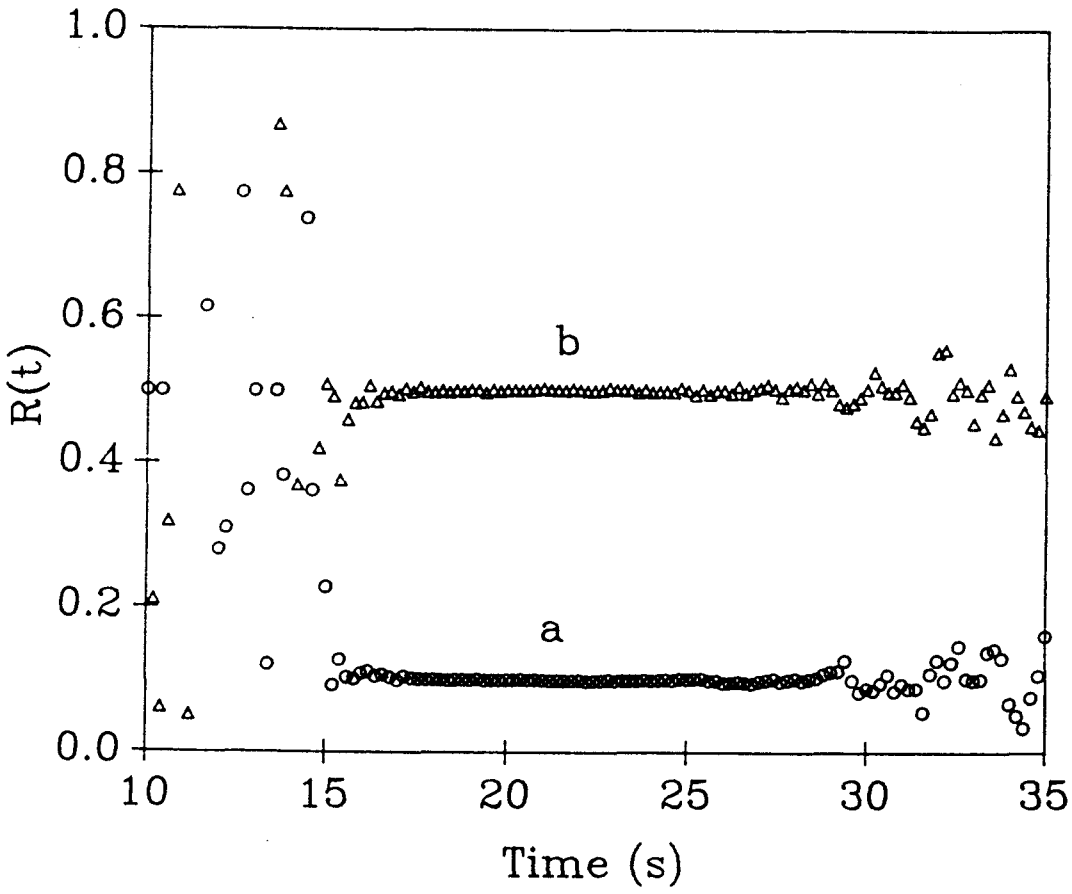

Figure V.1. Dependence of $S_r(t)/S_s(t)$ on time. Concentrations of QS of the test solutions are (a) 1 µg/mL, (b) 5 µg/mL. Reference solution, 10 µg/mL QS.

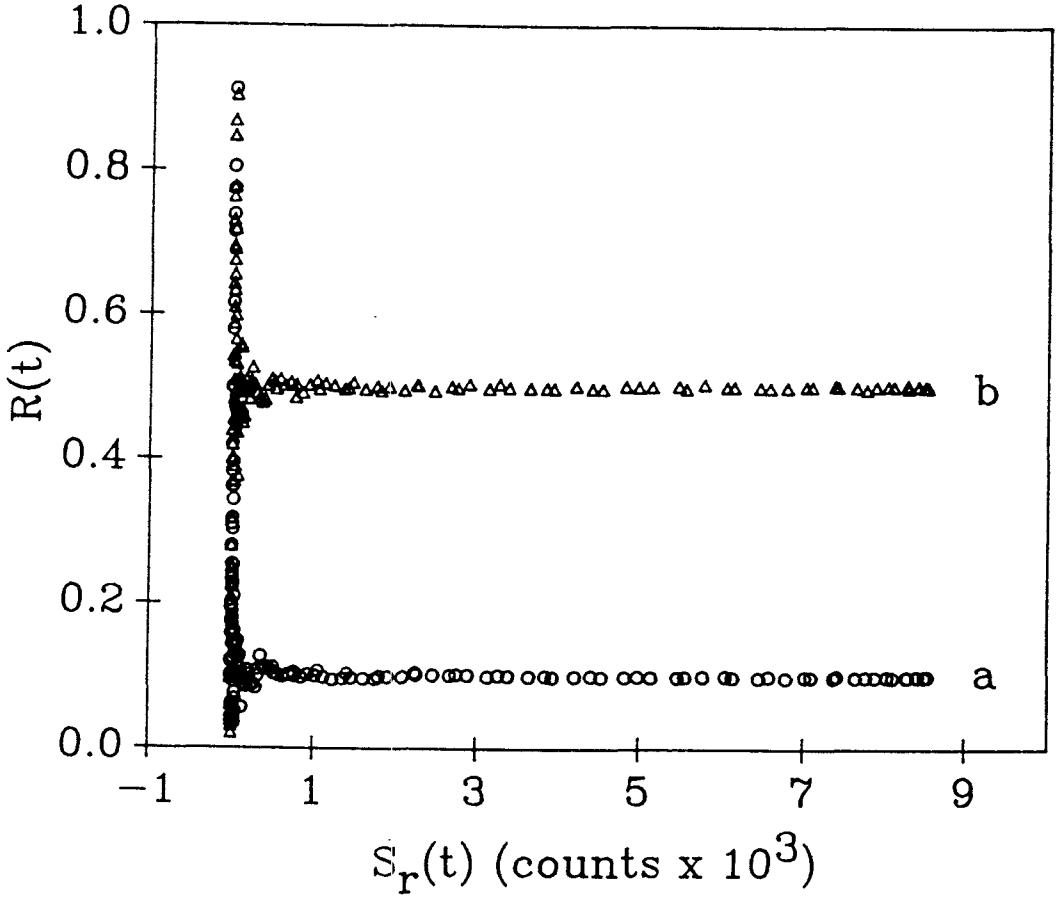

Figure V.2. Dependence of $S_r(t)/S_s(t)$ on the reference signal. Concentrations of QS of the test solutions are (a) 1 µg/mL, (b) 5 µg/mL. Reference solution, 10 µg/mL QS.

because it more directly indicates the value of R(t) at any point in the profile (i.e., the value of R(t) at the peak maximum or 50% of the peak maximum are easily obtained). Note that the abscissa is proportional to $D(t)^{-1}$ where D(t) is the dispersion coefficient.

Potassium Dichromate Interference

Sample solutions of 10 µg/mL QS solution containing 0.5 to 5 mg/mL of $K_2Cr_2O_7$ were used to evaluate the inner-filter effects on the fluorescence signal of QS. Because the absorbance of $Cr_2O_7^{2-}$ is a factor of 8 greater at the excitation wavelength than at the emission wavelength, primary absorption effects are dominant. A 10 µg/mL QS solution with no $K_2Cr_2O_7$ added was used to obtain the reference profile.

Figure V.3 shows how the peak profiles of QS solutions are affected by the $K_2Cr_2O_7$ concentration. Table V.II summarizes the peak height and peak area data. When the concentration of $K_2Cr_2O_7$ is 1.0 mg/mL or less, it is difficult to distinguish visually the difference between the shapes of the reference profile and the distorted sample profile. For the sample solution containing 1.0 mg/mL $K_2Cr_2O_7$, the peak area and height are reduced (relative to the reference profile) by 36 and 51%, respectively, and no shift of the peak time is observed for the data point integration time used (0.2 s). Thus, it is difficult to identify an interference effect causing a 40-50% error from visual inspection of the raw profile or the peak time.

For solutions containing $K_2Cr_2O_7$ concentrations of 1.5 mg/mL

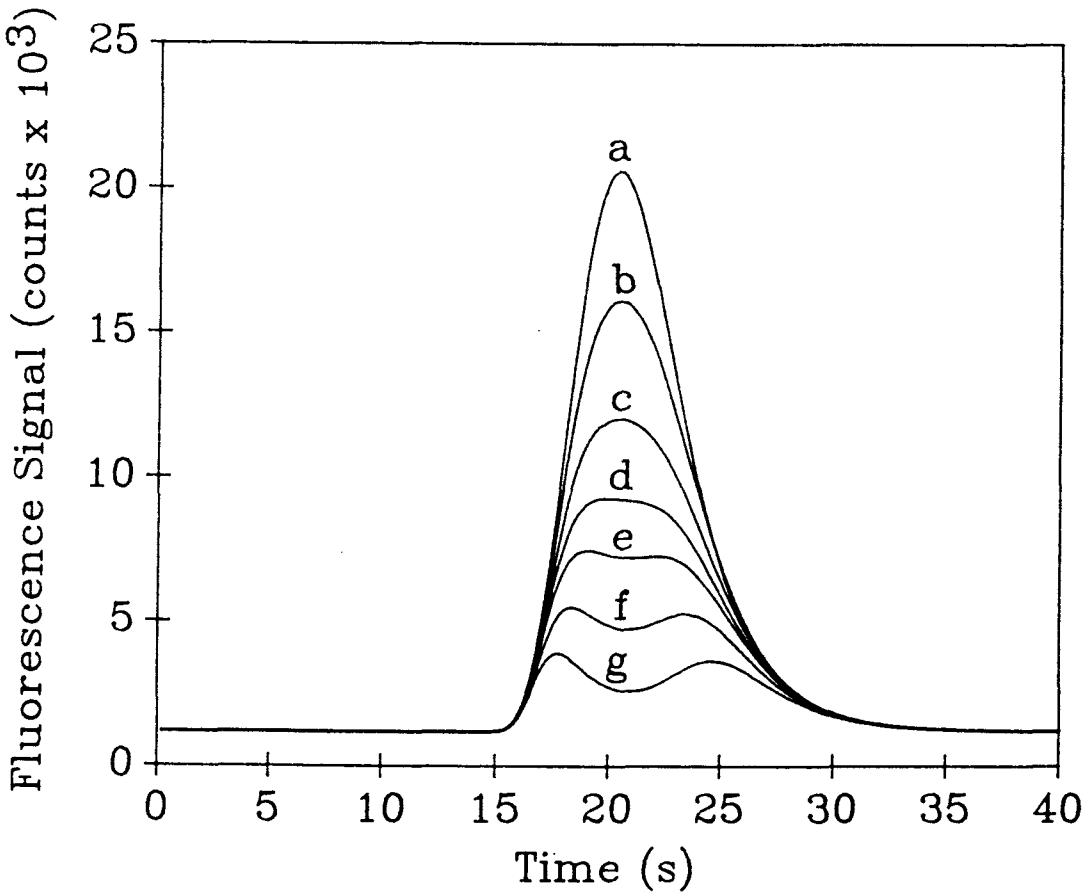

Figure V.3. Dependence of the shape of the FIA peaks of 10 µg/mL QS on the concentration of $K_2Cr_2O_7$. $K_2Cr_2O_7$ conc. (in mg/mL): (a) 0, (b) 0.5, (c) 1.0, (d) 1.5, (e) 2.0, (f) 3.0, (g) 5.0.

Table V.II. Effect of $K_2Cr_2O_7$ Concentration on Peak Parameters

$K_2Cr_2O_7$ Conc. (mg/mL)	Peak Height[a] (counts x 10^3)	Peak Area[b] (counts x 10^5)
0	22.3 (0.092)	6.62 (0.061)
0.5	14.9 (0.12)	5.21 (0.068)
1.0	10.8 (0.056)	4.21 (0.086)
1.5	8.07 (0.14)	3.51 (0.15)
2.0	6.07 (0.23)	2.94 (0.16)
3.0	3.58 (0.28)	2.13 (0.12)
5.0	1.47 (0.35)	1.31 (0.38)

[a]Peak height at maximum time for reference; % RSD in ( ).
[b]% RSD in ( ).

and greater, the distortion of the profile shape is obvious and the true maximum is not observed. For 2 mg/mL of $K_2Cr_2O_7$, for which the peak area is reduced by 44%, dual peaks are observed around the true peak maximum. Note that the first peak maximum is highest and that this peak maximum value shifts to shorter times with increasing interferent concentration. In the case of higher interferent concentration, the distortion of the peak can be easily detected by visual inspection or by comparing the peak time parameter of the sample to that of the reference.

Figure V.4 shows plots of log (R(t)) versus the reference signal for the different concentrations of $K_2Cr_2O_7$ tested. Note that these plots are similar to those in Figure V.2 except that the log of the ratio is taken as the dependent variable. The attenuation of the fluorescence signal is obvious for even the lowest interferent concentration tested and increases as the peak maximum is approached. The RSD for peak maximum and peak area in all cases are less than 0.4%. When the signals are taken at 16.6 s which corresponds to 9.2% of peak maximum of the reference, the RSD was ranged from 0.66 to 1.1% for all $K_2Cr_2O_7$ concentrations tested.

Note especially in curves e and f of Figure V.4 that R(t) oscillates around a mean value. The greater values of R(t) correspond to points taken after the peak maximum while the lower values correspond to points on the profile before the peak maximum. This behavior is attributed to the axial concentration distribution. The concentration of QS or $K_2Cr_2O_7$ is greater in the center of the tubing (and the flow cell) than near the walls. Thus for two points on either side of the profile where the dispersion coefficient

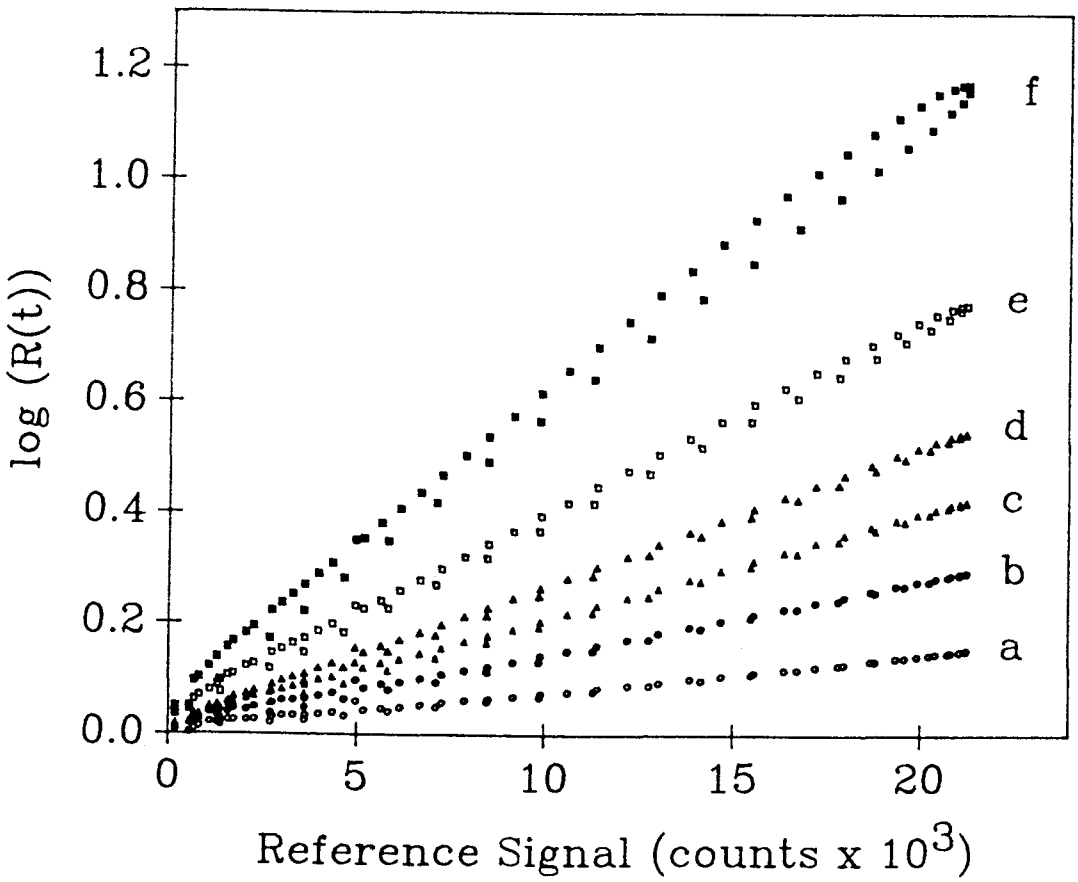

Figure V.4. Dependence of log (R(t)) on the dispersed $K_2Cr_2O_7$ concentration throughout the sample zone. $K_2Cr_2O_7$ conc. (in mg/mL): (a) 0.5, (b) 1.0, (c) 1.5, (d) 2.0, (e) 3.0, (f) 5.0

and "average" analyte and interferent concentration are equal, the effect of the interferent on the observed fluorescence signals differs.

Inner-filter effects are complex to model. As an approximation, the observed fluorescence signal (E_F) is related to true fluorescence signal observed in the absence of significant solution absorption (E^0_F) by

$$E_F = E^0_F \times 10^{-\epsilon_{ex}bc/2} \times 10^{-\epsilon_{em}bc/2} \qquad (2)$$

where ϵ_{ex} and ϵ_{em} are molar absorptivities at the excitation and emission wavelengths, respectively, b is the cell pathlength, and c is the concentration of the absorber. Rearrangement of equation 2 yields

$$\log (E^0_F/E_F) = kc \qquad (3)$$

where $k = b(\epsilon_{ex} + \epsilon_{em})/2$. Thus a plot of $\log (E^0_F/E_F)$ versus c should be linear.

Figure V.5 shows such plots from the data in Figure V.3 where E_F and E_F^0 are taken as the fluorescence signals at different times during the profiles [$E_F^0 = S_r(t)$ and $E_F = S_s(t)$] or as the areas of the peaks. The plots generally follow the model but negative deviation is significant above 2 mg/mL $K_2Cr_2O_7$ for signals at or near the maximum of the profile and for the peak area. The model used is based on a point source approximation and breaks down at higher solution absorbances. The non-uniform axial

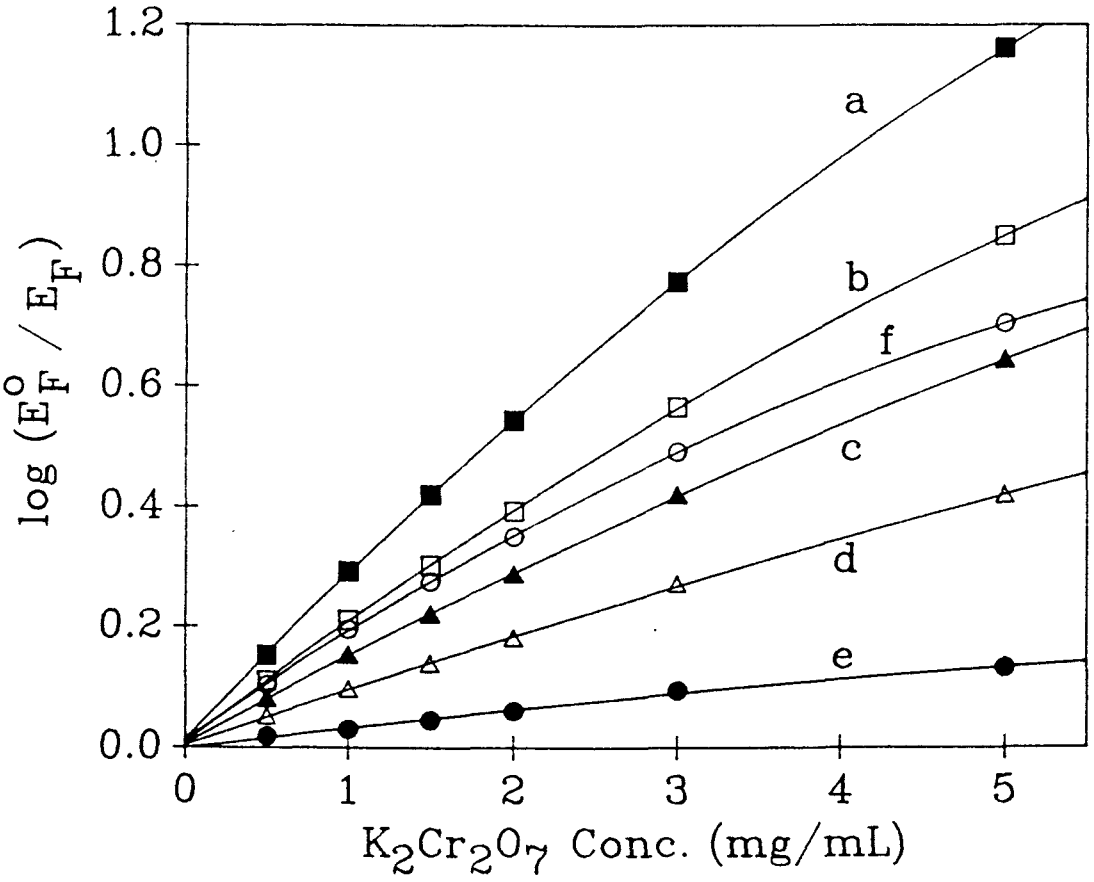

Figure V.5. Dependence of log (E^o_F/E_F) on the concentration of $K_2Cr_2O_7$. Signals are taken at different times throughout the peak profile except the peak area (f): (a) 20.4 s (peak maximum), (b) 18.8 s (70% of peak maximum), (c) 18.2 s (50% of peak maximum), (d) 17.6 s (30% of peak maximum), (e) 16.6 s (10% of peak maximum).

concentration may also contribute to the nonlinearity.

The plots in Figure V.4 for a given concentration of $K_2Cr_2O_7$ are also reasonably linear. This is expected from equation 3 because the average concentration of $K_2Cr_2O_7$ at any point in the profile is proportional to the reference signal at that point in the profile.

Potassium Iodide Interference

Test sample solutions of 10 µg/mL QS containing 1 to 15 mg/mL of KI were injected to demonstrate the effect of quenching. Figure V.6 shows that the attenuation and the distortion of the FIA peak increase as the concentration of KI increases. Table V.III summarizes the peak height and area information. Two peaks are not observed until the concentration of KI is 10 mg/mL or the peak area decreases to about 38% of its value without KI (i.e., at a higher value of overall attenuation than observed with $K_2Cr_2O_7$).

Figure V.7 shows the plots of R(t) versus the reference signal for different concentrations of KI. The distortion of the profile is obvious from the increase in R(t) as the peak maximum is approached for all KI concentrations tested. The oscillation of signals between points on either side of the peak maximum is ascribed to the non-uniform axial concentration distribution.

Quenching can be modeled with the Stern-Volmer equation which relates the observed fluorescence signal (E_F) to that true fluorescence signal observed without quenching (E_F^o) by

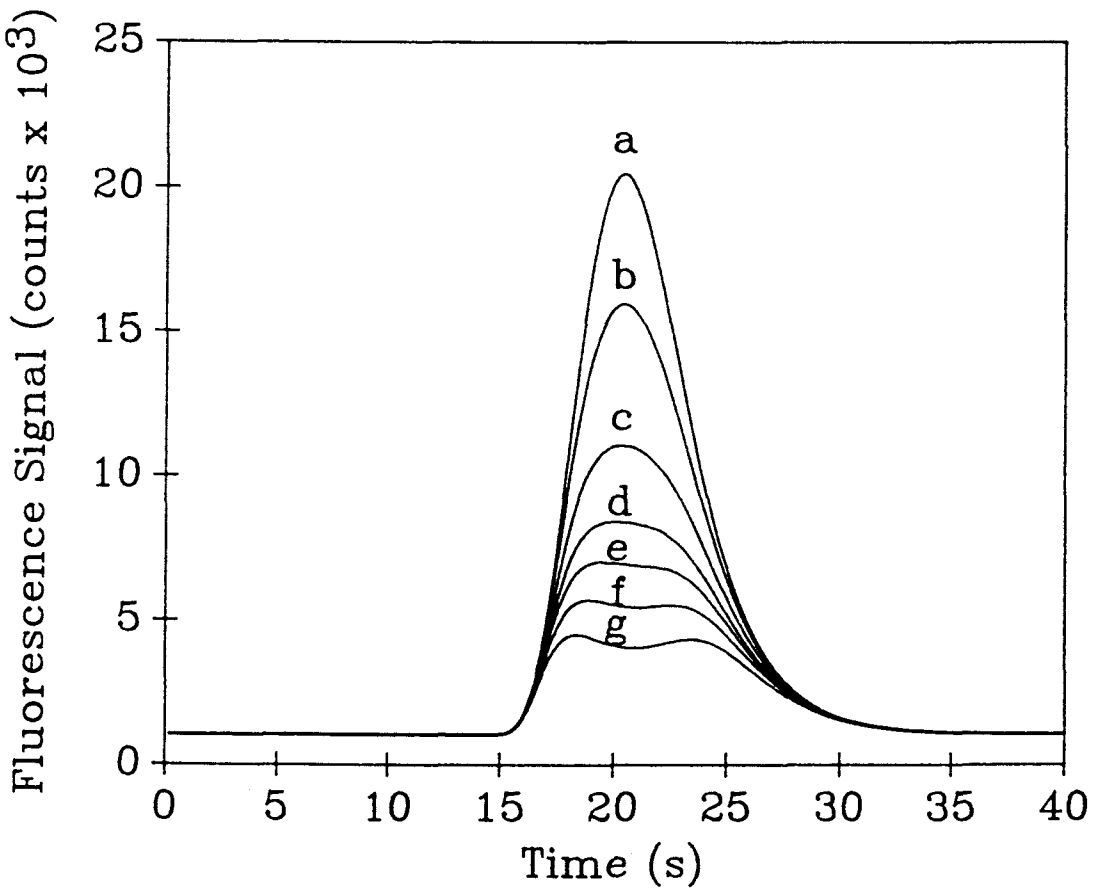

Figure V.6. Dependence of the shape of the FIA peaks of 10 µg/mL QS on the concentration of KI. KI conc. (in mg/mL): (a) 0, (b) 1, (c) 2, (d) 5, (e) 7, (f) 10, (g) 15.

Table V.III. Effect of KI Concentration on Peak Parameters

KI Conc. (mg/mL)	Peak Height[a] (counts x 10^3)	Peak Area[b] (counts x 10^5)
0	19.4 (0.17)	6.02 (0.092)
1	14.9 (0.20)	5.02 (0.058)
2	10.0 (0.093)	3.88 (0.14)
5	7.39 (0.069)	3.16 (0.072)
7	6.0 (0.40)	2.74 (0.036)
10	4.68 (0.073)	2.28 (0.19)
15	3.48 (0.26)	1.78 (0.13)

[a]Peak height at maximum time for reference; % RSD in ( ).
[b]% RSD in ( ).

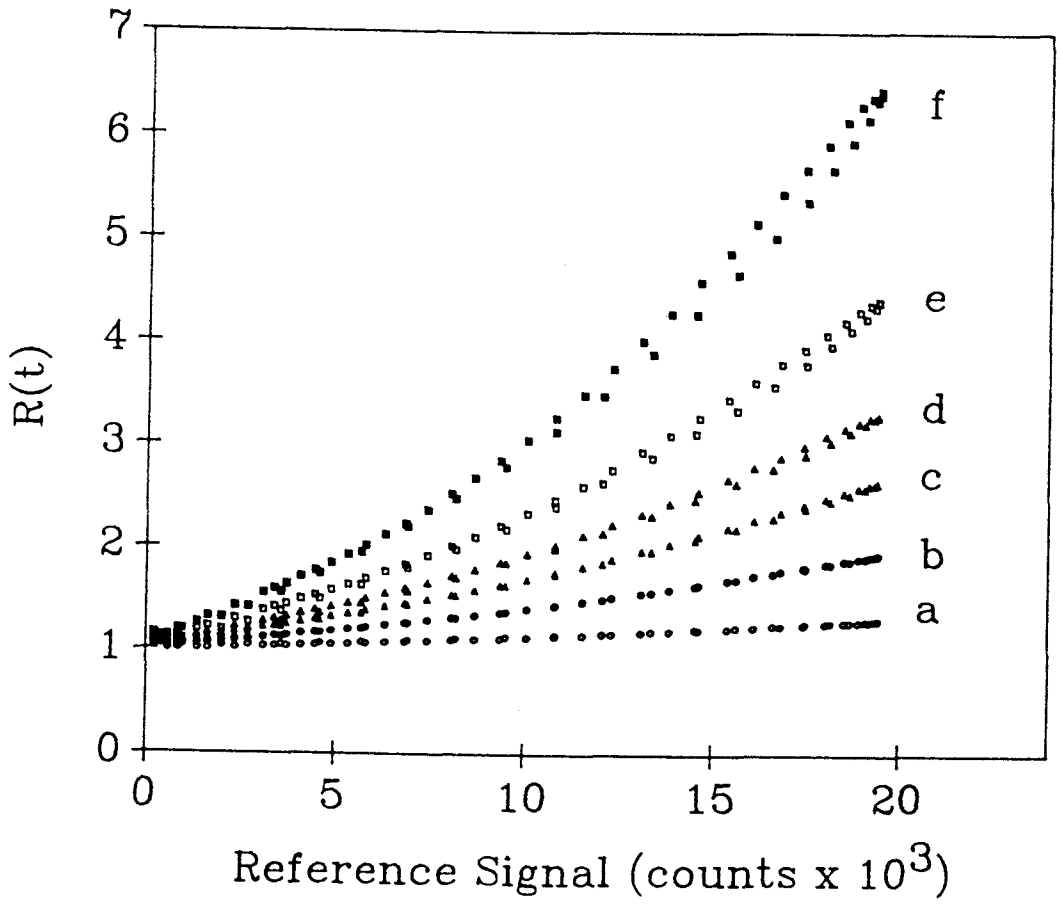

Figure V.7. Dependence of R(t) on KI concentration throughout the sample zone. KI conc. (in mg/mL): (a) 1, (b) 2, (c) 5, (d) 7, (e) 10, (f) 15.

$$E_F = E^0_F/(1 + K_q[Q]) \quad (4)$$

where [Q] is the quencher concentration and K_q is the Stern-Volmer constant. Rearrangement of equation 4 yields

$$E^0_F/E_F = 1 + K_q[Q] \quad (5)$$

A plot of E^0_F/E_F vs quencher concentration should be linear.

Figure V.8 shows such plots of E^0_F/E_F where E_F and $E_F{}^0$ are taken at different points in the profile or as the peak areas. When the concentration of KI is 7 mg/mL or less, a linear relationship is observed for the peak maximum signals. For higher concentrations of KI, a positive deviation from the ideal behavior is obtained. A linear relationship is observed up to higher KI concentrations for points of the profile away from the maximum and for the peak area.

Most of the plots in Figure V.7 are quite nonlinear even though the average concentration of KI is proportional to reference signal at all points in the profile. Equation 5 is not a good model for predicting how quenching varies across the profile.

Characteristics of the New Function

To evaluate the degree of the peak distortion in a different way, the stored raw data for the $K_2Cr_2O_7$ and the KI interference studies (Figures V.3 and 6) were used to construct plots of the function (F(t)) as shown in Figures V.9 and 10. Although the raw FIA profiles exhibit different shapes depending on the amount of

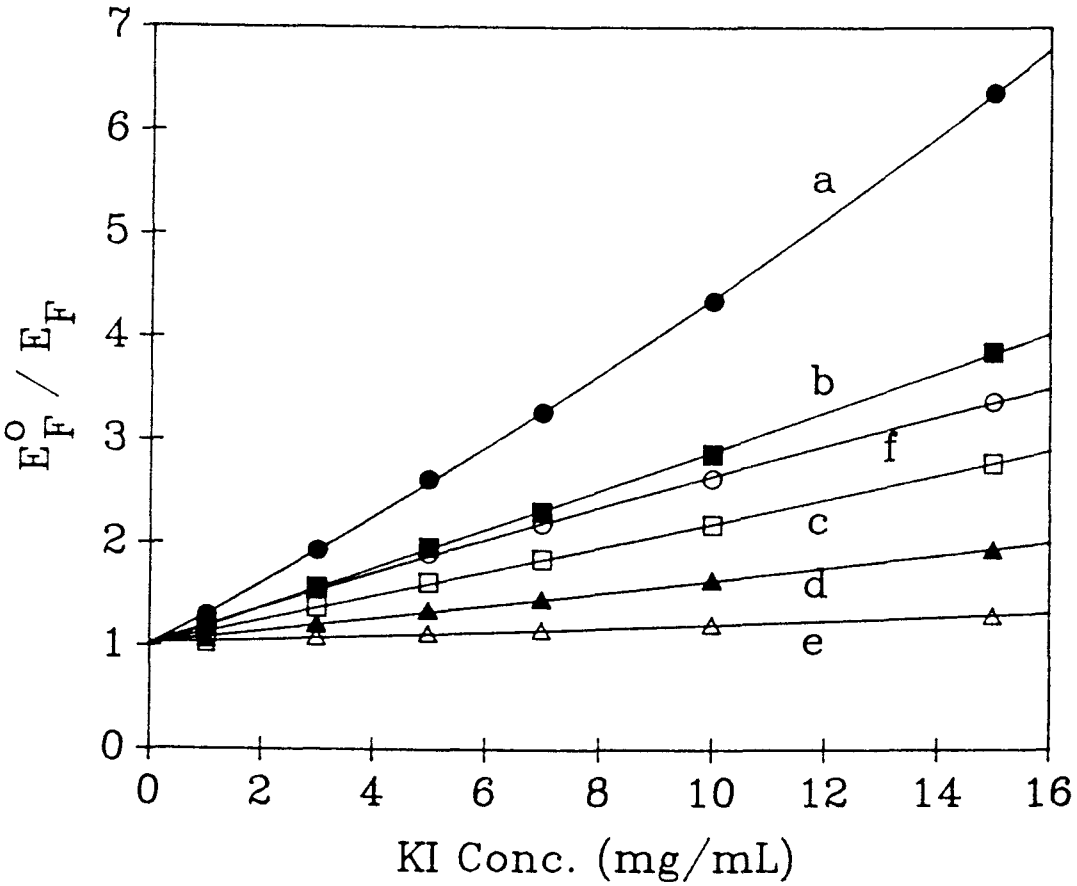

Figure V.8. Dependence of E^o_F/E_F on the concentration of KI. Signals are taken at different times throughout the peak profile except the peak area (f): (a) 20.4 s (peak maximum), (b) 18.8 s (70% of peak maximum), (c) 18.2 s (50% of peak maximum), (d) 17.6 s (30% of peak maximum), (e) 16.6 s (10% of peak maximum).

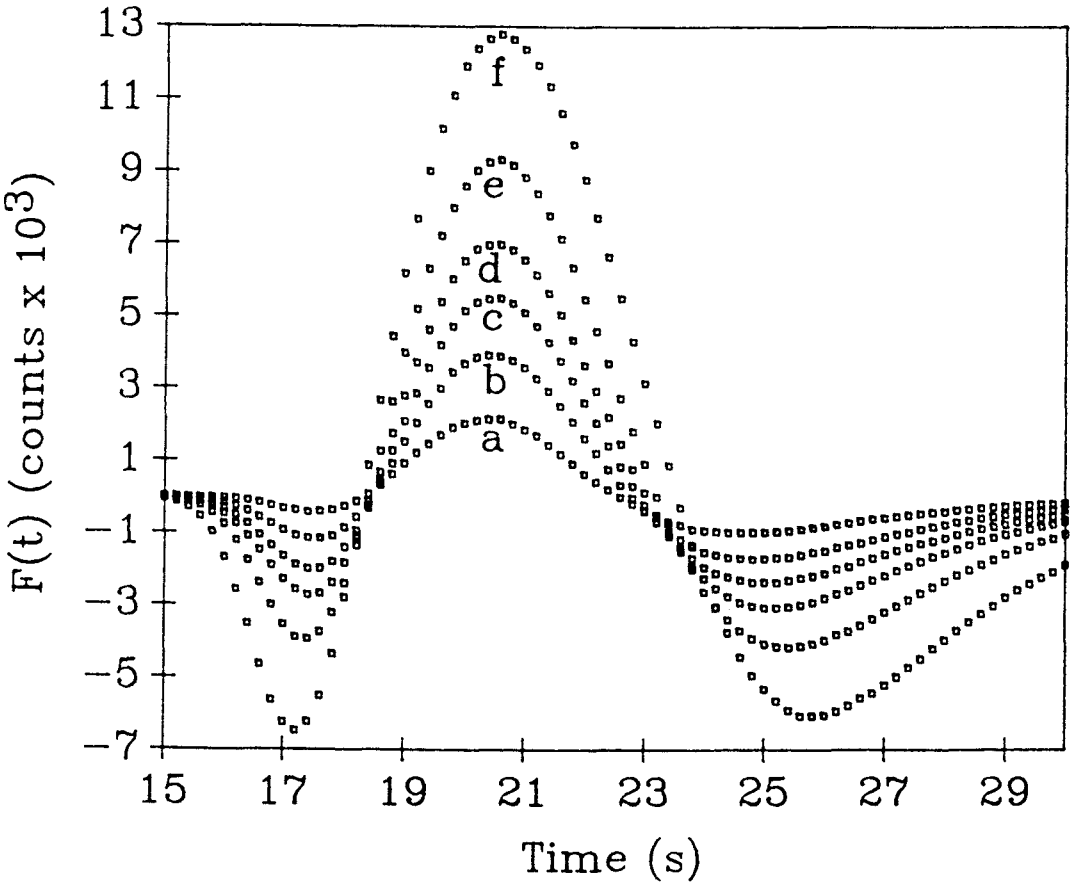

Figure V.9. Dependence of F(t) on the concentration of $K_2Cr_2O_7$. $K_2Cr_2O_7$ conc. (in mg/mL): (a) 0.5, (b) 1.0, (c) 1.5, (d) 2.0, (e) 3.0, (f) 5.0.

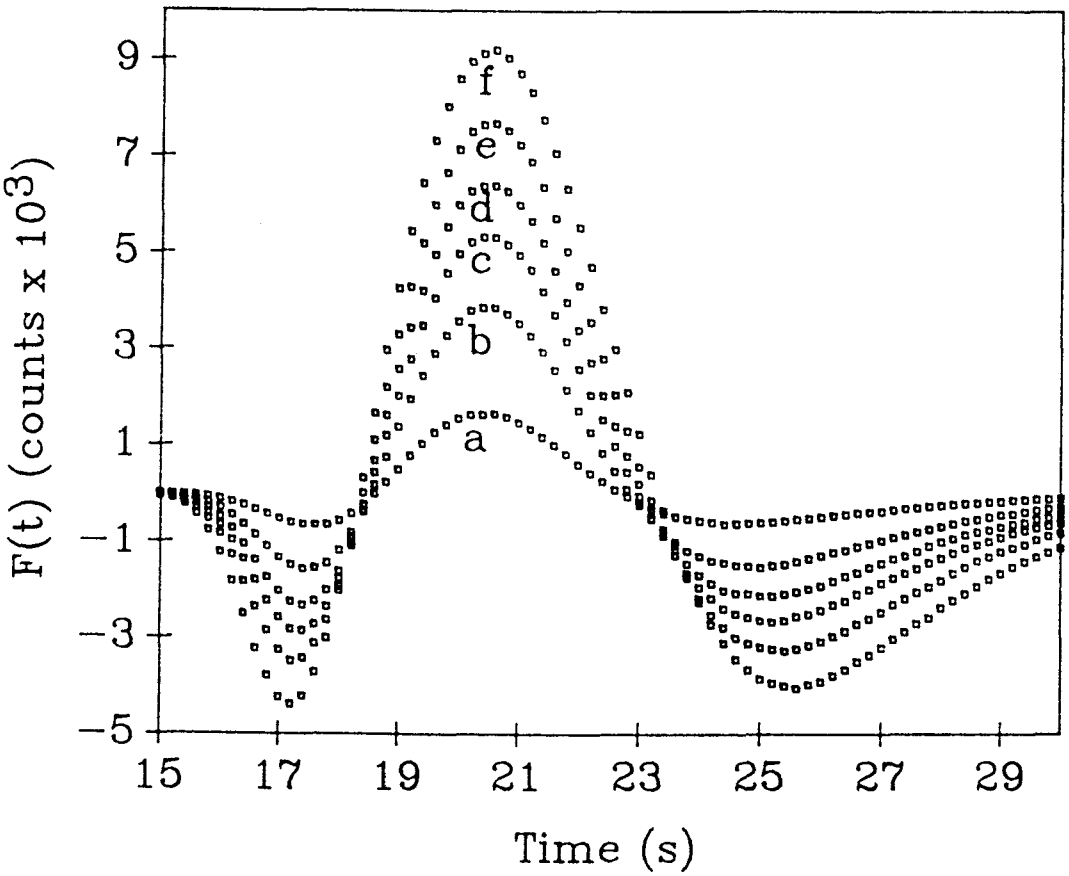

Figure V.10. Dependence of F(t) on the concentration of KI. KI conc. (in mg/mL): (a) 1, (b) 2, (c) 5, (d) 7, (e) 10, (f) 15.

interferent added, the shape of the new function appears to be relatively independent of the amount of the interferent. As the concentration of interferent increases, the size of the positive and negative peaks increase. Thus the information of the peak size can be applied to determine the effect of interference quantitatively. From the beginning of the peak (15.8 s) to ca. 70% of the peak maximum (18.8 s), F(t) is negative. From 18.8 to 23.6 s, F(t) is positive. After 23.6 s, F(t) again becomes negative. The times at which F(t) changes sign are very reproducible. The time at which F(t) becomes negative after the reference profile maximum increases slightly as the interferent concentration increases. The time at which F(t) first becomes positive appeared to be independent of the interferent concentration with an average RSD of 0.5%.

Determination of the Corrected Fluorescence Signal

The function F(t) was used to characterize interference effects in the following way. Both the maximum positive value of F(t) (F_{max}) and the summation of positive values of F(t) ($\Sigma F(t)$) were taken as measures of the relative interference effect. Although negative values of F(t) are also related to the distortion of the peak profile, better reproducibility is provided by using the positive values because of the relatively large variance in the leading and ending zones of the sample zone.

The peak height and area of F(t) were plotted versus the correction factor which is the ratio of analytical signal without interferences to the analytical signal with interferences present.

For this work the peak area was taken as the analytical signal where A_r is the peak area of the reference and A_s is the peak area of the sample solution. Thus the correction factor is A_r/A_s. The correction for the peak height of the raw peak was not performed due to the variation of the position for different different amount of the interference.

Table V.IV summarizes the data for the interference of $K_2Cr_2O_7$. With the data acquisition system employed in this study, excellent reproducibility in correction factor was obtained. The RSDs in the correction factors and the values of $\Sigma F(t)$ and F_{max} were typically better than 1%. The data in Table V.II are plotted in Figures V.11 and 12 and are fit with a 3rd order polynomial regression equation.

The data in Table V.V and Figures V.11 and 12 for KI show similar trends and precision. Note that correction plots for both types of interferences are very similar and almost identical up to a correction factor of 2.0.

To determine the minimum level of interferent that can be detected, ten repetitive injections of the reference solution (no interferents added) were made. From the plots of F(t), the SD of $\Sigma F(t)$ or F_{max} was obtained. The minimum correction factor that can be detected is defined as 1 plus twice the SD of $\Sigma F(t)$ or F_{max} for an interference-free analyte solution (229 and 16.2 counts, respectively) divided by the initial slope of correction curve (1.02×10^5 and 8.35×10^3 counts/(mg/mL KI), respectively). It is 1.0045 for peak area and 1.0034 for peak height. In other words, an error of less than 0.5% due to inner-filter effects or quenching can

Table V.IV. Correction Table for the Determination of QS with $K_2Cr_2O_7$ Interferent

$K_2Cr_2O_7$ Conc. (mg/mL)	Correction Factor[a]	$\Sigma F(t)$[a] (counts x 10^4)	F_{max}[a] (counts x 10^3)
0.5	1.27 (0.068)	2.70 (0.67)	2.12 (0.87)
1.0	1.57 (0.087)	5.10 (0.26)	3.91 (0.21)
1.5	1.89 (0.15)	7.44 (0.29)	5.52 (0.45)
2.0	2.25 (0.16)	9.78 (0.29)	6.99 (0.33)
3.0	3.10 (0.012)	13.8 (0.084)	9.30 (0.31)
5.0	5.05 (1.0)	20.9 (0.38)	12.8 (0.26)

[a]% RSD in ( ).

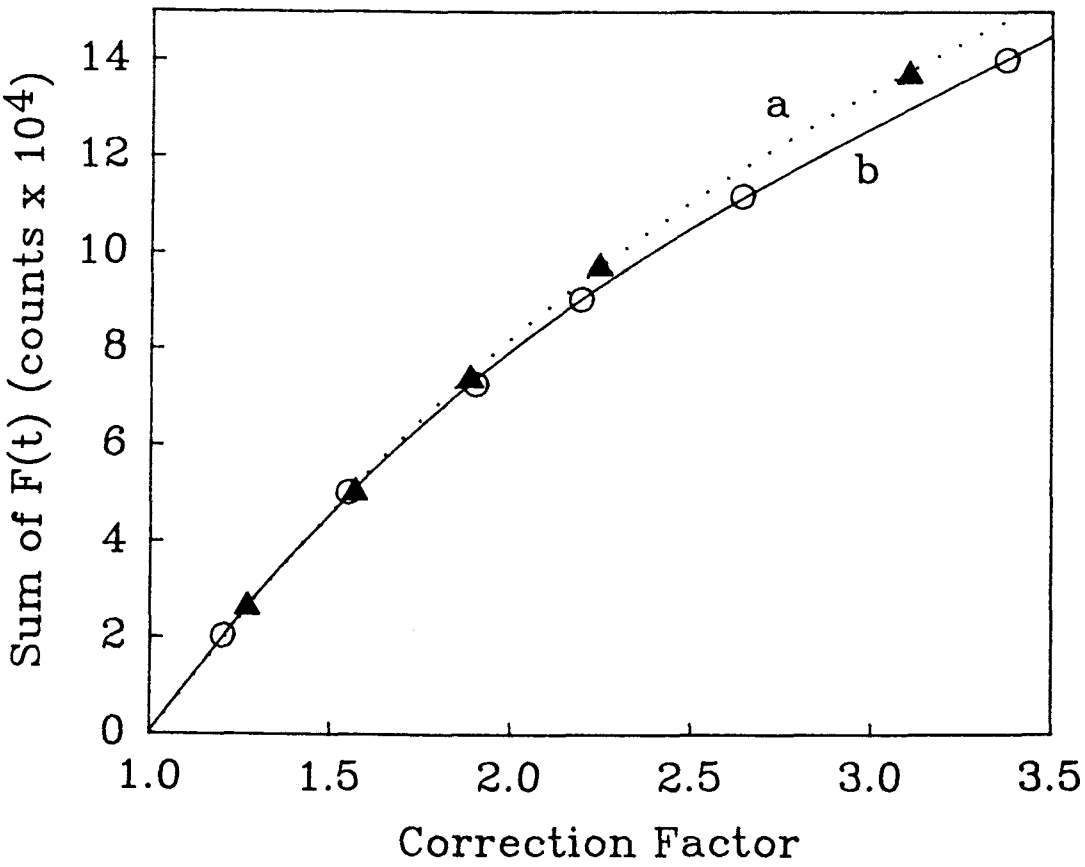

Figure V.11. Fluorescence correction curve for QS based on peak area. The data were taken from Figures V.9 and 10. (a) $K_2Cr_2O_7$, (b) KI. The correction factors were calculated by dividing the peak area of reference solution (10 µg/mL QS) by the peak area of the test solutions. The zero, first, second, and third order coefficients for the 3rd order polynomial regression fit are -1.22×10^5, 1.45×10^5, -2.47×10^4, and 1.57×10^3 for (a) and -1.38×10^5, 1.76×10^5, -4.23×10^4, and 4.30×10^3 for (b).

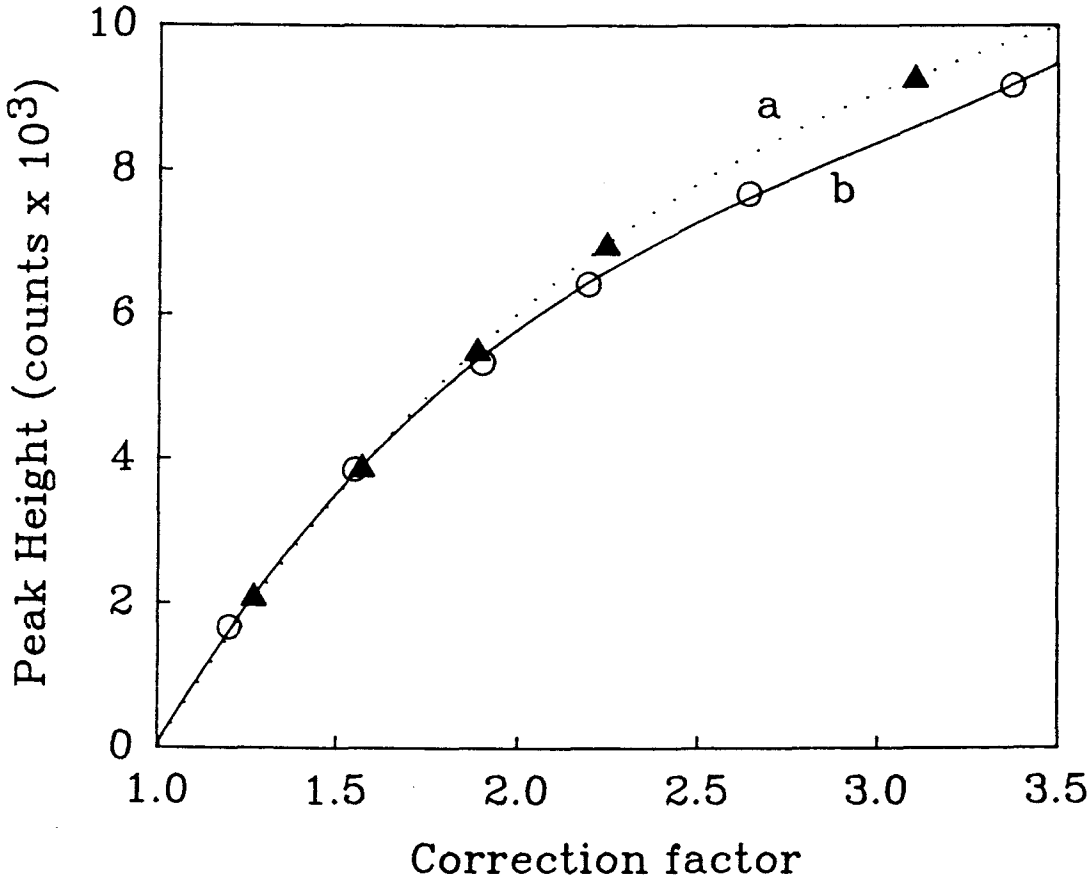

Figure V.12. Fluorescence correction curve for QS based on peak height. Conditions are the same as in Figure V.11 [(a) $K_2Cr_2O_7$, (b) KI]. The zero, first, second, and third order coefficients for the 3rd order polynomial regression fit are -1.11×10^4, 1.44×10^4, -3.61×10^3, and 3.55×10^2 for (a) and -1.20×10^4, 1.62×10^4, -4.71×10^3, and 5.21×10^2 for (b).

Table V.V. Correction Table for the Determination of QS with KI Interferent

KI Conc. (mg/mL)	Correction Factor[a]	$\Sigma F(t)^a$ (counts x 10^4)	$F_{max}{}^a$ (counts x 10^3)
1	1.200 (0.058)	2.04 (0.12)	1.67 (1.57)
2	1.551 (0.014)	5.04 (0.29)	3.86 (0.18)
5	1.903 (0.073)	7.28 (0.061)	5.34 (0.37)
7	2.194 (0.036)	9.04 (0.22)	6.43 (0.60)
10	2.638 (0.19)	11.2 (0.19)	7.68 (0.31)
15	3.375 (0.13)	14.0 (0.064)	9.17 (0.36)

[a]% RSD in ( ).

be detected. For this study this corresponds to a $K_2Cr_2O_7$ concentration of 8.3 µg/mL or a KI concentration of 23 µg/mL for peak area measurements.

To simulate real samples, test solutions of 5 µg/mL QS with different concentrations of KI or $K_2Cr_2O_7$ were injected. Sample solution containing both interferents could not be tested because $Cr_2O_7^-$ oxidizes I^-. From the FIA profiles and the profile from a 10 µg/mL QS reference solutions, the values of $\Sigma F(t)$ and F_{max} were obtained. These values were used to determine the correction factor from the previously established correction curve and the corrected signal (i.e., correction factor x measured peak area). Table V.VI shows the observed and corrected peak areas. The results shows that the correction can be made within 2% and the RSD values are less than 2.2% for all cases.

Table V.VI. Corrected Peak Area Based on the Correction Curve[a]

KI Conc. (mg/mL)	$K_2Cr_2O_7$ Conc. (mg/mL)	Observed Peak Area[b] (counts x 10^5)	Corrected Peak Area[b] (counts x 10^5)	
			by $\Sigma F(t)$	by F_{max}
0	0	3.02 (0.060)		
1.0	0	2.54 (0.036)	3.08 (0.11)	3.07 (2.21)
3.0	0	1.94 (0.17)	3.04 (0.71)	3.10 (1.37)
0	0.5	2.39 (0.16)	3.02 (0.65)	3.02 (1.45)
0	1.0	1.92 (0.34)	2.96 (0.39)	2.97 (1.03)

[a]5 µg/mL QS.
[b]% RSD in ( ).

CONCLUSIONS

A single-line FIA system has been proven to be a simple and effective diagnostic tool to study multiplicative interferences in fluorescence measurements. With the FIA system described in this paper, time-dependent signals can be precisely obtained. For a given system with a constant flow rate, the shape of the peak can serve as an important descriptor as well as the peak height or area. Comparison of a reference peak profile which characterizes physical dispersion to a sample profile allows detection and compensation for the peak distortion due to quenching or inner-filter effects. This method can not identify the type of concentration-dependent interference.

Although this method was tested for the case that the analyte does not react with reagents, it should be applicable to cases where a fluorescent product is formed and detected. In this case, the reference profile would be established with an interference-free standard injected into the reagent carrier stream.

This method should be extendable to FIA systems using detection by methods other than fluorescence. It is only necessary that the interference effect is dependent on the relative interferent concentration and independent of the analyte concentration. In general, the proposed method will not detect additive interferences as the signal due to interferent would vary as analyte signal such that the shape of the peak profile would not change.

REFERENCES

1. J. D. Ingle, Jr. and S. R. Crouch, "Spectrochemical Analysis", Prentice Hall, New Jersey, 1988.

2. K. Adamson, J. E. Sell, J. F. Holland, and A. Timnick, Am. Lab. 1984, **16(11)**, 16.

3. M. C. Yappert, M. W. Schuyler, and J. D. Ingle, Jr., Anal. Chem. 1989, **61**, 593.

4. K. W. Street, Jr. and M. Tarver, Analyst 1985, **110**, 1169.

5. G. M. Hieftje and G. R. Haugen, Anal. Chim. Acta 1981, **123**, 255.

6. G. L Campi and J. D. Ingle, Jr., Anal. Chim. Acta 1989, **224**, 225.

7. D. Betteridge, Anal. Chem. 1978, **50**, 832A.

8. J. Ruzicka and E. H. Hansen, Anal. Chim. Acta 1978, **99**, 37.

9. M. Valcarcel, M. D. Luque de Castro, "Flow Injection Analysis: Principles and Applications", Ellis Horwood, U. K., 1987.

10. J. Ruzicka, Anal. Chem. 1983, **55**, 1040A.

11. S. Olsen, J. Ruzicka, and E. H. Hansen, Anal. Chim. Acta 1982, **136**, 101.

12. J. Ruzicka, E. H. Hansen, and H. Mosbaek, Anal. Chim. Acta 1977, **92**, 235.

13. A. U. Ramsing, J. Ruzicka, F. J. Krug, and E. A. G. Zagatto, Anal. Chim. Acta 1981, **129**, 1.

14. R. L. Wilson and J. D. Ingle, Jr., Anal. Chem. 1977, **49**, 1060.

15. M. A. Ryan and J. D. Ingle, Jr., Anal. Chem. 1980, **51**, 2177.

CHAPTER VI

EXTRACTION OF ANALYTICAL KINETIC DATA FROM INDIVIDUAL PEAK PROFILES CORRECTED FOR DISPERSION IN FLOW INJECTION ANALYSIS: APPLICATION TO THE DETERMINATION OF ALUMINUM

H. K. Chung and J. D. Ingle, Jr.*

Department of Chemistry

Oregon State University

Gilbert Hall 153

Corvallis, Oregon 97331-4003

ABSTRACT

A new procedure for obtaining analytical kinetic information in single-line flow injection analysis (FIA) system is described. A microcomputer-controlled FIA system is used first to acquire and store the peak profile of a non-reacting reference solution and calculate the relative dispersion coefficient due to the physical dispersion as a function of time. Next the peak profile of a sample is acquired and stored and the previously determined dispersion coefficients are used to normalize the sample FIA response in the time domain by multiplying the signal response by the dispersion coefficient throughout the sample zone. In the absence of a chemical reaction, these normalized signals are time-independent and equal to the peak maximum signal for the sample. When a slow chemical reaction is in progress during the time between injection and detection, the signal varies across the normalized profile and depends on the reaction time and the ratio of the analyte to reagent (carrier stream) concentrations such that the chemical information can be extracted for kinetic determinations. Chemical and instrumental variables were optimized for a fluorometric kinetic determination of Al^{3+} with the fixed-time method. A 13 ng/mL detection limit was achieved. The proposed method is shown to discriminate against the interference from riboflavin, a non-reacting fluorescent species.

INTRODUCTION

Kinetic information can be obtained from FIA measurements if the time for a reaction to reach completion is much longer than the time between sample injection and detection. Several techniques have been suggested to extract kinetic information [1,2]. In a single-line FIA manifold with injection of the sample into a reagent stream, the peak height or area is proportional to the amount of product formed in a fixed-time period [1,2]. This single-point kinetic method does not provide true kinetic information because an absolute signal rather than a change in signal is measured. A non-reacting species in the sample that contributes to the detector response will cause error.

To measure a change in the detector signal due to a chemical reaction, several methods have been suggested. Hansen et al. used two flow detector cells to perform a two-point kinetic assay [3]. The difference in signals is measured and related to the amount product formed during the travel time between the flow cells. The stopped-flow technique is widely used for kinetic assays [4-6]. In this technique, the sample zone dispersed in the reagent carrier stream is stopped when it reaches the detection cell for a pre-determined period during which the reaction-rate measurement is performed. Fernandez et al. employed two serial injection valves for the simultaneous injection of the same sample into one reagent carrier stream [7]. The difference in the peak heights of the two peaks is related to the rate. Valcarcel and co-workers [8] demonstrated that kinetic information can be obtained in a single-line manifold by injecting a relatively large sample volume

(e.g., 1000 µL) into the reagent stream. Two reaction zones and two peaks are produced because little or no reagent/sample mixing occurs in the middle of the sample zone. The two-peak profile when a chemical reaction is in progress was compared to the single-peak profile with a plateau due to physical dispersion that occurs when a dye solution is injected. For the kinetic determinations, reaction-rate information was obtained from the difference in peak heights or area.

A number of researchers have described the effect of chemical kinetics on the shape of the peak profile and obtained kinetic information from the peak profile. Painton and Mottola [9] measured the contribution of a chemical reaction on dispersion and demonstrated that it changes noticeably (at relatively low flow rates). Hooley and Dessy constructed a multiple detector system based on light emitting diode sources/photodetector sensors that were located along the observation tube [10]. Dispersion phenomena were investigated to characterize the peak height and peak area. The peak area was constant when no chemical reaction is involved. When a chemical reaction is in progress throughout the detection time, the peak profile changes and is used to extract reaction-rate information. Recently, reagent dispersion in addition to sample dispersion [11] has been considered to investigate the kinetic aspects [12-14]. Hungerford and Christian [14] developed a theoretical model considering the effect of reagent dispersion in which simultaneous chemical and physical dispersion kinetics are taken into account.

Vanderslice and co-workers [15] developed a laminar flow

diffusion-convection equation that describes the peak profile with and without a chemical reaction. The equation was used for the determination of first-order reaction rate constants from the ratio of the peak heights and areas of reaction peaks to those of non-reaction peaks. This approach suggests that kinetic information can be obtained from the peak profile. The chemical contribution to the total dispersion at any point can be extracted because the physical dispersion without a chemical reaction can be described by the sample dispersion coefficient. If the dispersion coefficients are characterized, the steady-state signal due to the sample plug (prior to physical dispersion) can be obtained.

In this paper, a new method is described for obtaining rate information from the peak profile shape in a single-line FIA manifold. A reference profile is first obtained with a non-reacting sample and used to determine the relative physical dispersion coefficients. These dispersion coefficients are then used to normalize the FIA profile when a chemical reaction is occurring. Over a portion of the normalized profile, an increase in signal with time is observed and rate information is extracted with the fixed-time method. The technique is demonstrated by adapting a kinetic procedure developed by Campi and Ingle [16] for the determination of Al^{3+} to the FIA system. It is based on the formation of a fluorescent complex between Al^{3+} and acid alizarin garnet R.

EXPERIMENTAL

Instrumentation

All measurements were performed with a single-line FIA manifold system consisting of a positive displacement valveless pump (model RH1CKC, Fluid Metering, Inc.) driven by a stepper motor with a computer interface (model Super Lox SO-1, Ivek Corp. Springfield, VT), a 4-way double-stack slide-bar type injection valve (model 30520, Dionex Corp. Sunnyvale, CA) with pneumatic activators, a reaction coil, and a fluorescence flow cell (20 μL volume, 1-mm pathlength, model P\N 8830, Precision Cells Inc., Hicksville, N.Y.). The flow cell was inserted into the sample holder of a previously described spectrofluorometer [17]. A Lab pump Jr. (model RHSY, Fluid Metering, Inc.) was used to aspirate sample solutions into the sample loop from the sample reservoir. All connecting tubing in the main line was 0.5 mm i.d. Teflon tubing. The total length of the flow manifold between the injector and the flow cell is approximately 500 cm including a reaction coil of 400 cm.

A microcomputer (an IBM PC compatible) was used to control the FIA system and for data acquisition. Through signals on the I/O lines, the flow rate of the carrier stream pump, the load/inject position of the injection valve, and the on/off state of the sample loop filling pump are controlled. For data acquisition, the fluorescence signal from the photomultiplier tube (PMT) of the spectrofluorometer after current-to-voltage conversion and compensation for source fluctuations is directed to a V/F converter.

The output pulse train from the V/F converter is counted for a given time (integration time per a data point) with a CTM-05 timer-counter board expansion board (MetraByte) which is programmed as a frequency counter. The voltage resolution is 100 μV with a 0.1-s integration time.

The software, which was written in BASIC with an assembly subroutine for data acquisition (QuickBASIC version 4.5 and Macroassembler version 4.0 from Microsoft), was developed to control the FIA system, acquire and store the signal information, and process the data.

The excitation and emission monochromators are used with 2-mm (17-nm spectral bandpass) and 2.5-mm (21-nm spectral bandpass) slits, respectively. The PMT bias voltage was 800 V. A feedback resistance (current-to-voltage converter) of 1 MΩ and a time constant of 0.1 s are used to obtain a voltage signal.

Solution Preparation

All chemicals were reagent grade with the exception of the 2,4,2'-trihydroxyazo-benzene-5'-sulfonic acid (AAGR) reagent which is supplied by Berncolors-Poughkeepsie, Inc., as a sample from large batches of the dye. The major stock solutions were 100 μg/mL quinine sulfate (QS) in 0.1 N H_2SO_4, 100 μg/mL Al^{3+} in 0.01 M HNO_3, 500 μg/mL AAGR, 100 μg/mL riboflavin, and an acetate buffer (2 mol of acetic acid adjusted to pH 4.75 with 10 M NaOH and diluted to 1 L for most studies). The buffer solution was further cleaned with an ion-exchange resin (Chelex-100) to remove the metal contamination as

previously described [16]. The AAGR carrier stream solutions were prepared by adding the appropriate volume of AAGR and 50 mL of the acetate buffer and diluting to 100 mL with water at the time of analysis. All water used for solution preparation, rinsing glassware was double deionized water from a Millipore Milli-Q system.

Procedures

Under computer control, the sample loop was filled with a flow rate of 3 mL/min for 15 s. After a delay time of 3 s, the sample was injected and the data were collected for a user specified measurement time (typically 40 s) with a integration time of 0.1 or 0.2 s per each data point. The data file (fluorescence signal [S(t)] vs. time) was stored on a floppy diskette for later data analysis. A chart recorder was also used to monitor the signal continuously. The flow rate was varied in the range of 1.0 - 4.0 mL/min. The sample loop was varied in the range of 15 - 200 cm, corresponding to sample volumes of 30 - 500 μL. Unless otherwise specified, standard and sample solutions were injected in triplicate, and thus all rate values are the average rates of three runs.

QS solutions were injected into 0.1 N H_2SO_4 carrier stream to evaluate the physical dispersion of a sample zone. The excitation and emission wavelengths were 366 and 460 nm, respectively. To prepare an equilibrated solution of the Al^{3+}-AAGR complex, 4 mL of a 0.05 μg/mL Al^{3+} solution was mixed with 2 mL of a reagent mixture which contained 50 μg/mL AAGR in a 1.0 M HAc/NaOH buffer solution of pH 4.75 and allowed to reach equilibrium (over 30 min). This

solution was injected into a AAGR reagent carrier stream and the dispersion coefficients were calculated. The same concentration of AAGR reagent was used as a carrier stream for injections of Al^{3+} standards to carry out the chemical reaction. The excitation and emission wavelengths were 366 and 435 nm, respectively.

Software for Data Analysis

After the measurement period is completed, the FIA response curve is plotted on the monitor. Software was also written to characterize the FIA profile. The baseline signal is first calculated by averaging the signal values for given period of time (e.g., for 5 s) before the sample zone appears and then subtracted from all data points to obtain the net fluorescence signal at all times in the measurement period. The baseline corrected data file is searched to obtain the signal and time for the peak maximum. Then the beginning and end times of the peak profile, which correspond to the times the signal is 1% of the peak maximum, are obtained and the difference is taken as the peak baseline width. The points within the baseline width are summed to calculate the area. This initial program is used for routine FIA analysis if the shape of the peak profile is not considered.

A separate BASIC program was written for further data processing. This program performs baseline signal correction, blank correction, averaging of the signal value at time t, and normalization of the signal for dispersion. The disk files of reference profiles, which involve purely physical dispersion, are

loaded, averaged, and used to calculate the dispersion coefficient at time t throughout the sample zone. For most studies, the relative dispersion coefficient ($D'(t) = S_{max}/S(t)$) was calculated where S_{max} is the peak maximum signal. The absolute dispersion coefficient ($D(t)$) can also be calculated if the fluorescence signal of the undiluted reference solution is measured. The files for the test solutions (up to 10 repetitive measurements) are loaded and the dispersion-normalized signals ($S^0(t) = D'(t) \times S(t)$) are calculated. The blank profiles for the reference and the test solutions are also loaded and averaged for blank correction before normalization for dispersion.

For the proposed method for calculation of the reaction rate, the fixed-time method is applied to the dispersion-normalized data files for the test solutions. The initial time and total computation time are specified by the operator. The sum of the data points over the first half of the computational period are subtracted from the sum of the data points over the second half of the computational period. For the final studies involving the determination of Al^{3+} with a 200-μL sample loop, the initial time was selected as the time in the center of the normalized profile at which the signal is at its minimum value, and the computation time was the time between the initial time and the time at which the signal for the reference was 10% of its maximum value.

RESULTS AND DISCUSSION

Dispersion Coefficients of a Sample Zone

For later studies, it was necessary to obtain well defined and reproducible dispersion coefficients of a sample zone for which there is no chemical contribution to the overall dispersion values. To test the reproducibilities of dispersion coefficients in the FIA system, repetitive injections of 30 µL of a 10 µg/mL QS solution were made into a 0.1 N H_2SO_4 carrier stream. From the digitized signals over the profile, the relative dispersion coefficients (D'(t)) were calculated for selected times corresponding to the maximum down to about 1% of the maximum. Table VI.I shows that the signals over most of the peak can be utilized for the analytical measurement if the flow rate is reproducible and a digital data collection system is employed. At greater than 75% of the peak maximum, the relative standard deviation (RSD) of the signal is less than 0.4% and 1.1% or better for values as small as 1% of the peak maximum.

To evaluate peak height and area measurements, repetitive injections of 1, 3, 5, and 10 µg/mL of QS solutions were made. From the stored profile data, the dispersion-corrected signals over different time intervals from the peak maximum to selected longer times were calculated. The signals from each of the n time intervals were corrected for dispersion with the dispersion coefficients previously determined with 10 µg/mL QS as the reference, summed, and divided by n. The value of n varied from 1 to 62 corresponding to

Table VI.I. Comparison of the Signal Values for Different Points of the Sample Profile[a]

Time Delay[b] (s)	Mean Signal[c] (counts)	Percent of Peak Maximum	Relative D value	RSD (%)
20.4	8526 (14)	100	1.00	0.17
22.4	6468 (24)	76	1.32	0.37
23.8	4225 (25)	50	2.01	0.59
24.8	2910 (21)	34	2.93	0.73
27.6	854.0 (8.4)	10	9.98	0.97
29.0	439.7 (4.7)	5.2	19.4	1.1
32.6	85.7 (0.9)	1.0	99.6	1.0

[a]All values from five repetitive measurements; flow rate, 2.0 mL/min.
[b]Relative to time of injection.
[c]Counts accumulated in 0.2 s; std. dev. in ().

time intervals from 0.2 to 12.4 s. Calibration curves of the dispersion-corrected signals versus QS concentration for different time intervals were fit by a linear least squares program. Table VI.II summarizes the data. The calibration curves are linear with a correlation coefficient of greater than 0.99999 in all cases. The RSD in the slope of the calibration curve increases slightly as the total measurement time increases. The range of slopes is about 0.7% of the mean value. These results indicate that the long term reproducibility of the peak profile is quite good. For 1 μg/mL QS, the RSD in the normalized signal for different measurement times ranged from 0.42 to 0.68%.

Consideration of the Reference Solution

A reference solution is required to determine the peak shape and thus the dispersion coefficients across the profile. The reference carrier stream and reference solution must be similar to the carrier stream and analyte solutions used for analysis so that the relative dispersion coefficients of the reference apply to the analyte peaks. A volume of 200 μL of the equilibrated solution of the Al^{3+}-AAGR complex or the reagent mixture as a reference blank was injected into a H_2O carrier stream. The peak shapes are shown in Figure VI.1. The peak for the blank is inverted. At the emission wavelength of 575 nm, the fluorescence signal of H_2O is higher than that of AAGR solution. This may be caused by absorption of a significant fraction of the excitation radiation by the AAGR which reduces the scattering or background fluorescence signal. The net peak area and maximum

Table VI.II. Comparison of QS Calibration Data[a]

Time Interval (s)	Slope (counts x 10^4/μg/mL)	RSD[b] (%)	RSD of slope (%)
0.2	2.718	0.68	0.25
2.2	2.711	0.42	0.30
3.6	2.713	0.58	0.35
4.6	2.711	0.67	0.36
7.4	2.708	0.62	0.34
8.8	2.708	0.62	0.38
12.4	2.698	0.64	0.44

[a]All values from three repetitive measurements; sample volume, 30 μL; other conditions same as Table VI.I.

[b]In the normalized signal for 1 μg/mL QS.

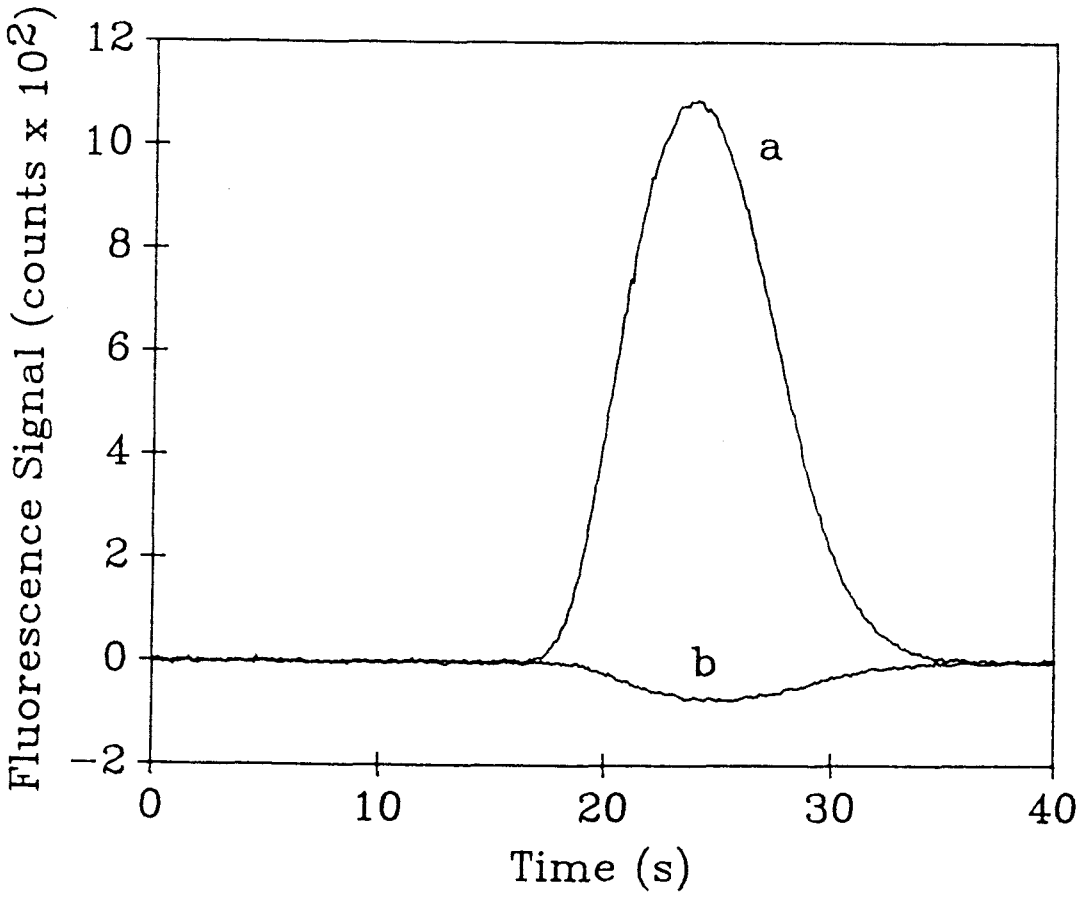

Figure VI.1. Peak shape of the Al^{3+}-AAGR complex and blank solution: (a) 1 µg/mL Al^{3+}; (b) reagent mixture without Al^{3+}. Conditions: carrier stream, H_2O; flow rate, 2.5 mL/min; injection volume, 200 µL.

values of the blank-corrected product (Al^{3+}-complex) profile are 6.0 and 5.8%, respectively, greater than those of the uncorrected profile.

In order to determine the effect of blank correction on the proposed reaction rate method, 200 µL of a 1 µg/mL Al^{3+} solution was injected into a reagent carrier stream of 150 µg/mL AAGR. The reaction rate was calculated over a 2.5 s time interval from the dispersion normalized profiles with the equilibrated Al^{3+}-AAGR solution as the reference. The mean rate calculated with the blank-corrected D'(t) values was lower by 0.43%, compared to that calculated with the uncorrected D'(t) values. These results indicate that blank correction does not significantly affect the reference profile. This is because the background signal due to reagent mixture also undergoes the same well-defined physical dispersion as the analyte signal. Thus, in routine analysis, the blank solution would not be necessary.

The possibility of using a different reference solution such as QS, which is much convenient and stable, was also tested. A QS solution in 0.1 M H_2SO_4 was injected into a 0.1 M H_2SO_4 carrier stream. Unfortunately QS does not fluoresce if injected into the AAGR carrier stream because the pH is too high. The relative D'(t) values obtained were applied to the above data set of 1 µg/mL Al^{3+} standards for the calculation of the reaction rates with the proposed method. The average difference caused by using QS instead of the Al^{3+}-AAGR complex as the reference was 0.43%.

For further studies, the reference solution was prepared by mixing the appropriate concentration of Al^{3+} with 50 µg/mL AAGR

solution in buffer. Then the equilibrated solution of Al^{3+}-AAGR mixture and reagent blank were injected into the AAGR reagent carrier stream to obtain blank-corrected dispersion coefficients as a function of time. This procedure assures that viscosity of the reference, analyte, and carrier stream solutions are similar. When the blank solution (reagent mixture) is injected into a AAGR carrier stream instead of H_2O, a positive-going peak is observed.

Effect of Sample Loop Volume

To determine the effect of sample loop volume, QS solutions were first injected into the single-line FIA manifold with a 0.1 N H_2SO_4 carrier stream to obtain non-kinetic peaks. The sample volume ranged from 30 to 500 µL. The shapes of the non-kinetic profiles, shown in Figure VI.2 (dashed line), depend purely on physical dispersion (or dilution). The peak height and area determined increase with increasing injected sample volume. Even though the peak area yields no information about the shape of the peak, it gives more direct information about the nature of the peak than the peak height. The linear relationship between the peak area and the injected sample volume observed indicates that there is no chemical reaction involved as the area is proportional to the total number of moles of analyte injected.

To test the effect of sample volume in the FIA system for the situation involving a chemical reaction, the same volumes of Al^{3+} samples were injected in the reagent carrier (150 µg/mL AAGR in a 1 M HAc pH 4.75 buffer) without changing the FIA manifold. Figure VI.2

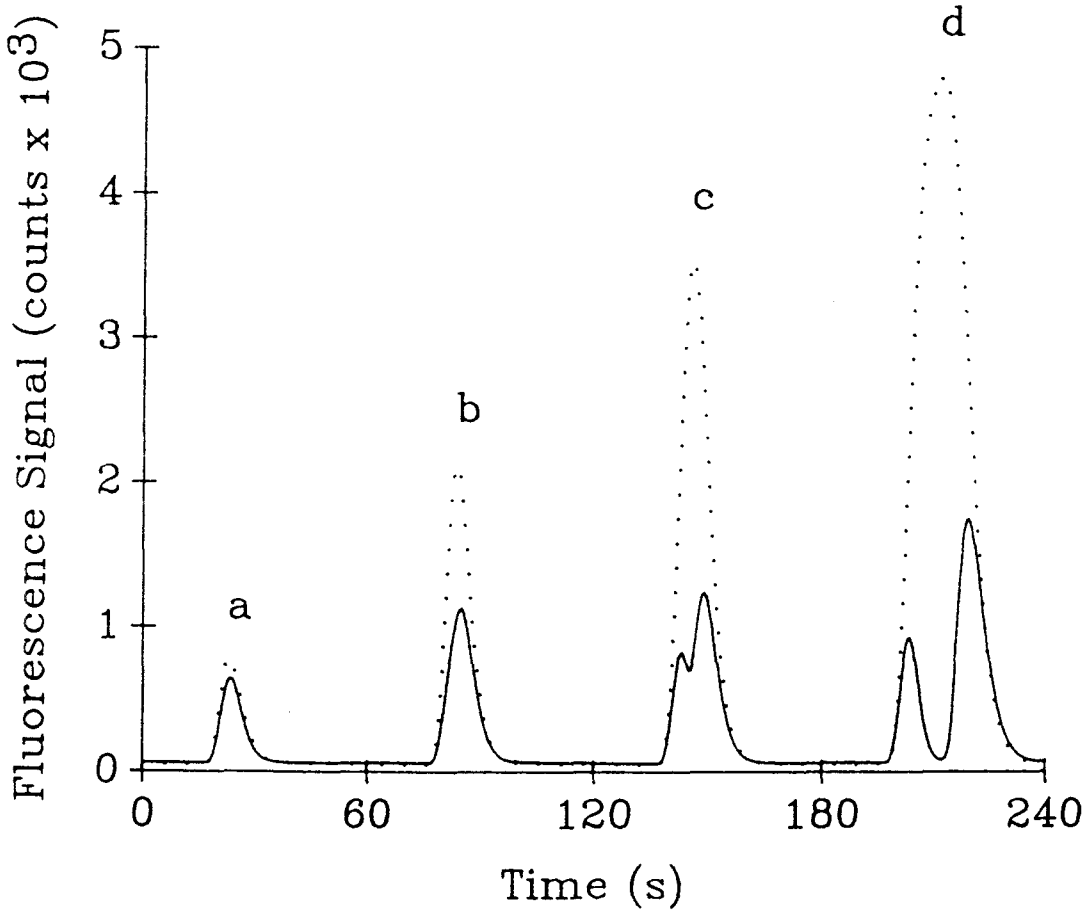

Figure VI.2. Dependence of the shape of the peak on the injected sample volume for QS (dotted line) and Al^{3+} (solid line) injected into an AAGR carrier stream. Injection volume: (a) 30 µL; (b) 100 µL; (c) 200 µL; (d) 500 µL. QS conc., 1 µg/mL; Al^{3+} conc., 1 µg/mL; flow rate, 2.0 mL/min.

shows superimposed detector responses of non-kinetic (dashed line) and kinetic (solid line) cases. The sample loop volume affects the shape of peak much more dramatically when a relatively slow chemical reaction is involved. When a chemical reaction is still in progress at the time of detection, the peak shape is affected both by physical dispersion and reaction kinetics.

Consider a second order reaction between the analyte and a reagent in a single-line FIA manifold for which the product is monitored. The amount of product formed, and hence the signal observed, at any point in the dispersed sample zone at the detector depends on several competing factors. First, the concentration of analyte varies throughout the sample zone as given by $C_A^o/D(t)$, where C_A^o is the initial analyte concentration, and is greatest at the maximum of the profile for a non-kinetic sample. This factor by itself would result in more product being formed in the center of the profile than at the edges of the profile. Second, the reagent concentration varies throughout the sample zone as described by $C_R^o(D(t) - 1)/D(t)$, where C_R^o is the reagent concentration in the carrier stream, and is least at the maximum of the profile for a nonreacting sample. This factor by itself would result in more product being formed away from the center of the profile. Note however, for small sample volumes yielding a large dispersion, $(D(t) - 1)/D(t) \simeq 1$ throughout the sample zone and effect of reagent dispersion is minor. Third, the analyte at the edges of the initial sample plug injected is in contact with the reagent longer than the analyte in the center of the plug. Thus, this factor by itself would result in more product being formed at the edges of the profile due

to a longer reaction time.

The shapes of the kinetic profiles shown in Figure VI.2 illustrate how the relative importance of these competing factors varies with the sample injection volume. For lower injected sample volumes (30 or 100 μL), the time for the peak maximum for kinetic peaks shifts slightly to longer times relative to non-kinetic peaks but the profiles are similar in shape. The dominant factor which affects the profile shape is the dispersion of the analyte. For smaller sample volumes, the absolute dispersion coefficient at the maximum is 3 or greater such that the reagent concentration (C_R) throughout the sample is relatively constant (i.e., $2C_R^0/3 < C_R < C_R^0$). However, for larger sample volumes (200 μL or larger), dual peaks are observed, which indicates that the shape of peak is affected more by the dispersion of the reagent and the reaction time. With the largest sample volume tested (500 μL), no mixing occurred between the sample and carrier stream in the middle of the sample zone (i.e., a steady-state signal due to undiluted analyte is observed). Near the region of no mixing, the limiting factor for the formation of product is the low concentration of the reagent and the short reaction time.

The data in Figure VI.2 also show that the shape of the profile in the leading region of the sample zone is fairly independent of the sample volume. This occurs because the dispersion coefficients ($D'(t)$) in the leading region are independent of the sample volume.

As shown in Figure VI.3, the shape of the dispersion-corrected profiles change significantly with the injected sample volume. For the 30-μL sample volume, the corrected profile is similar in shape to

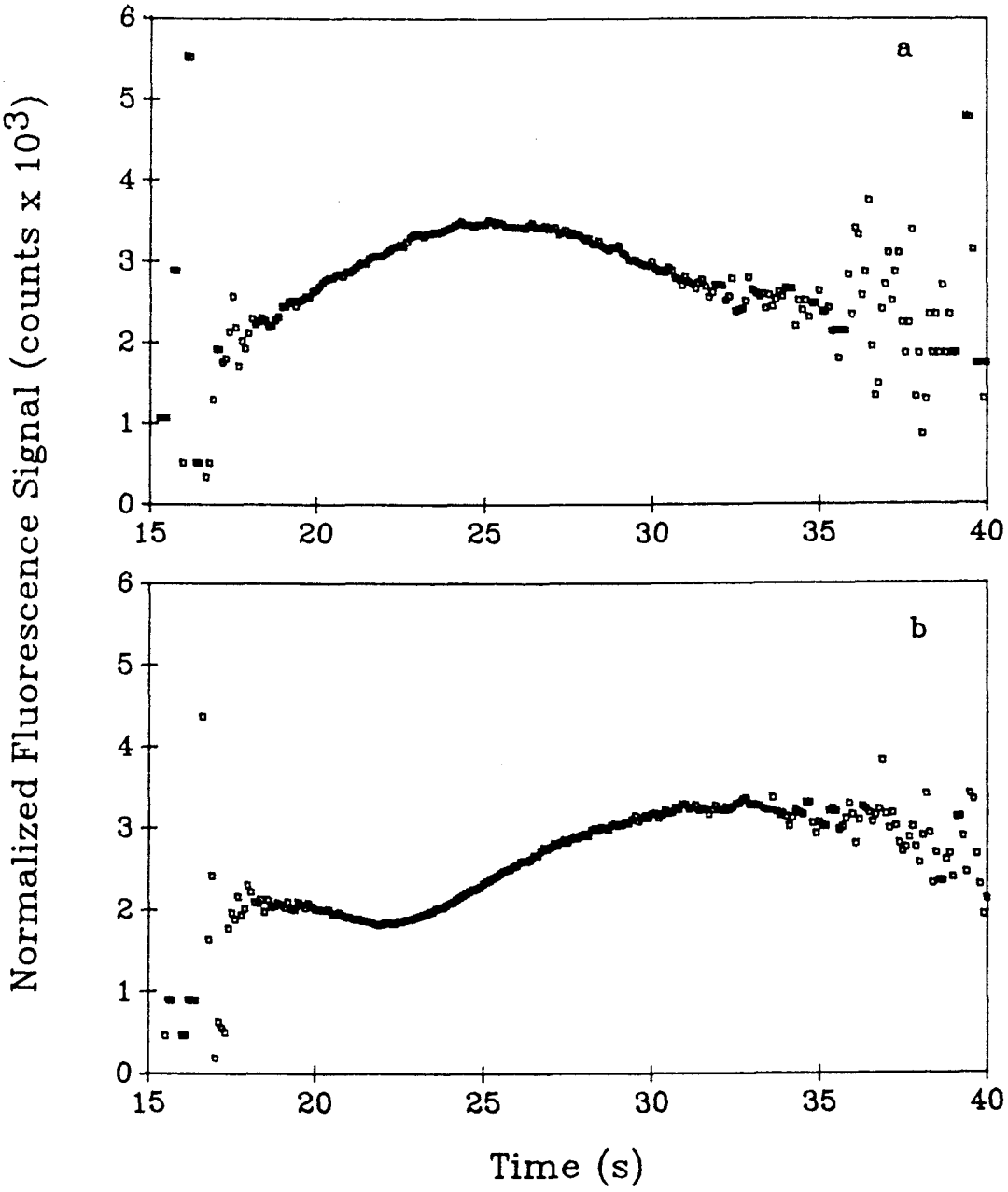

Figure VI.3. Dependence of dispersion-normalized profiles on injection volume: (a) 30 µL; (b) 100 µL; (c) 200 µL; (d) 500 µL. The absolute dispersion coefficients were used for normalization (6.54, 2.30, 1.37, and 1.00, respectively, at the maximum). Injected sample, 1 µg/mL Al^{3+}; flow rate, 2.0 mL/min.

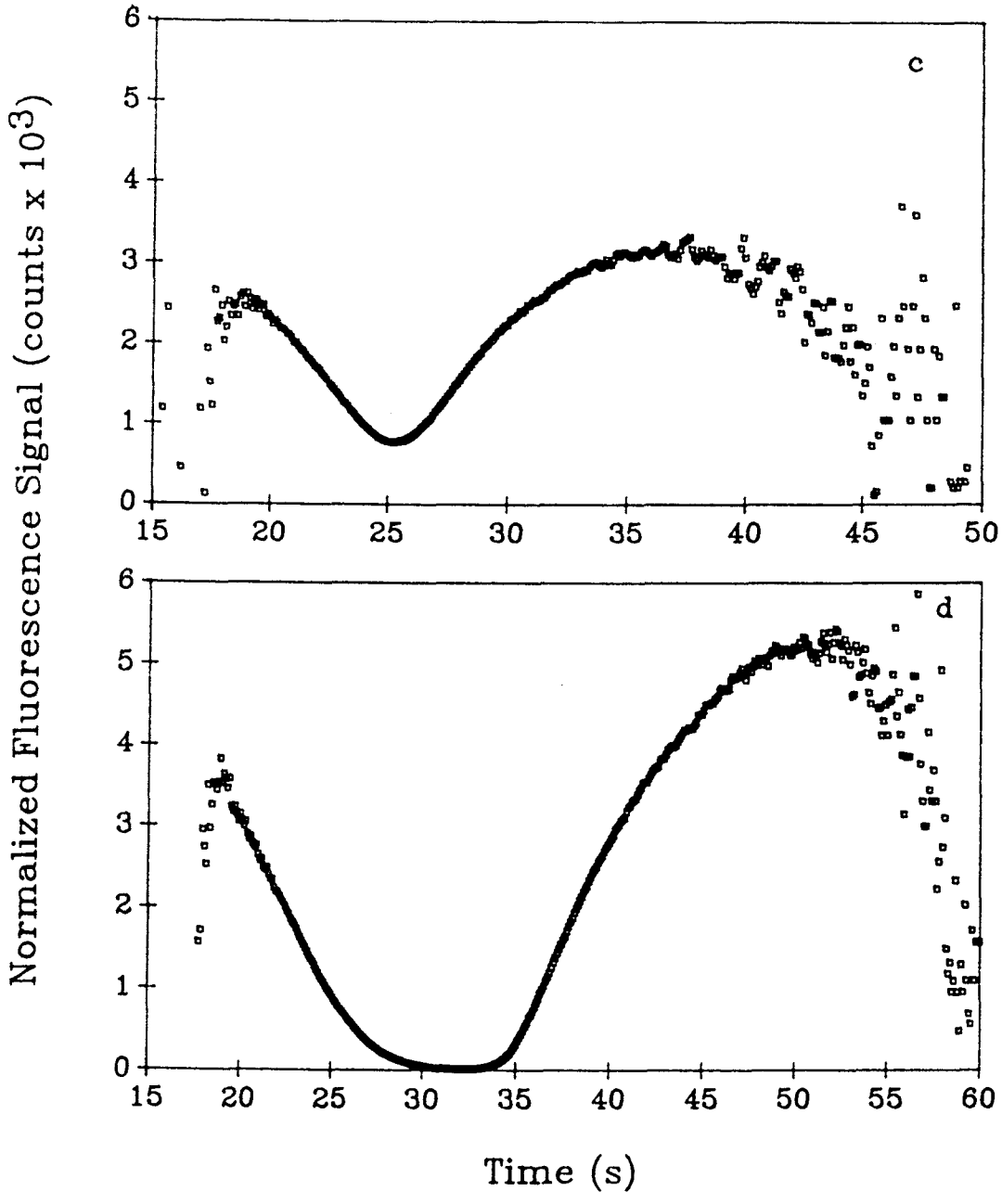

Figure VI.3. Continued

a normal FIA profile without a kinetic contribution. In this case, the absolute dispersion is relatively large throughout the profile such that the reagent concentration and the reaction time are similar throughout the profile. The maximum is near the center of the profile because the Al^{3+} concentration is the highest. When the sample volume is increased, the concentration of the reagent is significantly less near the center of the sample zone than at the edges. Also the Al^{3+} originally in the center of the sample zone has had much less time to react with the reagent. For sample volumes of 200 and 500 µL, dual peaks in the uncorrected profile and V-shaped corrected profile (Figures VI.3c and d) are observed. At or near the dip of the profile, there is little contribution from the chemical reaction because of the low reagent concentration and short reaction time. For the 500-µL sample volume, the fluorescence signal is effectively zero because no product has formed in the undiluted central sample zone.

Even though the ratio of reagent to sample concentrations varies throughout the sample profile due to the inherent characteristics of a single-line manifold, the fixed-time method can be applied to obtain reaction-rate information which compensates for the background signal due to non-reacting species. The fixed-time method was applied to the dispersion normalized profiles. The total measurement time was fixed (4.2 s) and the initial time for the calculation was adjusted to obtain the greatest rate for all cases. Figure VI.4 shows the effect of injected sample volume on the reaction rate. The RSD in the rate did not vary significantly with the sample volume. The calculated rate increases about a factor of 3 as the sample

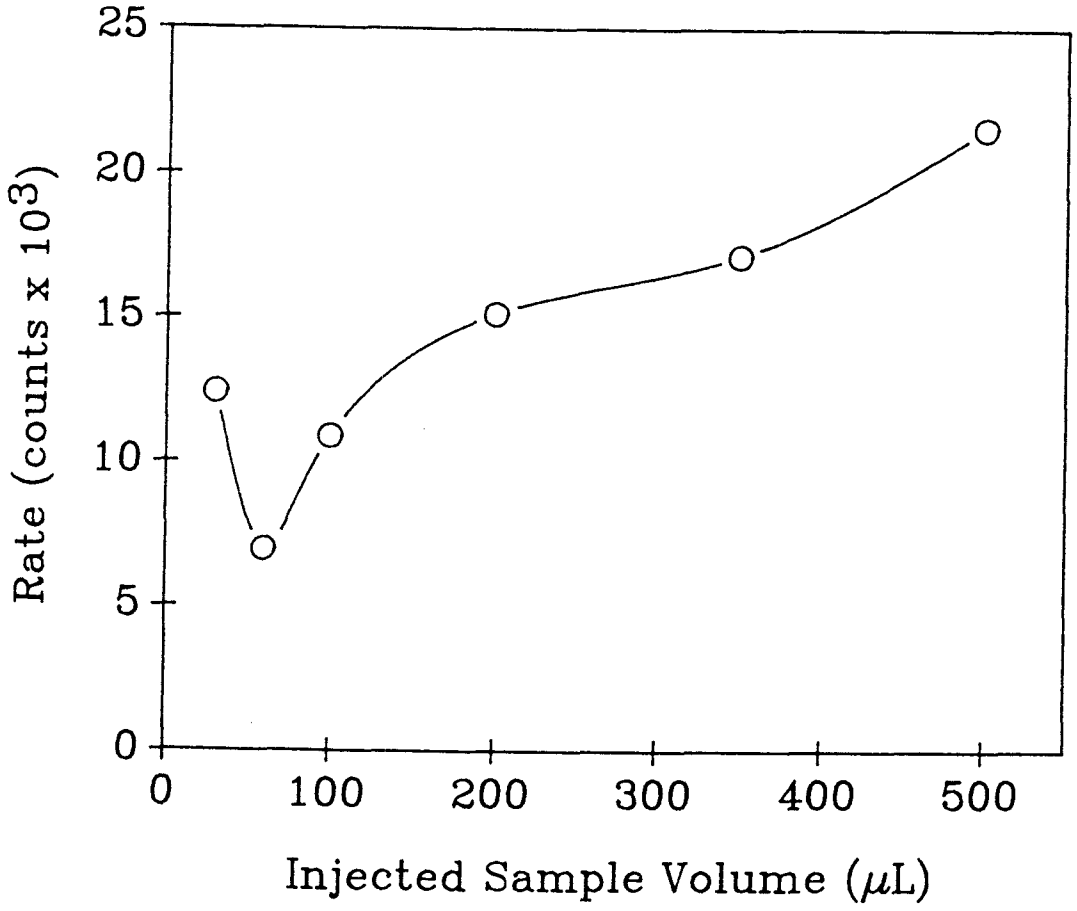

Figure VI.4. Dependence of the reaction rate on the injected sample volume. The starting times for the fixed-time calculation were 18.2, 21.1, 23.1, 27.1, 32.0, and 36.1 s for 30, 60, 100, 200, 350, and 500-µL injection volumes, respectively. Other conditions were same as in Figure VI.3.

volume is increased from 60 to 500 µL. The rate for the 30-µL sample size is greater than that for 60-µL sample size.

Note from the normalized profiles in Figure VI.3 that as the sample volume increases, a longer computational time for the fixed-time method can be used because the dispersed sample zone is larger. For further studies, a 200-µL sample volume was chosen. This sample volume yields a rate within 30% of that obtained with the largest sample volume tested (500 µL). Use of a 200-µL rather than 500-µL size has several advantages including lower sample consumption, higher sample throughput, and the fact that the minimum value of the normalized profile is at the maximum of the profile of the reference solution. The last factor makes it simple to identify the starting time for the fixed-time calculation. With a 500-µL sample loop, the central portion of the profile cannot be used because the dispersion coefficients are at or near 1.

Effect of Flow Rate

With a non-reacting sample (e.g., QS), the dispersion coefficient at the profile maximum (D_{max}) decreases in a non-linear fashion with increasing flow rate, indicating less dilution or a higher peak maximum. The peak area and the baseline width time decrease with increasing flow rate. Also, the rate of change of the dispersion coefficient of the sample zone with respect to time is greater at higher flow rates.

To observe the effect of flow rate on the chemical contribution of the sample profile, a 1 µg/mL Al^{3+} solution was injected into

the reagent carrier stream with flow rates varying from 1 to 4 mL/min. As shown in Figure VI.5, increasing the flow rate decreases both the peak height and the peak area. The peak height decreases with increasing flow rate in contrast to that observed for non-kinetic sample, primarily due to the smaller reaction time between the sample and reagent (the residence time between sample injection and detection). However, the general shape of the profiles appears to be independent of flow rate, indicating that the contribution of the concentration gradient to the shape of the profile of a sample zone is about same in all cases.

To calculate the reaction rate based on the fixed-time method, the time for the maximum of the reference profile was selected for the initial time with a total computational time of 4.0 s. Figure VI.6 shows that the calculated reaction rate increases somewhat with increasing flow rate up to about 2.5 mL/min and then varies little with flow rate. This behavior is due to the decrease in the total reaction time with increasing flow rate. When the flow rate is 2.5 mL/min or greater, a small enough fraction of Al^{3+} reacts over the 4-s computational period that the kinetics are pseudo-zero order. A flow rate of 2.5 mL/min was selected for further studies. The RSD of the rate did not significantly vary with flow rate.

Effect of the Reagent Concentration

As previously discussed, the reagent concentration varies throughout the sample zone. With a 200-μL sample size and 2.5 mL/min flow rate, the absolute dispersion coefficient varies from 1.5 to ∞

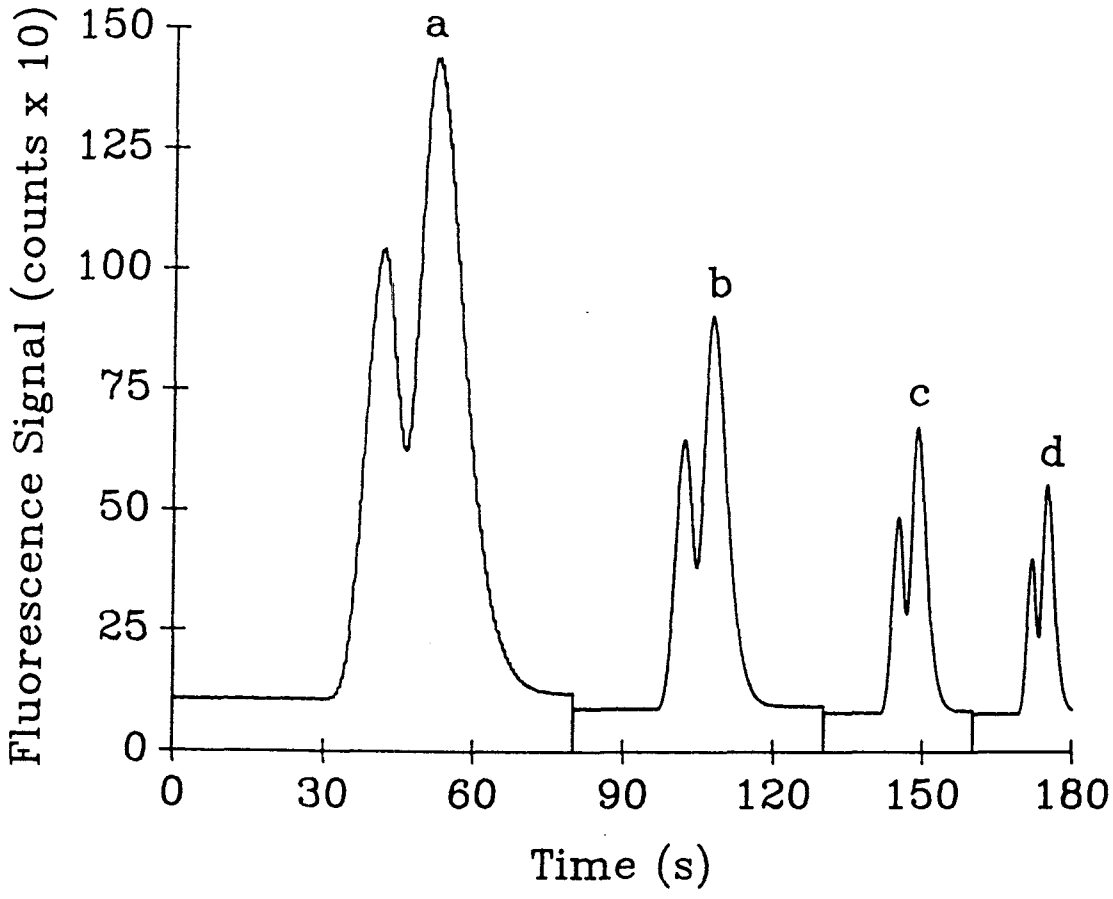

Figure VI.5. Effect of flow rate on the FIA profiles for Al^{3+} injected into a AAGR reagent carrier stream: (a) 1.0 mL/min; (b) 2.0 mL/min; (c) 3.0 mL/min; (d) 4.0 mL/min. Injected sample, 1 µg/mL Al^{3+}; Injection volume, 200 µL.

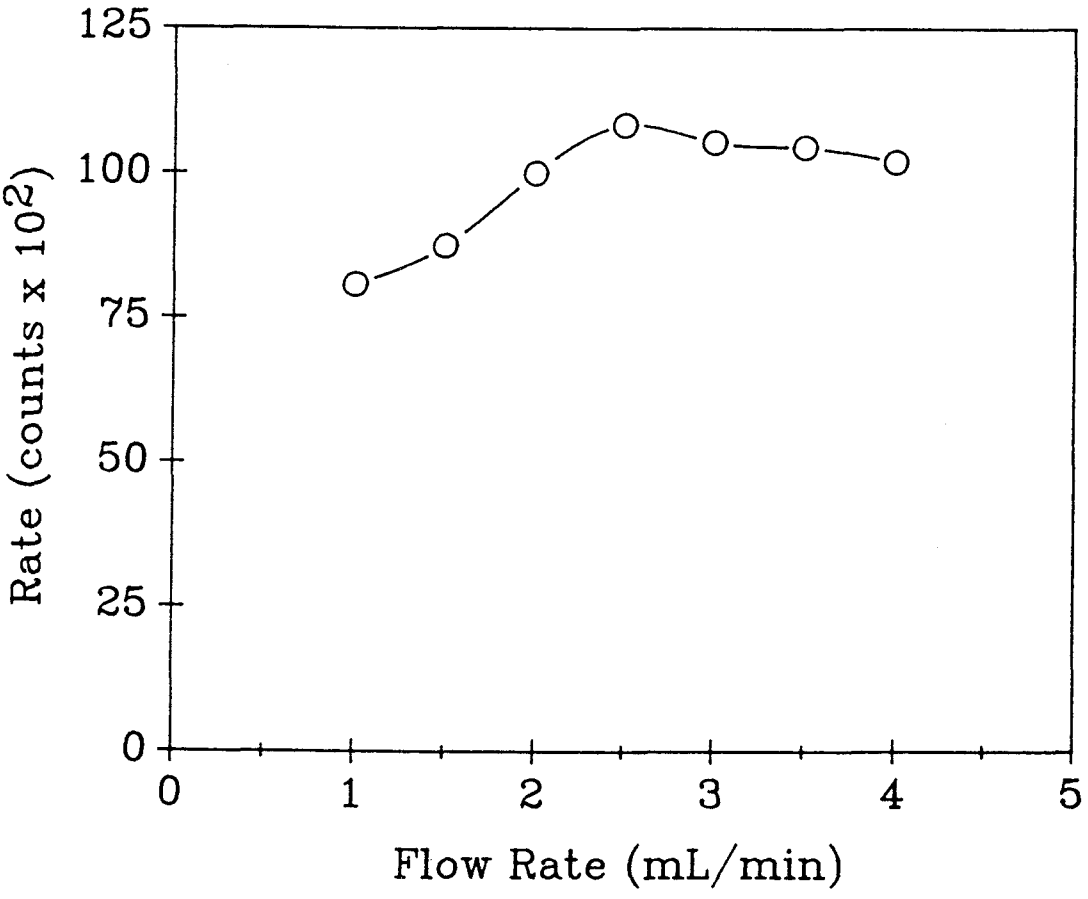

Figure VI.6. Dependence of the reaction rate on the flow rate. Injected sample, 1 µg/mL Al^{3+}; injection volume, 200 µL.

which means that the reagent concentration varies from its initial value to about 33% of the initial value at the center of the sample zone. To evaluate the effect of the reagent concentration on the profile of the peak and the reaction rate, 200 µL of a 1 µg/mL Al^{3+} solution was injected into carrier streams containing five different AAGR concentrations (50 - 250 µg/mL). As shown in Figure VI.7, the peak area, which provides more direct information about the peak size, increases as the AAGR concentration increases. Also the two peak maxima shift toward the center of the sample zone.

The rate with a fixed-time interval of 2.6 s and an initial time of 19.5 s was calculated from the dispersion normalized profiles. The effect of the AAGR concentration on the total peak area and reaction rate are compared in Figure VI.8. The peak area continually increases with increasing AAGR concentration, while the calculated reaction rate reaches a maximum value at about 150 µg/mL. This concentration was chosen for further studies because the dependence of the rate on AAGR concentration is slight.

Campi found that the rate measured in a conventional sample cell was fairly independent of AAGR concentration above a reaction mixture AAGR concentration of about 40 µg/mL [16]. With a 150 µg/mL AAGR carrier stream, the AAGR concentration at the center of the profile is about 50 µg/mL. Thus the results observed in this study are consistent with the data reported by Campi.

Characteristics of the Analytical Method

With the optimized experimental conditions described in the

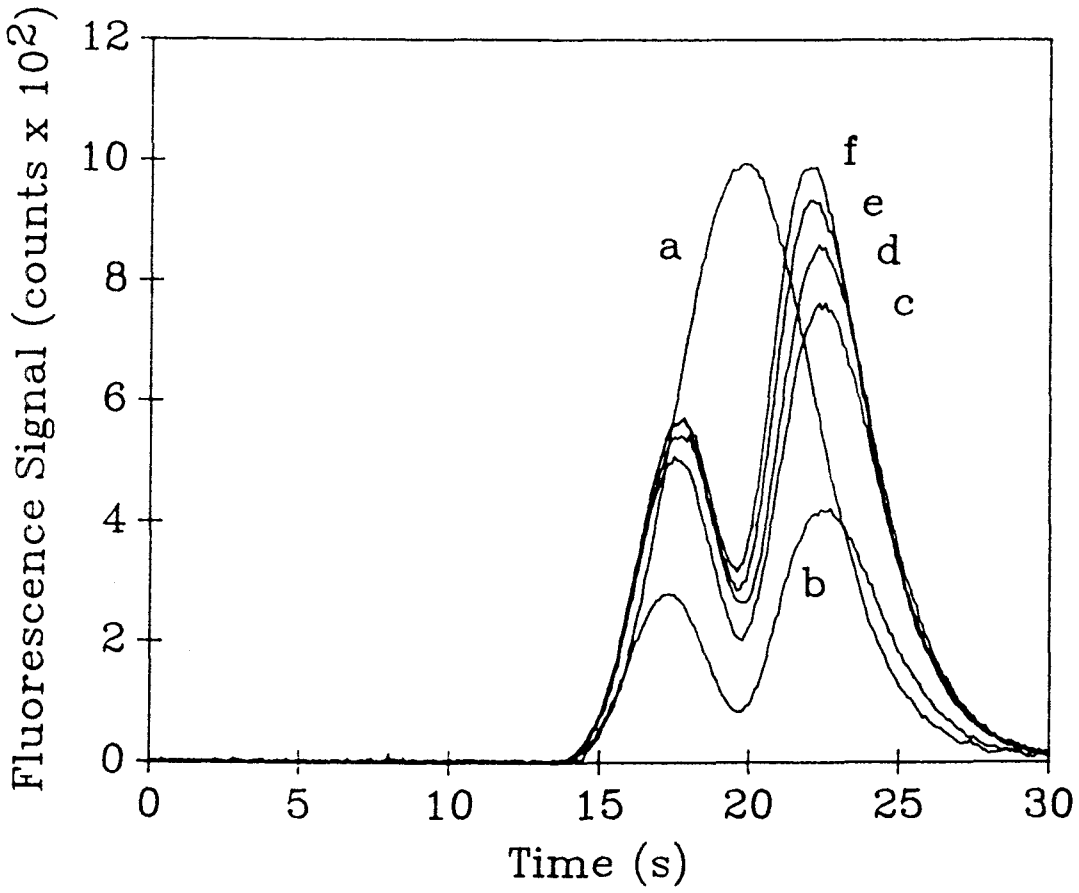

Figure VI.7. Dependence of the FIA profiles for Al^{3+} injected into a AAGR carrier stream on the concentration of AAGR: (a) equilibrated Al^{3+}-AAGR solution; (b) 50 µg/mL; (c) 100 µg/mL; (d) 150 µg/mL; (e) 200 µg/mL; (f) 250 µg/mL. Al^{3+} conc., 1 µg/mL; injection volume, 200 µL; flow rate, 2.5 mL/min.

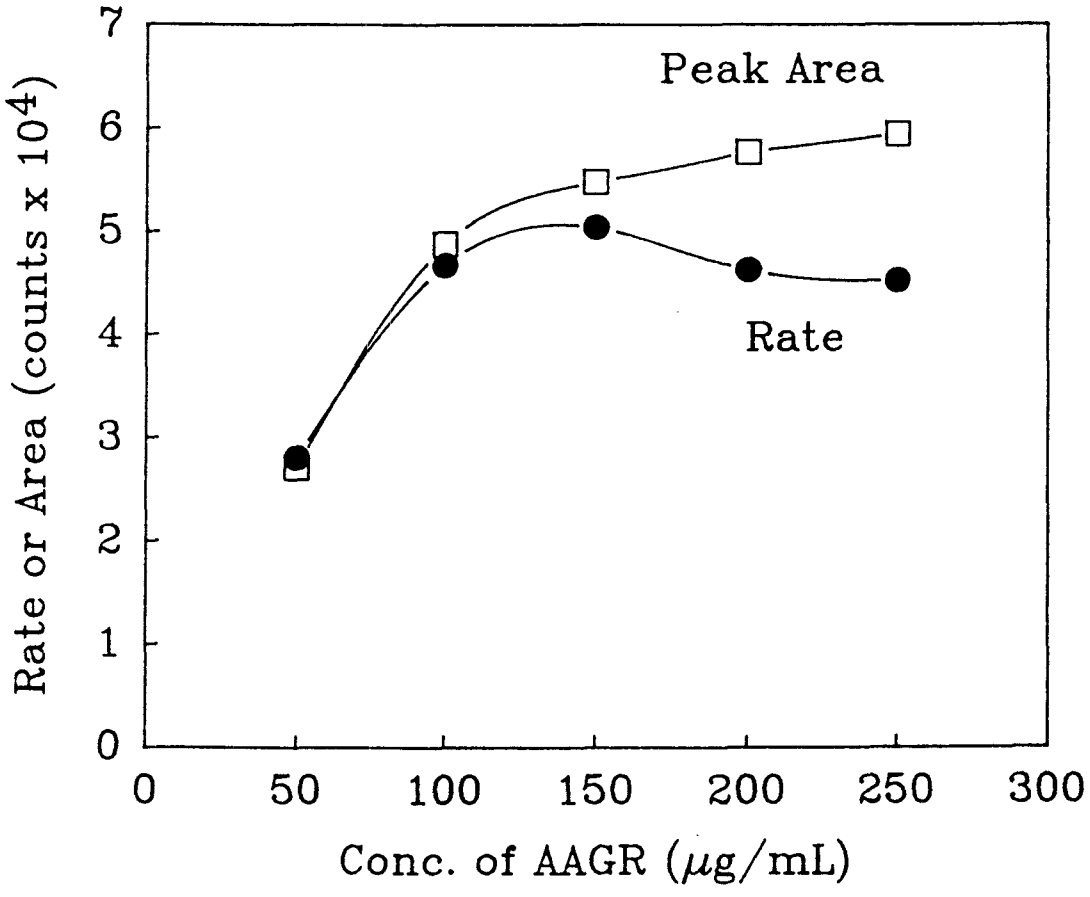

Figure VI.8. Dependence of the reaction rate on the concentration of AAGR. Al^{3+} conc., 1 µg/mL; injection volume, 200 µL; flow rate, 2.5 mL/min.

previous sections, the FIA peak profiles for the Al^{3+} standards of 0.025 to 10 µg/mL were obtained and saved as disk files for further analysis. The rate computational period was 6.4 s, which corresponds to the time between the maximum and 10% of the maximum for the reference profile (equilibrated Al^{3+} and reagent) in the same FIA manifold. Over this time interval, the dispersion coefficient varies from 1.4 to 14. The baseline-width time was 14.9 s for the reference and 20.6 s for the sample.

The calibration curves based on the peak height (2nd peak) and the area, which are most common descriptors of flow injection peaks, are linear. This is expected because the relative dispersion remains constant at every point of a given sample profile, but the amount of product formed at any point is proportional to the Al^{3+} concentration. The double-peak method of Valcarcel and co-workers [8] (i.e., the difference between the heights of the two maxima) also provides a linear plot. The calibration curve based on the proposed reaction rate method, shown in Figure VI.9, is linear up to 7 µg/mL Al^{3+}. This suggests that the reaction kinetics are near pseudo-first order in Al^{3+}.

Table VI.III summarizes the calibration data for the peak height, peak area, double-peak, and reaction-rate methods. For the peak height method, the maximum signal value for the second peak of the dual peaks (corresponding to a longer reaction time) was obtained with the computer program. The blank signal for the peak height, peak area, or double-peak methods were obtained at the same times or over the same time interval used for sample injections. The precision at 1 µg/mL Al^{3+} is best for the peak height method. The

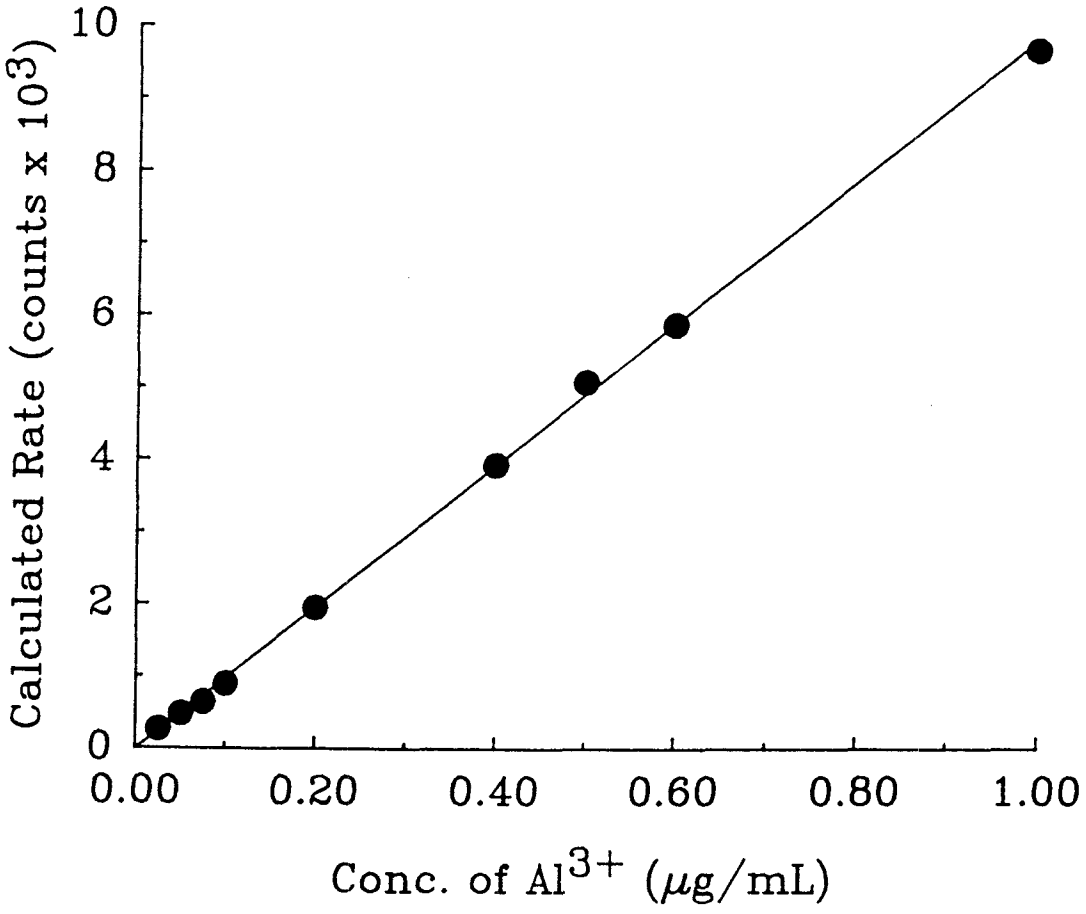

Figure VI.9. Calibration curve for the determination of Al^{3+} based on the rate method. Injection volume, 200 µL.

Table VI.III. Calibration Data Based on the Peak Height, Peak Area, Double-Peak, and Reaction-Rate Methods

Method	Slope (counts/(μg/mL))	RSD[a] (%)	DL (ng/mL)
peak height	431	0.33	7
peak area[b]	405×10^2	1.1	9
double-peak	150	0.96	24
rate	198×10^2	0.98	13

[a]For 1 μg/mL Al^{3+}.

[b]Area from peak maximum to 1% of maximum.

peak height would be expected to be least affected by the variance in dispersion due to between-run variations in injection time or flow rate. The peak area, double-peak, and rate methods yield comparable reproducibility.

The detection limits for Al^{3+} with the four methods, also shown in Table VI.III, are within a factor of 3 of each other. The detection limit is defined as twice the SD of the blank signal divided by the slope of the calibration curve. The SD of the blank signal was obtained from ten repetitive injections of the true blank solution into the reagent carrier stream. The detection limit with the rate method or the other methods in this study is considerably worse than that reported by Campi (0.1 ng/mL). The difference is due in part to the use of a shorter effective measurement time (6.4 s vs. 16 s), the use of a 1-mm pathlength flow cell in place of a 10-mm pathlength cuvette, and the greater average dilution of the Al^{3+}. According to these results, the proposed reaction rate method in a single-line manifold can be used as a true kinetics-based technique without a significant loss in detectability.

Determination of Al^{3+} with Riboflavin

To evaluate the accuracy and applicability of the proposed reaction-rate method for samples containing a fluorescent interferent, mixtures of Al^{3+} and riboflavin were tested. Riboflavin was chosen as a test interferent because it does not react with AAGR reagent mixture but fluoresces significantly with the excitation and emission conditions used for the Al^{3+} determination. The presence

of riboflavin in a sample containing Al^{3+} causes the signal at all points in the profile to be too high as determined by the dispersion of the riboflavin and its concentration as shown in Figure VI.10.

FIA profiles were obtained in triplicate for synthetic samples containing 1 or 2 μg/mL Al^{3+} and different concentrations of riboflavin. From the profiles, the peak height, peak area, rate with the double-peak method, and rate with the proposed method were obtained and are summarized in Table VI.IV. The proposed reaction method does discriminate against the interference from a non-reacting fluorescent species. The maximum error is 4%. The peak height, area, and double-peak methods suffer significant interference due to riboflavin. The increase in peak area and peak height for a given concentration of Al^{3+} is proportional to the concentration of riboflavin.

The double-peak method is not a true kinetic method because it does not in general discriminate against non-reacting fluorescent species. Moreover, the presence of an interfering species causes the times for the peak maxima to shift. The double-peak method would discriminate against a non-reacting species if the peak values were normalized for dispersion before the difference was taken.

Figure VI.11 shows the FIA normalized profiles with and without riboflavin present. Note that the shape of the normalized profile and the slope are not affected by the presence of riboflavin. The riboflavin just contributes a dc level to the profile.

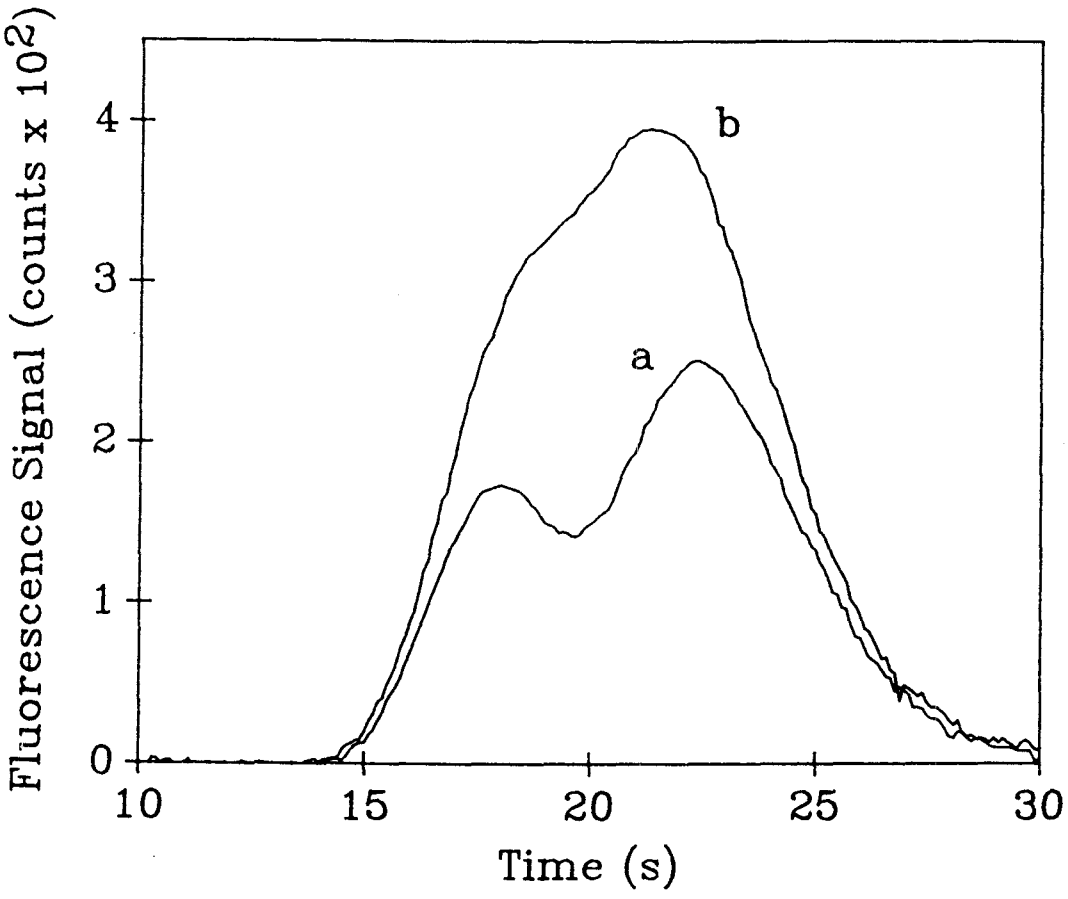

Figure VI.10. Effect of riboflavin on the peak profile of Al^{3+}: (a) without riboflavin; (b) with riboflavin. Al^{3+} conc., 1 µg/mL; riboflavin conc., 5 µg/mL.

Table VI.IV. Determination of Al^{3+} in Synthetic Samples Containing Riboflavin

Al^{3+} conc. (µg/mL)	Riboflavin conc. (µg/mL)	Peak area[a] (counts x 10^2)	Error (%)	Peak height[a] (counts)	Error (%)
1	0	179 (0.81)		245 (4.4)	
1	1	199 (1.0)	11	277 (2.9)	13
1	2	221 (1.6)	23	302 (3.8)	23
1	3	244 (1.3)	36	329 (1.6)	34
1	5	288 (5.1)	61	392 (3.9)	60
2	0	350 (3.9)		464 (7.6)	
2	1	371 (4.0)	6.0	487 (6.8)	4.9
2	2	392 (1.3)	12	509 (3.3)	9.7
2	3	411 (1.6)	17	537 (5.2)	16
2	5	457 (2.9)	30	590 (3.8)	27

[a]% RSD in ( ).

Table VI.IV. Continued

Al^{3+} conc. (μg/mL)	Riboflavin conc. (μg/mL)	Double Peak[a] (counts)	Error (%)	Reaction Rate[a] (counts x 10^2)	Error (%)
1	0	72 (4.4)		93.0 (2.8)	
1	1	77 (4.3)	6.9	90.8 (2.3)	2.4
1	2	81 (4.7)	13	95.1 (2.3)	2.4
1	3	87 (6.0)	21	93.6 (4.5)	0.68
1	5	94 (2.0)	31	92.3 (3.7)	0.77
2	0	136 (1.4)		193 (0.93)	
2	1	142 (1.6)	4.4	197 (3.0)	2.1
2	2	146 (3.6)	7.4	193 (1.8)	0.27
2	3	149 (3.8)	9.6	192 (2.7)	0.86
2	5	165 (2.9)	21	187 (2.4)	3.5

[a]% RSD in ( ).

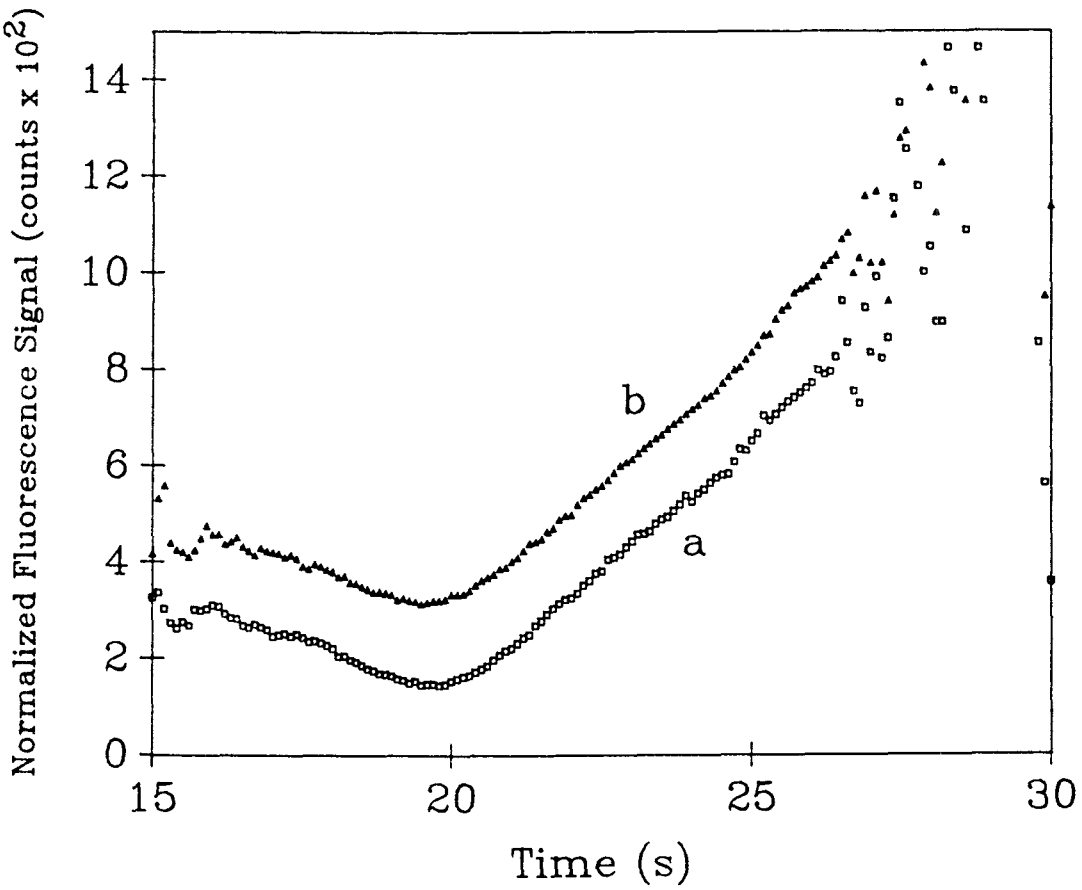

Figure VI.11. Normalized profiles from the data in Figure VI.10: (a) without riboflavin; (b) with riboflavin.

CONCLUSIONS

The signal in dispersion-normalized FIA profiles varies across the profile if the reaction between the analyte and reagents is relatively slow. It is demonstrated that analytical kinetic information can be extracted from the normalized profile. The kinetic method discriminates against non-reacting interferents that yield a detector signal because the normalized signal due to these interferences does not vary with time.

A primary advantage of the proposed kinetic measurement technique is that it can be used with simple single-line FIA systems without additional flow components or detectors. Thus it is simpler than FIA kinetic methods based on dual-injection values or multiple detectors. The sample throughput rate is greater than for the stopped-flow technique. The proposed technique does require microcomputer control and data acquisition and precise flow rates which is becoming more commonplace. Although the technique was demonstrated with fluorometric detection and monitoring of a reaction product, it is applicable to other detection techniques and for monitoring the disappearance of reactants. In the latter case, the normalized profile would be inverted relative to those presented (i.e., the normalized signal would decrease from the center to the edge of the profile.).

To use the new kinetic measurement technique, several conditions must be met. First, the reaction kinetics and the reagent concentrations must be adjusted such that it takes about a minute to tens of minutes for the reaction to reach completion in a normal

sample cell. Second, the amount of product formed at any point in the sample profile across the time interval used to extract kinetic information must be proportional to the analyte concentration. This condition requires that the reaction be first order in the analyte concentration and that the reagent concentrations be in sufficient excess relative to the maximum analyte concentration determined such that an insignificant amount of the reagents is consumed (effectively pseudo-first order in the analyte at any point in the profile). Note that the reagent concentration necessarily does vary across the profile such the normalized signal is not linear with time unless the reaction is zero-order in the reagents. Third, the carrier stream flow rate, the sample injection volume, and reaction coil length must be adjusted so that the criteria for condition two above are met and that a detectable change in product concentration occurs over the rate computational period (typically 5 to 15 s). In general, relatively large sample loop volumes (200 μL or greater) must be used so that the dispersion at peak maximum of the reference solution is low (D_{max} = 1-2) and the peak width is large enough (20-40 s) to obtain a sufficient reaction time. Under these conditions, the reaction time (the time the analyte and reagents are in contact before detection) increases from the center of the profile to the trailing edge as a first approximation, and the minimum signal in the normalized profile is convenient point for the beginning of the rate computational period.

REFERENCES

1. J. Ruzicka and E. H. Hansen, "Flow Injection Analysis", 2nd ed., Wiley, New York, 1988.

2. M. Valcarcel and M. D. Luque de Castro, "Flow Injection Analysis: Principles and Applications", Ellis Horwood, U. K., 1987.

3. E. H. Hansen, J. Ruzicka, and B. Rietz, Anal. Chim. Acta 1977, **89**, 241.

4. J. Ruzicka and E. H. Hansen, Anal. Chim. Acta 1979, **106**, 207.

5. J. Ruzicka and E. H. Hansen, Anal. Chim. Acta 1980, **114**, 19.

6. H. Kagenow and A. Jensen, Anal. Chim. Acta 1983, **145**, 125.

7. A. Fernandez, D. D. Luque de Castro, and M. Valcarcel, Analyst 1987, **112**, 803.

8. A. Fernandez, M. D. Luque de Castro, and M. Valcarcel, Anal. Chim. Acta 1987, **193**, 107.

9. C. C. Painton and H. A. Mottola, Anal. Chem. 1981, **53**, 1713.

10. D. J. Hooley and R. E. Dessy, Anal. Chem. 1983, **55**, 313.

11. J. F. Tyson, Anal. Chim. Acta 1986, **179**, 131.

12. A. A. Woods, J. Ruzicka, and G. D. Christian, Anal. Chem. 1987, **59**, 2767.

13. J. M Hungerford and G. D. Christian, Anal. Chim. Acta 1987, **200**, 1.

14. H. Wada, S. Hiraoka, A. Yuchi, and G. Nakagawa, Anal. Chim. Acta 1986, **179**, 181.

15. J. T. Vanderslice, G. R. Beecher, and A. G. Rosenfeld, Anal. Chem. 1984, **56**, 268.

16. G. L. Campi and J. D. Ingle, Jr., Anal. Chim. Acta 1989, **224**, 363.

17. M. A. Ryan and J. D. Ingle, Jr., Anal. Chem. 1980, **52**, 2177.

CHAPTER VII

CONCLUSIONS

The PC-based data acquisition and control system developed in this research has been shown to be a powerful and versatile tool. It provides the high resolution and wide dynamic range necessary for accurate characterization of time-varying signals in FIA and kinetics measurements with fluorometric monitoring. By controlling instrumental components such as injectors, sample-loop valves, and pumps, reproducibility is enhanced through synchronization of the data acquisition with the start of an experiment. Programs were written to display the acquired data on the monitor, save data files on floppy disks, and analyze the data. A critical feature is the ability to analyze the stored data with different computational parameters (e.g., a specific time segment of the data) or to analyze the data at a later time with new programs.

The fluorometric kinetic method for the determination of AA based on the condensation reaction between dehydroascorbic acid and OPDA has been shown to be a rapid, sensitive, and selective because the rate can be obtained in less than 30 s and steady-state background fluorescence can be discriminated. The reaction can be performed in a standard fluorometric sample cell without prior heating or column oxidation steps which are required in previous procedures based on the OPDA condensation reaction. It has been proved that $HgCl_2$ is a very effective oxidant for conversion of ascorbic acid to dehydroascorbic acid and does not cause spectral and

chemical interference. Studies have shown that photodecomposition of the OPDA and/or the monitored fluorescent product should be taken into consideration. When the measurement period is 25 s or less, the greatest rate and best detection limit are obtained with 0.1 M OPDA without significant photodecomposition. Although the fixed-time method for data reduction was used, other computational techniques such as the initial rate, variable-time, or curve fitting methods can also be employed with modification of software. This reaction should be also be suitable for FIA or HPLC post-column derivatization.

The single-line flow injection system used in this research has been shown to be a simple, fast, and effective diagnostic tool. With a valveless piston pump to provide accurate flow rate and precise control of the FIA components, the run-to-run reproducibility of the dispersed sample zone (fluorescence signal versus time) is excellent and allows the peak shape to be used to obtain additional information about a sample. Studies with QS show that the RSD of the signal is 1.1% or better for values as small as 1% of the peak maximum. Since the physical dispersion of the analyte solution for a given system can be defined by the dispersion coefficients, the peak shape for a sample of interest can be evaluated and compared to that of a reference solution for which only physical dispersion controls the peak profile. This concept has been used for the detection of concentration-dependent interferences and for the extraction of analytical kinetic data in FIA.

In fluorescence measurements, the shape of an FIA profile is distorted in the presence of absorbers or quenchers. It has been shown that these multiplicative interferences can be observed with a

single injection because the relative attenuation of the fluorescence signal varies throughout the sample zone and interference is greatest at the peak maximum where the analyte and interferent concentration are highest (lowest dispersion). The ratio of the reference peak profile (analyte solution with no interferences) which characterizes physical dispersion to a sample profile is shown to vary across the peak profile if a multiplicative interference is significant.

An empirical function introduced in this thesis normalizes for the difference in the analyte concentrations in the sample and the reference solutions and is used to determine the effect of the profile distortion quantitatively. A correction curve based on a plot of the relative attenuation of the peak height or area versus the value of the function was established. This curve and the value of the function for a sample are then used to determine a correction factor to multiply the peak height or area by. Although the type of concentration-dependent interference can not be identified, up to a 60% attenuation due to a multiplicative interference can be corrected without prior information. This method can not be used to detect additive interferences because the peak profile does not change. The correction method described in this thesis should also be applicable to cases where a fluorescent product is formed and detected because the reference profile can be established with an interference-free standard injected into the reagent carrier stream.

It has been proven that the dispersion coefficients established with a reference solution can be utilized to extract analytical kinetic information. The dispersion-normalized FIA profiles in the case that a slow chemical reaction occurs between the injected

analyte solution and a carrier reagent stream yields a signal that increases from the center to the trailing edge of the sample zone due to increased reaction time. The change in signal with time provides rate information and discriminates against species that do not react but that contribute a fluorescence signal.

To use the proposed kinetic method, the reaction should be first order in the analyte concentration at any point and a significant change in product concentration should occur during the measurement period (typically 5 to 15 s). Because the reagent concentration necessarily does vary across the profile, a non-linear signal as a function of time is observed. FIA variables such as the carrier stream flow rate, the sample injection volume, and reaction coil length must be adjusted to satisfy above conditions. A relatively large sample loop (e.g., 200 μL) is advantageous because the peak width is large enough (20-40 s) to obtain a sufficient reaction time and the reaction time increases from the center of the profile to the trailing edge. In this case, the beginning of the rate computational period can be chosen at the minimum signal in the normalized signal. In general, the fixed-time computational method is recommended because the different reaction conditions at all points in the profile need not be controlled.

The proposed method has been demonstrated for the determination of Al^{3+} in a sample containing a non-reacting fluorescent species (riboflavin). The non-reacting interferent does not contribute to the rate because the normalized signal due to the interferent is constant over the profile. The proposed kinetic measurement technique offers advantages over conventional FIA-kinetic methods. A

simple single-line FIA system can be used without additional flow components or detectors. The sample throughput rate is greater than for the stopped-flow technique.

In this thesis, a single-line FIA system with a digital data acquisition system has shown to be a powerful analytical tool to develop new methods utilizing the shape of the peak. The overall dispersion at the time of detection has been the basis of the research. Future studies might be concerned with using theoretical models describing sample dispersion which would allow a more comprehensive optimization of experimental conditions. The effect of the type and length of reaction coil, which was not studied in this thesis, should be explored.

It might be possible to apply dispersion normalization techniques to extract kinetic information with the merging zone method. For example, the concentration of the reagent could be adjusted to be constant throughout the dispersed sample zone. To satisfy this condition, a volume of reagent solution much larger than the sample volume could be injected with a reagent injection loop. The dispersion of the analyte in the mixture after the confluence of the two streams would determine the reaction time. In this case, the reaction time would increase for the analyte from the leading edge to the falling edge of the sample zone. Thus, normalization of the peak profile can provide more direct information about the chemical kinetics without the complication of a varying reagent concentration throughout the profile due to dispersion. Addition of a injection valve for the reagent would also minimize reagent consumption.

The kinetic method described in this thesis should be applicable

to FIA systems using other detection techniques such as spectrophotometric monitoring. The proposed kinetic method should also be applicable for monitoring the disappearance of reactants. Many chemical reactions whose initial rate can be measured in a standard sample cell can be adapted to the proposed FIA kinetic measurement technique.

The general concept of comparing the FIA profile of a reference solution (i.e., a pure analyte standard) to the profile of a sample solution should become a powerful general tool for detecting certain types of interferences with any detection technique. If the ratio of the profiles is constant across the sample zone, physical dispersion controls the sample profile. However, if this ratio varies across the profile, then species in the sample, but not the standard, are affecting the response from the analyte. Even if a chemical reaction is occurring, the shape of the profile will be changed by interferences that affect the kinetics or the signal derived from the analyte.

BIBLIOGRAPHY

K. Adamson, J. E. Sell, J. F. Holland, and A. Timnick, Am. Lab. 1984, 16(11), 16.

H. A. Baines, J. Soc. Chem. Ind. 1930, 49 PT, 481T

M. Z. Barakat, M. F. Abdel-Wahab, and M. M. El-Sadr, Anal. Chem. 1955, 27, 536.

M. Z. Barakat, S. K. Shehab, N. Darwish, and A. El-Zoheiry, Anal. Biochem. 1973, 53, 245.

H. Bergamin, E. A. G. Zagatto, F. J. Krug, and B. F. Reis, Anal. Chim. Acta 1978, 101, 17.

H. U. Bergmeyer, A. Hagen, Fresenius Z. Anal. Chem. 1972, 261, 333.

O. A. Bessey and C. G. King, J. Biol. Chem. 1933, 103, 687.

D. Betteridge, Anal. Chem. 1978, 50, 832A.

W. J. Blaedel and G. P. Hicks, Anal. Chem. 1962, 34, 388.

W. J. Blaedel and D. L. Petitijean, Anal. Chem. 1958, 30, 1958.

S. H. Brolks, D. V. Leff, M. A. Hernandez Torres, and J. D. Dorsey, Anal. Chem. 1988, 60, 1737.

G. L Campi and J. D. Ingle, Jr., Anal. Chim. Acta 1989, 224, 225.

G. L Campi and J. D. Ingle, Jr., Anal. Chim. Acta 1989, 224, 363.

P. W. Carr, Anal. Chem. 1978, 50, 1602.

G. D. Clark, G. D. Christian, J. Ruzicka, G. F. Anderson, and J. A. van Zee, Anal. Instr. 1989, 18, 1.

E. Cordos, S. R. Crouch, and H. V. Malmstadt, Anal. Chem. 1968, 40, 1812.

S. R. Crouch, Anal. Chem. 1969, 41, 880

J. E. Davis and B. Renoe, Anal. Chem. 1979, 51, 529.

M. J. Deutsch and C. E. Weeks, J. Assoc. Off. Anal. Chem. 1965, 48, 1248.

F. T. M. Dohmen and P. C. Thijssen, Talanta 1986, 33, 107.

D. C. Egberg, R. H. Potter, and J. C. Heroff, J. Assoc. Off. Anal. Chem. 1977, 60, 126.

C. B. Elliott, Ph.D. thesis, Oregon State University, 1982.

D. F. Evered, Analyst 1960, **85**, 515.

A. Fernandez, M. D. Luque de Castro, and M. Valcarcel, Anal. Chim. Acta 1987, **193**, 107.

A. Fernandez, D. D. Luque de Castro, and M. Valcarcel, Analyst 1987, **112**, 803.

G. G. Guilbault, CRC Crit. Rev. Anal. Chem. 1970, 377.

G. G. Guilbault, P. Brignac, Jr., and M. Zimmer, Anal. Chem. 1968, **40**, 190.

D. Gupta, P. D. Sharma, and Y. K. Gupta, Talanta 1975, **22**, 913.

E. H. Hansen, J. Ruzicka, and R. Rietz, Anal. Chim. Acta 1977, **89**, 241.

L. Hargis, Anal. Chem. 1969, **41**, 597.

G. M. Hieftje and G. R. Haugen, Anal. Chim. Acta 1981, **123**, 255.

D. J. Hooley and R. E. Dessy, Anal. Chem. 1983, **55**, 313.

J. M Hungerford and G. D. Christian, Anal. Chim. Acta 1987, **200**, 1.

J. D. Ingle, Jr. and S. R. Crouch, Anal. Chem. 1970, **42**, 1055.

J. D. Ingle, Jr. and S. R. Crouch, Anal. Chem. 1971, **43**, 697.

J. D. Ingle, Jr. and S. R. Crouch, "Spectrochemical Analysis", Prentice Hall, New Jersey, 1988.

J. D. Ingle, Jr. and M. A. Ryan, "Reaction Rate Methods in Fluorescence Analysis" in "Modern Fluorescence Spectroscopy", E. L. Wehry, ed., Plenum Press, New York, 1981, Vol 3, Chap. 3, pp 95-141.

J. D. Ingle, Jr., M. J. White, and E. D. Salin, Anal. Chem. 1982, **54**, 56.

G. E. James and H. L. Pardue, Anal. Chem. 1969, **41**, 1618.

T. Janjic, G. Milovanovic, and M. Celap, Anal. Chem. 1970, **42**, 27.

H. Kagenow and A. Jensen, Anal. Chim. Acta 1983, **145**, 125.

M. I. Karayannis, Anal. Chim. Acta 1975, **76**, 121.

S. D. Kolev and E. Pungor, Anal. Chem. 1988, **60**, 1700.

E. E. Kriss, G. T. Kurbatova, and K. B. Yatsimirskii, Zhurnal Analiticheskoi Khimii 1976, **31**, 598.

J. B. Landis, M. Rebec, and H. L. Pardue, Anal. Chem. 1977, 49, 785.

F. Lazaro, M. D. Luque de Castro, and M. Valcarcel, Anal. Chim. Acta 1984, 165, 177.

O. H. Lowry, N. R. Roberts, and J. I. Kapphahn, J. Biol. Chem. 1957, 224, 1047.

M. D. Luque de Castro, and M. Valcarcel, Analyst 1984, 109, 413.

L. J. Machlin, "Handbook of Vitamins: Nutritional, Biomedical, and Clinical Aspects", M. Dekker, New York, 1984.

H. V. Malmstadt and S. R. Crouch, J. Chem. Educ. 1966, 43, 340.

H. A. Malmstadt, C. J. Delaney, and E. A. Cordos, CRC Crit. Rev. Anal. Chem. 1972, 559.

H. V. Malmstadt and T. P. Hadjiioannou, Anal. Chem. 1962, 34, 452.

H. V. Malmstadt and T. P. Hadjiioannou, Anal. Chem. 1962, 34, 455.

H. V. Malmstadt and T. P. Hadjiioannou, Anal. Chem. 1963, 35, 14.

H. V. Malmstadt and G. P. Hicks, Anal. Chem. 1960, 32, 394.

H. V. Malmstadt and H. L. Pardue, Anal. Chem. 1961, 33, 1040.

G. E. Mieling and H. L. Pardue, Anal. Chem. 1978, 50, 1611.

H. A. Mottola, CRC Crit. Rev. Anal. Chem. 1975, 229.

H. A. Mottola, Anal. Chem. 1981, 53, 1312A.

H. A. Mottola and H. B. Mark, Jr., Anal. Chem. 1986, 58, 264R.

C. N. Murtyand N. G. Bapat, Z. Anal. Chem. 1963, 199, 367.

S. P. Mushran and M. C. Agrawal, J. Scient. Ind. Res. 1977, 36, 274

G. Nagy, Z. Feher, and E. Pungor, Anal. Chim. Acta 1970, 52, 47

S. Olsen, J. Ruzicka, and E. H. Hansen, Anal. Chim. Acta 1982, 136, 101.

J. Ottaway, J. Fuller, and J. Allan, Analyst 1969, 94, 522.

L. A. Pachla, D. L. Reynolds, and P. T. Kissinger, J. Assoc. Off. Anal. Chem. 1985, 68, 1.

C. C. Painton and H. A. Mottola, Anal. Chem. 1981, 53, 1713.

C. C. Painton and H. A. Mottola, Anal. Chim. Acta 1984, 158, 67.

K. S. Panwar, S. P. Rao, and J. N. kGaur, Anal. Chim. Acta 1961, 25, 218.

H. L. Pardue, Anal. Chim. Acta 1989, 216, 69.

H. L. Pardue, C. S. Frings, and C. J. Delaney, Anal. Chem. 1965, 37, 1426.

R. A. Parker and H. L. Pardue, Anal. Chem. 1970, 42, 56.

L. T. M. Prop , P. C. Thijssen, and L. G. G. Van Dongen, Talanta 1985, 32, 230.

A. U. Ramsing, J. Ruzicka, F. J. Krug, and E. A. G. Zagatto, Anal. Chim. Acta 1981, 129, 1.

C. B. Ranger, Anal. Chem. 1981, 53, 21A.

W. Roberts, Proc. Roy, Soc. London 1881, 32, 145.

B. Rocks and C. Riley, Clin. Chem. 1982, 28, 409.

J. H. Roe and C. A. Kuether, Anal. Biochem. 1943, 43, 399.

R. B. Roy and A. Conetta, Food Technology 1976, 94.

R. A. Roy, A. Conneta, and J. Saltpeter, J. Assoc. Off. Anal. Chem. 1976, 59, 1244.

J. Ruzicka, Anal. Chem. 1983, 55, 1040A.

J. Ruzicka and E. H. Hansen, Anal. Chim. Acta 1975, 78, 145.

J. Ruzicka and E. H. Hansen, Anal. Chim. Acta 1978, 98, 1.

J. Ruzicka and E. H. Hansen, Anal. Chim. Acta 1978, 99, 37.

J. Ruzicka and E. H. Hansen, Anal. Chim. Acta 1979, 106, 207.

J. Ruzicka and E. H. Hansen, Anal. Chim. Acta 1980, 114, 19.

J. Ruzicka and E. H. Hansen, Anal. Chim. Acta 1986, 179, 1.

J. Ruzicka and E. H. Hansen, "Flow Injection Analysis", 2nd ed., Wiley, New York, 1988.

J. Ruzicka, E. H. Hansen, and E. A. Zagatto, Anal. Chim. Acta 1977, 88, 1.

J. Ruzicka, E. H. Hansen, and H. Mosbaek, Anal. Chim. Acta 1977, 92, 235.

M. A. Ryan, Ph.D. thesis, Oregon State University, 1982.

M. A. Ryan and J. D. Ingle, Jr., Anal. Chem. 1980, 52, 2177.

M. A. Ryan and J. D. Ingle, Jr., Talanta 1981, 28, 539.

G. S. Sastri and G. G. Rao, Talanta 1972, 19, 212.

M. Schmall, C. W. Pifer, and E. G. Wollish, Anal. Chem. 1953, 25, 1486.

L. T. Skeggs Jr., Am. J. Pathol. 1957, 28, 311.

L. R. Snyder, Anal. Chim. Acta 1980, 114, 3.

R. H. Stehl, D. W. Dahl, and J. J. Latterell, Anal. Chem. 1967, 39, 1426.

R. H. Stehl, D. W. Margerum, and J. J. Latterell, Anal. Chem. 1967, 39, 1346.

K. K. Stewart, G. R. Beecher, and P. E. Hare, Anal. Biochem. 1976, 70, 167.

K. K. Stewart, J. F. Brown, and B. M. Golden, Anal. Chim. Acta 1980, 114, 119.

K. W. Street, Jr. and M. Tarver, Analyst 1985, 110, 1169.

A. Tello, Undergraduate Research Project Report, Oregon State University, 1985.

H. Theorell and A. Nygaard, Acta. Chem. Scand. 1954, 8, 877.

A. Townshend and A. Vaughan, Talanta 1969, 16, 929.

A. Townshend and A. Vaughan, Talanta 1970, 17, 299.

J. F. Tyson, Anal. Chim. Acta 1986, 179, 131.

M. Valcarcel and F. Grases, Talanta 1983, 30, 139.

M. Valcarcel and M. D. Luque de Castro, "Flow Injection Analysis: Principles and Applications", Ellis Horwood, U. K., 1987.

J. T. Vanderslice, G. R. Beecher, and A. G. Rosenfeld, Anal. Chem. 1984, 56, 268.

J. T. Vanderslice, K. K. Stewart, A G. Rosenfeld, and D. J. Higgs, Talanta 1981, 28, 11.

J. Velisek, J. Davidek, and G. Janicek, Collection Czechoslov. Chem. Commun. 1972, 37, 1465.

K. K. Verma and A. K. Gulati, Anal. Chem. 1980, 52, 2336.

H. Wada, S. Hiraoka, A. Yuchi, and G. Nakagawa, Anal. Chim. Acta 1986, 179, 181.

P. D. Wentzell and S. R. Crouch, Anal. Chem. 1986, 58, 2851.

P. D. Wentzell and S. R. Crouch, Anal. Chem. 1986, 58, 2855.

R. L. Wilson, Ph.D. thesis, Oregon State University, 1976.

R. L. Wilson and J. D. Ingle, Jr., Anal. Chim. Acta 1976, 83, 203.

R. L. Wilson and J. D. Ingle, Jr., Anal. Chem. 1977, 49, 1060.

R. L. Wilson and J. D. Ingle, Jr., Anal. Chim. Acta 1977, 92, 417.

A. A. Woods, J. Ruzicka, and G. D. Christian, Anal. Chem. 1987, 59, 2767.

M. C. Yappert, M. W. Schuyler, and J. D. Ingle, Jr., Anal. Chem. 1989, 61, 593.

K. B. Yatsimirskii, "Kinetic Methods of Analysis", Pergamon Press, Oxford, 1966.

APPENDICES

APPENDIX I

SINGLE-LINE FIA WITH TWO SERIAL INJECTION VALVES FOR KINETIC DETERMINATIONS

A single-line FIA configuration with two injection valves in series was tested for kinetic determinations. For both valves, the sample loop was 30 µL, and both sample loops were filled with the same test solution and switched to the injector position simultaneously under microcomputer control. Two FIA peaks are obtained. If a slow reaction occurs between the analyte and reagent carrier stream, the second peak is larger because the sample plug is in contact with the reagent stream a longer period of time (i.e., longer reaction time) and the system can be used to obtain kinetic information.

This FIA system was evaluated for the determination of AA based on the condensation reaction discussed in Chapter IV. A carrier solution of 1×10^{-3} M $HgCl_2$ and 5×10^{-2} M OPDA in a pH 4.75 acetate buffer was used. The two injection valves were separated by a reaction coil of 400-cm length, 0.5-mm i.d. tubing, and 50 cm of 0.5-mm i.d. tubing was used between the second injector and the flow cell. Instrumental conditions for fluorescence measurements are identical to those in Chapter IV unless specified otherwise.

Figure AI.1 shows the baseline-corrected FIA peaks. The rate was calculated from the differences in peak maximum signals and peak areas. Calibration plots for 2 - 10 µg/mL AA are shown in Figure AI.2 and the calibration data are shown in Table AI.1. The data show

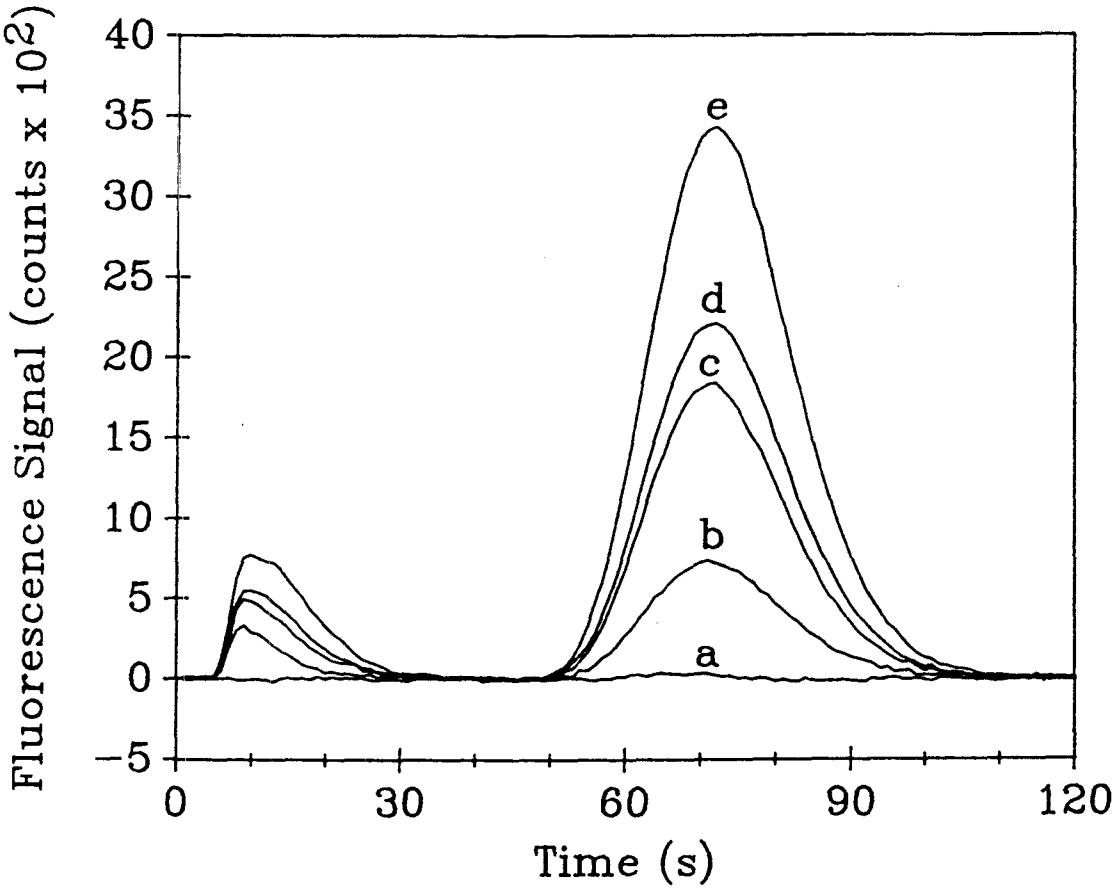

Figure AI.1. Baseline-corrected FIA peaks for the AA standards: (a) blank, (b) 1 µg/mL, (c) 5 µg/mL, (d) 6.25 µg/mL, (e) 10 µg/mL. Injected sample, 30 µL; flow rate, 1 mL/min; integration time per each data point, 1 s.

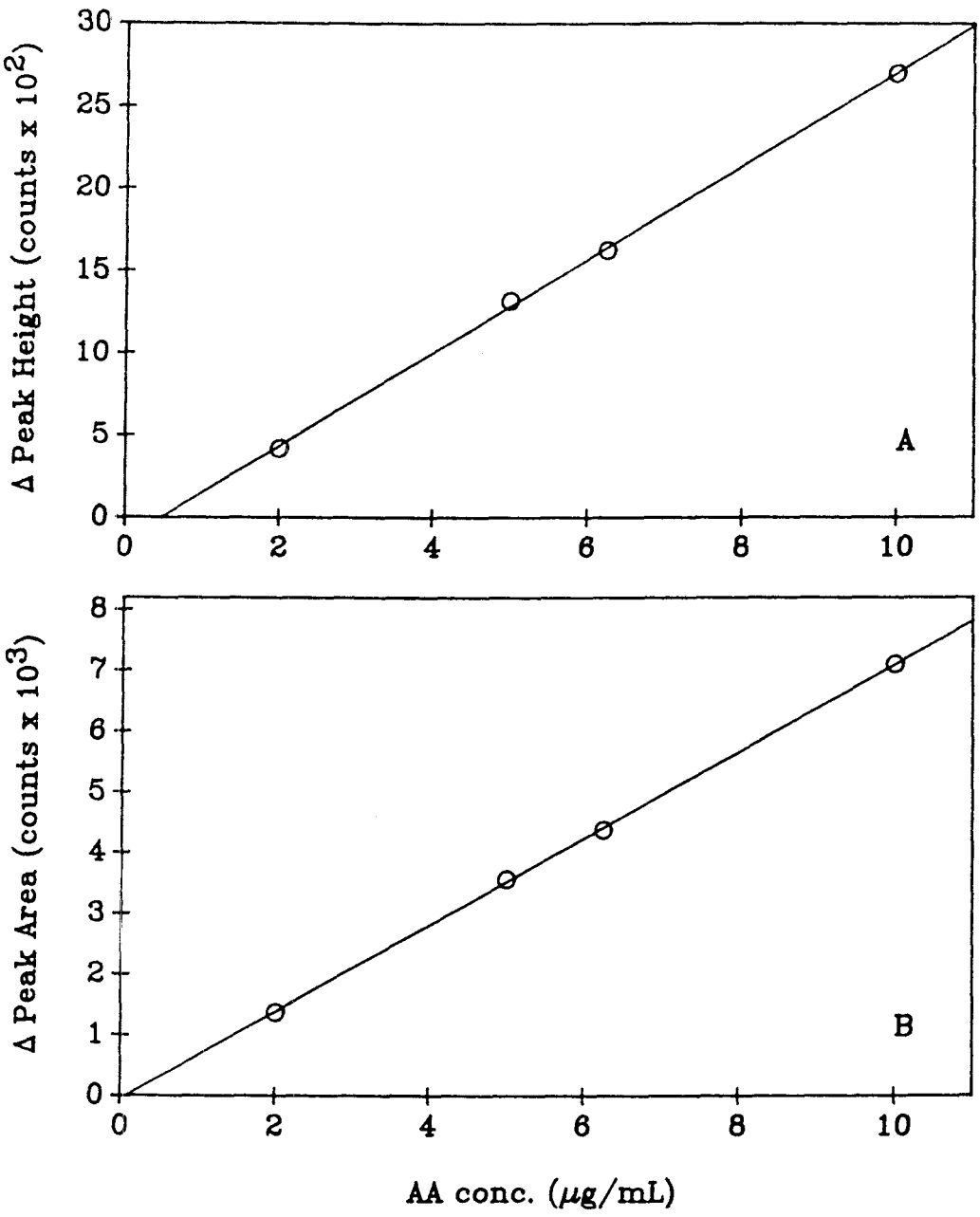

Figure AI.2. Calibration curve for the determination of AA based on the differences in (A) peak maximum signals and (B) peak areas. The data were taken from Figure AI.1.

Table AI.I. Calibration Data for the Determination of AA

Quantity[a]	Rate[b] (counts)	Slope[c] (counts/(μg/mL))	Intercept[d] (counts)
ΔS_m	2703 (1.5)	284 (5.0)	-134 (29)
ΔA	71014 (1.7)	7150 (70)	-519 (400)

[a] $\Delta S_m = (S_2)_m - (S_1)_m$, $\Delta A = A_2 - A_1$.
[b] For 10 μg/mL AA, %RSD in ( ).
[c] Standard error of slope in ( ).
[d] Standard error of intercept in ( ).

that the RSD values are less than 3.2 and 1.8% for the peak height and peak area differences, respectively.

With a constant flow rate and a sample containing a non-reacting fluorophore, the areas of both peaks should be equal if the sample loop volumes are equal. This was tested with a 1 µg/mL QS solution. The ratio of the peaks ($r_A = A_2/A_1$) was 1.012. A true rate method should discriminate against non-reacting species that contribute to the detector signal. For the sample loop volumes used, such species would contribute only 1.2% of their signal to AA. Complete discrimination can be achieved by calculating a corrected difference in area ($\Delta A'$) based on $\Delta A' = A_2/r_A - A_1$.

The effect of non-reacting interferents on the difference in peak maxima is much more serious as it depends on the difference in the sample loop volumes and the dispersion for the two peaks. From the peaks obtained from injecting the 1 µg/mL standard, the ratio of baseline-corrected peak heights (r_p) equals 0.342. The dispersion at the peak maximum is 2.95 and 8.50 for the first and second peak, respectively. Thus a non-reacting interferent would contribute 66% of its signal to the peak height difference. A compensated value ($\Delta S'_m$) can be obtained by calculating from $\Delta S'_m = (S_2)_m/r_p - (S_1)_m$. No such correction was suggested by Valcarcel and coworkers (A1) in their original work on the dual-injection kinetic method.

REFERENCES

A1. A. Fernandez, M. D. Luque de Castro, and M. Valcarcel, Analyst 1987, 112, 803.

APPENDIX II

COMPUTER PROGRAM LISTINGS

Main Program (BASIC)

```
'*****************************
'* FLOW INJECTION ANALYSIS  *
'*****************************
'Written by H. K. Chung
'Department of Chemistry
'Oregon State University
'Program name: KF41.BAS
'October, 1989

DIM dio%(10), din$(10), din(10), nfile$(2), file$(2), mode(3),
T1$(10)
DIM x(2500), y(2500), T1(10), mode$(3)
COMMON SHARED x(), y(), T1(), datnum%, rangelo%, rangehi%,
filename1$, mode$()
DECLARE SUB PlotProc ()
DECLARE SUB ResultProc ()

CLS
'Menu*****************************************************************
index = 0
measno% = 0
dvariable = 0
calcval = 1: calcval0 = 1
plotval = 1: plotval = 1
nfile$(1) = ""

'reset outputs of CTM05 ports
OUT &H303, &H0

DO
CLS
     GOSUB draw.box
     LOCATE 3, 25: PRINT "**** Flow Injection Analysis ****"
     LOCATE 7, 25: PRINT "1. Input User's Parameters"
     LOCATE 8, 25: PRINT "2. Review and Edit Parameters"
     LOCATE 9, 25: PRINT "3. Start FIA Analysis"
     LOCATE 10, 25: PRINT "4. Data Analysis"
     LOCATE 11, 25: PRINT "5. Quit!"
     LOCATE 17, 25: PRINT "Select Your choice:    "
     LOCATE 17, 48: PRINT "? "
     LOCATE 17, 48, 0, 7
     DO
          ch$ = INPUT$(1)
          LOCATE 17, 48: PRINT ch$
          LOCATE 17, 48: BEEP
```

```
     LOOP WHILE VAL(ch$) > 5 OR VAL(ch$) = 0
SELECT CASE ch$
     CASE "1"
     CLS : GOSUB init.para
     CASE "2"
     CLS : GOSUB review.edit
     CASE "3"
     CLS : GOSUB do.fia
     CASE "4"
     CLS : GOSUB data.anal
     CASE "5"
     EXIT DO
     CASE ELSE
     BEEP
END SELECT

LOOP
CLS
'reset outputs of PIO12
OUT &H383, &H80          'mode 1 (all ports are I/O ports)
OUT &H382, &H0           'write 00 to PC Ports

END

do.fia:
IF din(4) < .001 THEN BEEP: RETURN
IF din(5) / din(4) < 1 THEN BEEP: RETURN

'Sampling Procedure*****************************************************
COLOR 24, 7: LOCATE 1, 70: PRINT "WAIT"
COLOR 0, 7: LOCATE 23, 18
measno% = measno% + 1
PRINT "#"; measno%; "of"; repno%; "Repetitive Measurements"
COLOR 7, 0
LOCATE 2, 18: PRINT "Time for Sampling     :"; USING "###.##";
filltime
LOCATE 3, 18: PRINT "Time for Initial Delay:"; USING "###.##";
initdelay
IF filltime = 0 THEN GOTO inj.delay0
LOCATE 10, 18: PRINT "Elapsed Time for Sampling     :"
'turn on the sampling pump which uses OP3
'Base address of CTM05 is &H300
OUT &H303, &H4           '&H04 = 0000 0100 for sampling

     sfill0 = TIMER
filled:
     sfill1 = TIMER

     LOCATE 10, 50
     PRINT USING "###.##"; sfill1 - sfill0;
     IF sfill1 - sfill0 < filltime THEN GOTO filled
'turn off the sampling pump
     OUT &H303, &H0
```

```
BEEP
inj.delay0:
LOCATE 11, 18: PRINT "Elapsed Time before Count Meas:"

     IF initdelay = 0 THEN GOTO freq.meas
       sfill2 = TIMER
inj.delay1:
     sfill3 = TIMER
     initdelayed = initdelay - (sfill3 - sfill2)
     telapsed = (sfill1 - sfill0) + (sfill3 - sfill2)
     LOCATE 11, 50
     PRINT USING "###.##"; telapsed;
     IF initdelayed > 0 THEN GOTO inj.delay1

'Frequency Measurement Step ****************************************
freq.meas:

GOSUB printout1
COLOR 24, 7: LOCATE 1, 64: PRINT "DATA ACQUISITION"
LOCATE 1, 64: COLOR 7, 0

     index$ = STR$(index)
     IF index > 9 AND index < 100 THEN
     nchar = 2
     ELSEIF index < 9 THEN
     nchar = 1
     END IF
FINDEX$ = RIGHT$(index$, nchar)
filename1$ = "B:" + nfile$(1) + "." + FINDEX$
baseseg% = &H5500
     dio%(0) = 1              'low order counter = counter #1
     dio%(1) = dio%(0) + 1    'high order counter = counter #2
     dio%(2) = 2              'source #2 for input
     dio%(3) = baseseg%
'change inputs into milliseconds for assembly language subroutine
     dio%(4) = din(4) * 1000            'gate INTERVAL in ms
     dio%(5) = CINT((din(5)) / din(4))  'total # of dpoints
     N = dio%(5) * 2

     dio%(6) = din(6) / din(4)      '# of dpoints before injection
     dio%(7) = din(7) / din(4)      '# of dpoints between injections
     dio%(8) = din(8) / din(4)      '# of dpoints for sample injection
     dio%(9) = din(9) / din(4)
     dio%(10) = din(10) / din(4)

CALL CTM05(dio%(0))          'call assembly language
LOCATE 1, 60: PRINT "                "
COLOR 24, 7: LOCATE 1, 67: PRINT "DATA TRANSFER"
LOCATE 1, 67: COLOR 7, 0

     P = N * 2
     FOR i = 1 * 4 TO P STEP 4
     K = i / 4                      'data array starts with 1 ...
DEF SEG = baseseg%
```

```
     ARRAY1 = PEEK(i - 4)
     ARRAY2 = PEEK(i - 3)
     ARRAY3 = PEEK(i - 2)
DEF SEG
     y(K) = ARRAY1 + ARRAY2 * 256 + ARRAY3 * 65536
     x(K) = (K) * din(4)
     NEXT i
     x(0) = din(6)

LOCATE 1, 60: PRINT "           "
COLOR 24, 7: LOCATE 1, 71: PRINT "DATA SAVE"
LOCATE 1, 71: COLOR 7, 0
 ' GOTO drive.not.ready


OPEN filename1$ FOR OUTPUT AS #2
     PRINT #2, USING "###.###"; din(6); din(4)    'injection time
     P = N * 2
     FOR i = 1 * 4 TO P STEP 4
     K = i / 4
     PRINT #2, USING "#########"; y(K)
     NEXT i
CLOSE #2

'The following procedure prepares for early exit of main procedure
KEY 15, CHR$(0) + CHR$(1)        '<Esc> key
ON KEY(15) GOSUB EscapePressed
KEY(15) ON

plot.data:
datnum% = P / 4
     SOUND 3100, 10
     CLS : LOCATE 10, 1:
     IF mode$(2) <> "Y" THEN GOTO plot.done
datnum% = P / 4

PlotProc

'get parameters for the results before get into the result
plot.done:
SOUND 3100, 10
IF mode$(3) <> "Y" THEN GOTO skip.calc
IF mode$(1) = "1" THEN
GOSUB result.para
ELSE
GOSUB result.para.display
END IF

ResultProc

skip.calc:
index = index + 1

COLOR 7, 0: CLS
```

```
     IF Escape$ = "pressed" THEN
     GOTO EscapeMain
     ELSEIF measno% < repno% THEN
     KEY(15) OFF
     GOTO do.fia
     END IF
EscapeMain:
     Escape$ = " "
     measno% = 0

RETURN

'The following procedure allows to exit main routine after the
measurement.
EscapePressed:
BEEP: BEEP
Escape$ = "pressed"
RETURN

'END OF MAIN PROGRAM
**************************************************************************

printout1: CLS

PRINT "1. FLOW RATE CONTROL (0 - 9.9 mL/min) "
PRINT "   -Flow Rate of Pump    (mL/min)          :"; TAB(45); frate
PRINT
PRINT "2. FREQUENCY COUNT"
PRINT "   -Time Interval (sec)                    :"; TAB(45); din(4)
PRINT "   -Measurement Time (sec)                 :"; TAB(45); din(5)
PRINT
PRINT "3. INJECTION CONTROL DURING DATA COLLECTION"
PRINT "   -Time for First Injection (sec)         :"; TAB(45); din(6)
PRINT "   -Repetitive Injections (Y/N)            :"; TAB(46); repinj$
PRINT
PRINT
PRINT "4 .DATA FILE"
PRINT "   -File name (Maximum 8 letters)          :"; TAB(46);
nfile$(1)
PRINT "   -Index (Numerical Value 1-99)           :"; TAB(45); index
PRINT
PRINT "5. MEASUREMENT MODE"
PRINT "   -Number of Repetitive Measurements      :"; TAB(45); repno%
PRINT "   -Plot Data (Y/N)                        :"; TAB(46);
mode$(2)
PRINT "   -Calculate Results (Y/N)                :"; TAB(46);
mode$(3)
PRINT "   -Current Measurement Number             :";
COLOR 0, 7: PRINT TAB(45); ""; measno%; ""
COLOR 7, 0
RETURN

ques.1:
     COLOR 23, 0: LOCATE 2, 45: PRINT frate
```

```
      COLOR 0, 7: LOCATE 2, 60: LINE INPUT frate$
      IF frate$ <> "" THEN frate = VAL(frate$)
      COLOR 7, 0: LOCATE 2, 45: PRINT frate; "                    "
      IF frate > 9.9 THEN frate = 0
      FLOW% = INT(frate) * 6 + frate * 10
      OUT &H383, &H80             'set to mode 1 of PIO12
      OUT &H382, FLOW%            'issue flow rate to PC ports


RETURN
ques.2:
      FOR i = 4 TO 5
      COLOR 23, 0: LOCATE 1 + i, 45: PRINT din(i)
      COLOR 0, 7: LOCATE 1 + i, 60: LINE INPUT din$(i)
      IF din$(i) <> "" THEN din(i) = VAL(din$(i))
      COLOR 7, 0: LOCATE 1 + i, 45: PRINT din(i); "
"
      NEXT
      IF din(4) < .001 THEN
      BEEP: GOTO ques.2
      ELSEIF din(5) / din(4) > 2000 THEN
      BEEP: GOTO ques.2
      END IF

      intvl = din(4)
      datnum% = din(5) / din(4)
      calcval0 = 1     'reset the index
      plotval0 = 1     'rest the index
      RETURN
ques.3:
      COLOR 23, 0: LOCATE 9, 45: PRINT din(6)
      COLOR 0, 7: LOCATE 9, 60: LINE INPUT din$(6)
      IF din$(6) <> "" THEN din(6) = VAL(din$(6))
      COLOR 7, 0: LOCATE 9, 45: PRINT din(6); "                    "
'for repetitive injections during data collection
      COLOR 23, 0: LOCATE 10, 46: PRINT repinj$
      COLOR 0, 7: LOCATE 10, 60: LINE INPUT repinj$
      repinj$ = UCASE$(repinj$)
      IF repinj$ <> "Y" THEN repinj$ = "N"
      COLOR 7, 0: LOCATE 10, 46: PRINT repinj$; "                    "
      SELECT CASE repinj$
            CASE "Y"
            GOSUB for.rep.inj
            CASE ELSE
                  din(7) = din(5)       'time interval=measurement time
                  din(8) = din(5)
                  din(9) = din(5)
                  din(10) = din(5)
      END SELECT
      BEEP
      GOSUB sampling.proc
      GOSUB printout1
RETURN
for.rep.inj:
```

```
CLS
LOCATE 8, 1:
PRINT "REPETITIVE INJECTIONS ARE SELECTED!!!"
PRINT "TIME PARAMETERS SHOULD BE CHOSEN CAREFULLY"
LOCATE 12, 1: INPUT "Time Interval between Injections (sec): ";
din(7)
LOCATE 13, 1: INPUT "Time for Sample Injection (sec)       : ";
din(8)
LOCATE 14, 1: INPUT "Delay for Sampling (sec)              : ";
din(9)
LOCATE 15, 1: INPUT "Time for Sampling (sec)               : ";
din(10)

RETURN

sampling.proc:
CLS :
     LOCATE 8, 1:
     PRINT "** TIME PARAMETERS FOR SAMPLING BEFORE TAKING DATA **"
     LOCATE 10, 1: INPUT "Time for sampling      (sec) :"; filltime
     LOCATE 11, 1: INPUT "Time for initial delay (sec) :"; initdelay
RETURN
ques.4:
     FOR i = 1 TO 2
     COLOR 23, 0: LOCATE 13 + i, 46: PRINT nfile$(i)
     COLOR 0, 7: LOCATE 13 + i, 60: LINE INPUT file$(i)

     IF file$(i) <> "" THEN nfile$(i) = UCASE$(file$(i))

     IF LEN(nfile$(1)) > 6 THEN
     COLOR 7, 0: BEEP
     LOCATE 14, 60: PRINT "              ": GOTO ques.4
     END IF
     LOCATE 15 + i, 46: COLOR 7, 0
     LOCATE 13 + i, 46: PRINT nfile$(i); "                    "
     NEXT
     index = VAL(nfile$(2))
RETURN

QUES.5:
     FOR i = 1 TO 3
     COLOR 23, 0:
     LOCATE 17 + i, 46: PRINT mode$(i)
     COLOR 0, 7: LOCATE 17 + i, 60: LINE INPUT mod$(i)

     IF mod$(i) <> "" THEN
     repno% = VAL(mod$(1))
     mode$(i) = UCASE$(mod$(i))
     ELSE
     BEEP
     END IF

     COLOR 7, 0
     LOCATE 17 + i, 46: PRINT mode$(i); "                    "
```

```
     NEXT
     measno% = 0      'reset the measno%
     IF mode$(2) = "Y" THEN CLS : GOSUB plot.para
     IF mode$(3) = "Y" THEN CLS : GOSUB result.para
    GOSUB printout1
RETURN

plot.para:
IF plotval < plotval0 THEN GOTO plot.para2
CLS

'check for the valid parameters....
IF intv1 = 0 OR din(5) < intv1 THEN
BEEP: LOCATE 20, 10: PRINT "Check the Parameters for Frequency count"
FOR i = 1 TO 2000: NEXT
RETURN
END IF
Tinit = intv1: Tfin1 = din(5)
plotval0 = plotval0 + 1
plot.para2:
LOCATE 11, 1
PRINT "Time parameters for plot"
PRINT "Initial Time :     "; USING "###.#"; Tinit
PRINT "Final Time   :     "; USING "###.#"; Tfin1
LOCATE 12, 40: LINE INPUT Tinit$
IF Tinit$ <> "" THEN Tinit = VAL(Tinit$)
LOCATE 12, 20: PRINT USING "###.#"; Tinit
LOCATE 13, 40: LINE INPUT Tfin1$
IF Tfin1$ <> "" THEN Tfin1 = VAL(Tfin1$)
LOCATE 13, 20: PRINT USING "###.#"; Tfin1

plot.para.given:
COLOR 0, 7: LOCATE 23, 1: PRINT "1.CONTINUE"
         LOCATE 23, 14: PRINT "2.EDIT VARIABLES"
COLOR 7, 0
rangelo% = Tinit / intv1
rangehi% = Tfin1 / intv1

DO
ch21$ = INKEY$
LOOP WHILE VAL(ch21$) <> 1 AND VAL(ch21$) <> 2
IF VAL(ch21$) = 2 THEN GOTO plot.para

RETURN

result.para:
IF calcval < calcval0 GOTO result.para2
'Set up default variables
     T1(0) = intv1              'start with first data point
     T1(1) = intv1 * 10         'make 10 data points for baseline
     T1(3) = T1(1) + intv1
     T1(4) = datnum% * intv1
     pctmax = 10
LOCATE 1, 1:
```

```
T1(2) = intvl + T1(1) - T1(0)
T1(5) = intvl + T1(4) - T1(3)
T1(10) = .1
calcval0 = calcval0 + 1
result.para2:
GOSUB result.para.display
COLOR 0, 7: LOCATE 23, 1: PRINT "1.CONTINUE"
        LOCATE 23, 14: PRINT "2.EDIT VARIABLES"

 COLOR 7, 0
 DO
 ch7$ = INKEY$
 LOOP WHILE VAL(ch7$) <> 1 AND VAL(ch7$) <> 2

     IF VAL(ch7$) = 1 THEN GOTO para.given
     FOR i = 0 TO 1
     LOCATE 4, 17 + 14 * i: PRINT "        "
     LOCATE 4, 17 + 14 * i: LINE INPUT T1$(3 * i)
       IF T1$(3 * i) <> "" THEN T1(3 * i) = VAL(T1$(3 * i))
     LOCATE 5, 17 + 14 * i: PRINT "        "
     LOCATE 5, 17 + 14 * i: LINE INPUT T1$(3 * i + 1)
       IF T1$(3 * i + 1) <> "" THEN T1(3 * i + 1) = VAL(T1$(3 * i +
1))
       T1(3 * i + 2) = intvl + T1(3 * i + 1) - T1(3 * i)
     LOCATE 6, 16 + 14 * i: PRINT T1(3 * i + 2)
     NEXT
LOCATE 8, 31: PRINT "        "
LOCATE 8, 31: LINE INPUT pctmax$
IF pctmax$ <> "" THEN
pctmax = VAL(pctmax$)
T1(10) = pctmax * .01

END IF
GOTO result.para2
para.given:
RETURN
result.para.display:
CLS
PRINT "-------------------------------------"
PRINT "               Baseline     PEAK #1"
PRINT "               --------    --------- "
PRINT " Initial Time:"; TAB(17); T1(0); TAB(30); T1(3)
PRINT "   Final Time:"; TAB(17); T1(1); TAB(30); T1(4)
PRINT "  Time Period:"; TAB(17); T1(2); TAB(30); T1(5)
PRINT "-------------------------------------"
PRINT "   % peak max: "; TAB(30); pctmax; "%"
PRINT "-------------------------------------"
RETURN
init.para:
     GOSUB printout1
     GOSUB ques.1
     GOSUB ques.2
     GOSUB ques.3
     GOSUB ques.4
```

```
     GOSUB QUES.5
     COLOR 7, 0
RETURN

review.edit:              'review and edit:
     GOSUB printout1

DO
     COLOR 7, 0: LOCATE 23, 1: PRINT "
                 "
     COLOR 0, 7: LOCATE 23, 1: PRINT "1.FLOW COND "
            LOCATE 23, 14: PRINT "2.FREQ MEAS "
            LOCATE 23, 27: PRINT "3.INJ CONTL "
            LOCATE 23, 40: PRINT "4 .DATA FILE "
            LOCATE 23, 53: PRINT "5.MEAS MODE "
            LOCATE 23, 66: PRINT "6.MAIN MENU "
     COLOR 7, 0

ch3$ = INPUT$(1)

     SELECT CASE ch3$
      CASE "1"
       GOSUB ques.1
      CASE "2"
       GOSUB ques.2
      CASE "3"
       GOSUB ques.3
      CASE "4"
       GOSUB ques.4
      CASE "5"
       GOSUB QUES.5
      CASE "6"
       EXIT DO
      CASE ELSE

      BEEP
     END SELECT
LOOP
RETURN

'Raw data can be retrieved from disk file
'or current measurement can be performed

data.anal:

DO
     CLS
     PRINT : PRINT :
     PRINT "You may choose data file to obtain FIA result"
     PRINT : PRINT
     PRINT "    1. Current Measurement"
     PRINT "    2. Retrieve Data from the Disk"
     PRINT "    3. Back to Main Menu"
```

```
      DO
       ch4$ = INKEY$
      LOOP WHILE ch4$ = ""

      SELECT CASE ch4$
       CASE "1"
        GOSUB replot2
       CASE "2"
        GOSUB ret.file
       CASE "3"
       EXIT DO
       CASE ELSE
        BEEP
      END SELECT
LOOP
RETURN
ret.file:
      PRINT : PRINT : PRINT
      PRINT " The Files Available on Drive B: are "
is.drive.ready:
       PRINT : FILES "b:*.*"
       PRINT
filename:
       INPUT "Type the name of disk file(with  extension)  "; rfile$
       filename$ = rfile$
       filename1$ = "b:" + rfile$
    OPEN filename1$ FOR INPUT AS #2
     INPUT #2, din(6), din(4)
       datnum% = 1                    'array starts with 1...
     DO UNTIL EOF(2)
      INPUT #2, y(datnum%)

      x(datnum%) = datnum% * din(4)   'restore elapsed time
      datnum% = datnum% + 1
       LOOP
    CLOSE #2

      datnum% = datnum% - 1    'number of data points
      intvl = x(1)
      rangelo% = x(1) / intvl
      rangehi% = x(datnum%) / intvl
      PRINT : PRINT : PRINT " Successful to retrieve the file
asked..."
replot2:
mode$(1) = "1"
PlotProc
LOCATE 10, 1: INPUT "  Do you want to skip calculation?  ", a$
IF a$ = "y" OR a$ = "Y" THEN GOTO XXX
more.result:
x(0) = din(6)       'injection delay
GOSUB result.para
ResultProc
XXX:
COLOR 0, 7: LOCATE 23, 1: PRINT "1.MORE RESULT "
```

```
        LOCATE 23, 17: PRINT "2.REPLOT DATA "
        LOCATE 23, 34: PRINT "3.BACK TO MENU"
COLOR 7, 0
wait.key6:

     DO
       ch8$ = INKEY$
     LOOP WHILE ch8$ = ""
     ch8% = VAL(ch8$)
     IF ch8% = 1 THEN
     GOTO more.result
     ELSEIF ch8% = 2 THEN
     GOTO replot2
     ELSEIF ch8% <> 3 THEN
     BEEP: GOTO wait.key6
     END IF

RETURN    'back to the menu of data analysis

draw.box:      'drawing the box
LOCATE 1, 15: PRINT CHR$(201)
LOCATE 1, 65: PRINT CHR$(187)
LOCATE 5, 15: PRINT CHR$(200)
LOCATE 5, 65: PRINT CHR$(188)
FOR i = 2 TO 4 'vertical line
     LOCATE i, 15: PRINT CHR$(186)
     LOCATE i, 65: PRINT CHR$(186)
NEXT i
FOR i = 16 TO 64'horizontal line
     LOCATE 1, i: PRINT CHR$(205)
     LOCATE 5, i: PRINT CHR$(205)
NEXT i
RETURN


'******************
SUB PlotProc STATIC
'******************

GOTO plotting.data
replot1:
LOCATE 24, 1:
       INPUT "Initial Time:   ", Tinit
       INPUT "Final Time  :   ", Tfinl
       PRINT "Time range should be"; x(1); "thru "; x(datnum%)
       IF Tfinl > x(datnum%) OR Tinit < x(1) THEN BEEP: GOTO replot1
       rangelo% = Tinit / intvl
       rangehi% = Tfinl / intvl
       CLS : GOTO plotting.data

plotting.data:
CLS
SCREEN 2
LOCATE 25, 1
```

```
PRINT "1.CONTINUE     2.REPLOT"
LOCATE 25, 50: PRINT "FILE NAME: "; filename1$

'for the desired range of plot check for largest x and y values
intvl = x(2) - x(1)       'time interval
xlo = x(rangelo%): ylo = 0
xhi = x(rangehi%): yhi = y(rangelo%)
     FOR i = rangelo% TO rangehi%
       IF x(i) < xlo THEN xlo = x(i)
       IF x(i) > xhi THEN xhi = x(i)
       IF y(i) < ylo THEN ylo = y(i)
       IF y(i) > yhi THEN yhi = y(i): cursor = i
       NEXT
IF yhi = 0 THEN yhi = 10

'Define Division for x and y axis for the plot
     ndivx = 6: xsubd = 5
     ndivy = 7: ysubd = 5
     xdivlo = xlo - x(1)       'to start x=0 for the nice plot
     xdivhi = xhi
     ydivlo = 0                'to plot baseline inside the box
     ydivhi = yhi * 1

'640*200 pixel medium-resolution graphics
'x and y width maximum to be displayed are 639 and 199
'look for the character size of largest y
     IF LEN(STR$(ydivlo)) > LEN(STR$(ydivhi)) THEN
     ylength = LEN(STR$(ydivlo)) + 1
     ELSE ylength = LEN(STR$(ydivhi))
     END IF

'BOX DRAWING ON THE SCREEN
     xorg% = 60      '+ylength*7.5
     yorg% = 164
     xend% = 600: yend% = 10
     xwidth% = xend% - xorg% - 1         '7.5 pixel per one character
     ywidth% = yorg% - yend% - 1         'xwidth = 600 - 150 = 450:
ywidth=165-25=140
     LINE (xorg%, yorg%)-(xend%, yorg%)
     LINE (xorg%, yorg%)-(xorg%, yend%)

'DRAW TICS FOR MAJOR DIVISION AND SUB-DIVISION
xtic = CINT(xwidth% / ndivx)
ytic = CINT(ywidth% / ndivy)
xsub = xtic / xsubd
ysub = ytic / ysubd

FOR i = 1 TO ndivx
LINE (xorg% + xtic * i, yorg% - 3)-(xorg% + xtic * i, yorg%)
FOR j = 1 TO xsubd
LINE (xorg% + xtic * (i - 1) + xsub * (j - 1), yorg% - 1)-(xorg% +
xtic * (i - 1) + xsub * (j - 1), yorg%)
NEXT j
NEXT i
```

```
FOR i = 1 TO ndivy
LINE (xorg%, yorg% - ytic * i)-(xorg% + 4, yorg% - ytic * i)
NEXT i

'x AND y LABEL ROUTINE
     xdiv = (xend% - xorg%) / 8 / ndivx
       FOR i = 0 TO ndivx
            LOCATE 22, CINT(xorg%) / 8 + CINT(xdiv * i) - 2
            PRINT USING "####"; ((xdivhi - xdivlo) / ndivx) * i +
xdivlo
       NEXT
     ydiv = (yorg% - yend%) / 8 / ndivy
       ylabel = CINT((ydivhi - ydivlo) / ndivy)
       FOR i = 0 TO ndivy
            LOCATE CINT(yorg% / 8) + 1 - CINT(ydiv * i), 1
            PRINT USING "#######"; ylabel * i + ydivlo
       NEXT
LOCATE 23, 13: xlabel$ = "time,sec"

'calculate center of x axis
     xcenter = (xwidth% / 7.5 / 2)
     LOCATE 23, (CINT(xcenter - LEN(xlabel$) / 2) + ylength + 1)
     PRINT xlabel$

'DRAW DATA POINTS
newdx = xdivhi - xdivlo
newdy = ydivhi - ydivlo
FOR i = rangelo% TO rangehi%
       xx% = CINT((xend% - xorg%) / (newdx) * (x(i) - xdivlo))
       yy% = CINT((yorg% - yend%) / (newdy) * (y(i) - ydivlo))
       PSET (xorg% + xx%, yorg% - yy%)
       PSET (xorg% + 1 + xx%, yorg% - yy%)
     NEXT

'Draw line at peak maximum
      cursorX% = CINT((xend% - xorg%) / (newdx) * (x(cursor) -
xdivlo))
       LINE (xorg% + cursorX%, yorg%)-(xorg% + cursorX%, yend%)
DO
          SELECT CASE mode$(1)
          CASE IS <> "1"
          ch6$ = "0": EXIT DO
          CASE "1"
          END SELECT
     ch6$ = INKEY$
     LOOP WHILE VAL(ch6$) <> 1 AND VAL(ch6$) <> 2
     IF ch6$ = "2" THEN GOTO replot1


continue: SCREEN 0
END SUB
```

```
'**********************
SUB ResultProc STATIC
'**********************

COLOR 24, 7: LOCATE 1, 70: PRINT "WAIT"
COLOR 7, 0
injtime = x(0)
intvl = x(2) - x(1)

'Find baseline for Peak #1
     baselinesum1 = 0
     FOR i = T1(0) / intvl TO T1(1) / intvl
     baselinesum1 = baselinesum1 + y(i)
     NEXT

     avgbase1 = baselinesum1 / (T1(2) / intvl)

'Find Peak Maximum for Peak #1
     pmax1 = y(T1(3) / intvl)
     FOR i = T1(3) / intvl TO T1(4) / intvl
     IF y(i) > pmax1 THEN pmax1 = y(i): tmax1 = x(i)
     NEXT
     corpmax1 = pmax1 - avgbase1

'Find Travel Time and Return Time for Peak #1
     travel1 = 9999.9 + injtime     'for error value
     returntime1 = 9999.9 + injtime
     FOR i = T1(3) / intvl TO T1(4) / intvl
     IF y(i) - avgbase1 > .01 * corpmax1 THEN travel1 = x(i): i =
T1(4) / intvl
     NEXT
     FOR i = tmax1 / intvl TO T1(4) / intvl
     IF y(i) - avgbase1 < .01 * corpmax1 THEN returntime1 = x(i): i =
T1(4) / intvl
     NEXT

'Find Travel Time and Return Time for Peak #1
     travel2 = 9999 + injtime    'for error value
     returntime2 = 9999 + injtime
     FOR i = T1(3) / intvl TO T1(4) / intvl
     IF y(i) - avgbase1 > T1(10) * corpmax1 THEN travel2 = x(i): i =
T1(4) / intvl
     NEXT
     FOR i = tmax1 / intvl TO T1(4) / intvl
     IF y(i) - avgbase1 < T1(10) * corpmax1 THEN returntime2 = x(i):
i = T1(4) / intvl
     NEXT

'Find Area for Peak #1
     area1 = 0
     FOR i = T1(3) / intvl TO T1(4) / intvl
     area1 = area1 + y(i)
     NEXT
     corarea1 = area1 - avgbase1 * T1(5) / intvl
```

```
LOCATE 23, 1: PRINT "
"
LOCATE 1, 70: PRINT "          "
LOCATE 10, 1
dest$ = "scrn:"
GOSUB result.print

IF mode$(1) = "1" THEN
GOTO getresult
ELSEIF mode$(3) = "Y" THEN
dest$ = "LPT1:": GOSUB result.print: GOTO finish.result
ELSE BEEP
END IF

getresult:
LOCATE 23, 1: PRINT "1. Get Printout        2.Back to Menu"
COLOR 7, 0:

DO
     DO
      ch8$ = INKEY$
     LOOP WHILE ch8$ = ""
     SELECT CASE VAL(ch8$)
     CASE 1
     dest$ = "LPT1:": GOSUB result.print
     CASE 2
     EXIT DO
     CASE ELSE
     BEEP
     END SELECT
LOOP

GOTO finish.result

result.print:
OPEN dest$ FOR OUTPUT AS #3
PRINT #3,
PRINT #3, "-FILE: "; filename1$
PRINT #3, "========================================="

PRINT #3, TAB(21); "PEAK #1"
    PRINT #3, "     Baseline:";
    PRINT #3, TAB(27); USING "#######.##"; avgbase1
     PRINT #3, "     Peak Max:";
     PRINT #3, TAB(27); USING "#######.##"; corpmax1
      PRINT #3, "    Peak Area:";
      PRINT #3, TAB(27); USING "#######.##"; corarea1

PRINT #3, "-----------------------------------------"
PRINT #3, TAB(25); " 1 %";
PRINT #3, TAB(38); USING "###"; T1(10) * 100;
PRINT #3, TAB(42); "%"
PRINT #3, TAB(24); "--------------------"
```

```
 PRINT #3, "  Travel Time:";
 PRINT #3, TAB(23); USING "####.#"; travel1;
 PRINT #3, TAB(37); USING "####.#"; travel2
  PRINT #3, "Peak Max Time:";
  PRINT #3, TAB(30); USING "####.#"; tmax1
   PRINT #3, "  Return Time:";
   PRINT #3, TAB(23); USING "####.#"; returntime1;
   PRINT #3, TAB(37); USING "####.#"; returntime2
PRINT #3, "========================================="
CLOSE #3
RETURN

finish.result:
LOCATE 23, 1: PRINT "                                        "

END SUB
```

ASSEMBLY LANGUAGE SUBROUTINE FOR FIA

```
     PAGE 55, 132
     TITLE DATA COLLECTION SUBROUTINE FOR FIA

COMMENT \
     FILE NAME: CTM05C.ASM
     This subroutine should be used with FIA main program written in
     QuickBasic (version 4.5).  From the main program, timing
     parameters such as time interval, measurement time and other
     timing parameters for injector control should be passed.
\

DATA    SEGMENT WORD PUBLIC 'DATA'

BASADR  DW 0000H          ;CTM-5 base I/O address
BASEG   DW 0000H          ;BASIC's data segment

CTER1   DW 0000H          ;DI%(0) data, low order counter
CTER2   DW 0000H          ;DI%(1) data, high order counter
SINPUT  DW 0000H          ;DI%(2) data, source input
MEMSEG  DW 0000H          ;DI%(3) data, memory segment
INTVL   DW 0000H          ;DI%(4) data, measurement time interval
DPOINT  DW 0000H          ;DI%(5) data, # of data points
DI6     DW 0000H          ;DI%(6) data, first injection time
DI7     DW 0000H          ;DI%(7) data, interval between injection
DI8     DW 0000H          ;DI%(8) data, sample injection period
DI9     DW 0000H          ;DI%(9) data, sampling delay
DI10    DW 0000H          ;DIO%(10) data, sampling period

;following are time controlling counters

NINJ    DW ?              ;number of injection performed
INJDLY  DW ?              ;time delay for next injection
INJPRD  DW ?              ;sample injection period
```

```
SAMDLY  DW ?            ;sampling delay
SAMPRD  DW ?            ;sampling period
INJPRDO DW 0000H        ;index for sample injection period
SAMDLYO DW 0000H        ;index for sampling delay from 2nd peak
SAMPRDO DW 0000H        ;index for sampling period
DPTR    DW 0000H        ;data array pointer
POINTER DW 0000H        ;points to memory location

TAB     DW 0000H

DATA    ENDS
DGROUP                  GROUP DATA

CODE SEGMENT BYTE PUBLIC 'CODE'
     ASSUME CS:CODE, DS:DGROUP
     PUBLIC ctm05
ctm05                   PROC FAR

;DATA FETCH FROM BASIC
*************************************************

getdata:  CLI
          PUSH BP               ;save base pointer
          MOV BP,SP             ;set up pointer to arguments to be
                                ;passed
          PUSH ES               ;save segment registers
          PUSH BX
          PUSH SS
          PUSH DS               ;save BASIC's data segment

          PUSH DS
          MOV AX,DATA           ;get current data segment
          MOV DS,AX             ;set up DS as current data segment
          POP AX
          MOV BASEG,AX          ;store BASIC's segment
          MOV SI,[BP]+6         ;SI = pointer to DIO%(0)
          MOV DPTR,SI           ;store in data pointer

;Read DI%(0-10) into temporary data buffer variables in data segment
;note SI = DPTR data pointer
;source segment = BASIC's data segment
;destination segment = current data segment

FDATA:    PUSH ES               ;save ES
          PUSH DS               ;save current data segment
          PUSH DS
          POP ES                ;destination segment = current segment
          LEA DX,CTER1          ;get effective address of first data
          MOV DI,DX             ;set up destination offset
          MOV AX,BASEG          ;get BASEG
          MOV DS,AX             ;source segment = BASIC's data segment
          CLI                   ;no interrupts during block move
          CLD                   ;increment SI/DI
          MOV CX,11             ;move 11 words (D0-10)
```

```
REP       MOVSW                ;block move
          STI                  ;re-enable interrupts

          POP DS               ;restore current data segment
          POP ES               ;restore extra segment


;INITIALIZATION OF STC*************************************************
;issue Master reset

          MOV BASADR,300H      ;set up CTM-5 base address
          MOV DX,BASADR        ;get base address of CTM-5
          INC DX               ;address to command reg port
          MOV AL,0FFH          ;reset master master mode register
          CALL DELAY
          OUT DX, AL

;load data pointer register, 0001 0111 (17H)
;master mode register(10), for control group(111)

          MOV AL,17H
          CALL DELAY
          OUT DX,AL            ;point to master mode register

;set master mode register
;mode word = 1100 1010 1111 0000 (Hex CAF0)
;BCD Division(1), Disable increment(1), 8-bit bus(0),
;Fout gate off (0), Fout divider ratio of 10(1010),
;Fout source = F5(1111), Compare 2 ;disabled(0)
;Compare 1 disabled(0), Time of day disabled(00)

          DEC DX               ;DX = data port
          MOV AX,0CAF0H
          CALL DELAY
          OUT DX, AL
          MOV AL, AH
          CALL DELAY
          OUT DX, AL

O.k. data valid, now set timebase counter 5 mode register
;Mode word = 0000 1110 0010 0010 (Hex 0E22)
;No gating(000), count on rising edge(0), F4 source(1110)
;disable special gate(0), reload from load(1),count repetitively(1)
;binary(0), count down(0), toggled output(010).

          MOV DX,BASADR        ;CTM-5 base I/O address
          INC DX               ;address control
          MOV AX,0005H         ;set pointer to counter 5
          CALL DELAY
          OUT DX,AL            ;data port pointed to mode reg.
          DEC DX               ;address data port
          MOV AL,22H           ;low byte of mode word
          CALL DELAY
```

```
          OUT DX,AL           ;write low byte
          MOV AL,0EH          ;high byte of mode word
          CALL DELAY
          OUT DX,AL           ;write high byte (mode loaded)

;Now load divisor data into counter from DI%(4)
;load register counter 5, command code = 0000 1101

          INC DX              ;re-address control port
          MOV AX,000DH        ;pointer byte(load register counter 5)
          CALL DELAY
          OUT DX,AL           ;point to load register
          MOV AX,INTVL        ;get load data(gate interval)
          DEC DX              ;DX = data port
          CALL DELAY
          OUT DX,AL           ;low byte
          MOV AL, AH
          CALL DELAY
          OUT DX,AL           ;high byte (load reg. loaded)

;Set counter mode register of low order accumulator counter
;Mode register word = 0000 XXXX 0010 1001 (Hex 0X29)
;no gate(000), count on rising clock edge(0),source input(XXXX)
;disable special gate(0), reload from load(0), count repetitively(1)
;binary(0), count up(1), active high T.C.(001)

          INC DX              ;control port for command register
          MOV AX,CTER1        ;use low order counter
          CALL DELAY
          OUT DX,AL           ;point to mode register
          MOV AX, SINPUT
          MOV CL, 8
          SHL AX, CL
          OR AX,0029H         ;build mode word
          DEC DX
          CALL DELAY
          OUT DX,AL           ;low byte of mode word
          MOV AL, AH
          CALL DELAY
          OUT DX,AL           ;high byte,mode loaded

;load register of low order counter , command code = 0000 1XXX

          INC DX              ;re-address control port
          MOV AX, CTER1
          OR AX, 0008H        ;pointer byte(low order load register
                              ;counter)
          CALL DELAY
          OUT DX,AL           ;point to load register
          XOR AX,AX           ;clear register
          DEC DX              ;DX = data port
          CALL DELAY
          OUT DX,AL           ;low byte
          CALL DELAY
```

```
          OUT DX,AL           ;high byte (load reg. loaded)

;Set mode register of high order counter 3
;mode register word = 0000 0000 0010 1001 (0029H)
;no gating(0000), count on rising edge(0),
;source from internal TC of low order counter 2 (0000),
;disable special gate(0), reload from load(0), count repetitively(1)
;binary, count up(0),active high TC pulse(001)

          INC DX
          MOV AX,CTER2        ;get high order counter and set pointer
          CALL DELAY
          OUT DX,AL           ;issue to mode register
          DEC DX
          MOV AX, 0029H
          CALL DELAY
          OUT DX,AL
          MOV AL,AH
          CALL DELAY
          OUT DX,AL

;load register of hi order counter , command code = 0000 1XXX

          INC DX              ;re-address control port
          MOV AX, CTER2
          OR AX,0008H         ;pointer byte(low order load register
                              ;counter)
          CALL DELAY
          OUT DX,AL           ;point to load register
          XOR AX,AX           ;clear register
          DEC DX              ;DX = data port
          CALL DELAY
          OUT DX,AL           ;low byte
          CALL DELAY
          OUT DX,AL           ;high byte (load reg. loaded)

;Clear all the values in the memory locations to be used
          MOV TAB, 0000H
          PUSH ES
FLUSHMEM:
          MOV AX, memseg
          MOV ES, AX
          MOV AX, TAB
          MOV DI, AX
          MOV BX,0000h
          MOV ES:[DI],BX
          INC TAB
          MOV AX, 2710H       ;2710H= 10000/4 (=2500) data points
          CMP TAB, AX
          JLE FLUSHMEM
          POP ES

;set up the time control counters
          MOV AX,0000H
```

```
          MOV POINTER,AX      ;set up pointer to zero
          MOV NINJ,AX         ;set up number of injection as zero

          MOV INJPRDO,AX
          MOV SAMDLYO,AX
          MOV SAMPRDO,AX
BEGIN:
;check time for first injection
          MOV AX,0
          CMP AX,NINJ         ;check for # of injection performed
          JL NEXTINJ          ;check for next injection
          CMP AX,DI6          ;if AX(=0) < NINJ, jump
          JL DOWNDI6
          CALL VALVE          ;perform first injection
          JMP NEXTINJ
DOWNDI6:  DEC DI6
          JMP FREQ

;if injection occurs, INJDLY for next injection and INJPRD for
injection ;period are loaded in VALVE subroutine
;check for repetitive injection

NEXTINJ:
          MOV AX,0000H
          CMP AX,INJDLY       ;INJDEL is loaded from VALVE subroutine
          JL INJECTIONPRD     ;check time for subsequent injection
          CALL VALVE          ;inject sample and restore the
                              ;variables

;check injection period (sample loop on-line)
;during injection period, INJPRDO is 1 (sample-loop is on-line)

INJECTIONPRD:
          DEC INJDLY          ;countdown INJDLY for next injection
          MOV AX,0
          CMP AX,INJPRD
          JL DOWNINJPRD
          CMP AX,INJPRDO      ;INJPRDO=1 if bypass loop is on-line
          JL  DLYSAMPLING     ;if injection period done, jump
          MOV AX,0000H        ;prepare for bypass loop on-line
          CALL BPORT

;sample is all flushed, so prepare delay time

          MOV AX,DI9          ;get delay time for sampling
          MOV SAMDLY,AX       ;load value into SAMDLY
          MOV AX,0001H
          MOV INJPRDO,AX      ;make INJPRDO=1
          JMP DLYSAMPLING

DOWNINJPRD:
          DEC INJPRD
          JMP FREQ
```

```
DLYSAMPLING:
          MOV AX,0
          CMP AX,SAMDLY        ;more delay?
          JL DOWNSAMDLY        ;if more delay, count down
          CMP AX,SAMDLY0       ;if delay is done, SAMDLY0=0
          JL SAMPLING          ;if SAMDLY0 =0, then continue
          MOV AX, 04H          ;prepare for sampling 04H=0000 0100
          CALL BPORT           ;delay is done, so start sampling
          MOV AX,0001H
          MOV SAMDLY0,AX
          MOV AX,DI10          ;prepare for time for sampling
          MOV SAMPRD,AX
          JMP SAMPLING

DOWNSAMDLY:
          DEC SAMDLY
          JMP FREQ

SAMPLING:
          MOV AX,0
          CMP AX,SAMPRD        ;more sampling?
          JL DOWNSAMPRD        ;if more sampling, count down
          CMP AX,SAMPRD0
          JL FREQ
          MOV AX,00H           ;prepare for reset injection valve
          CALL BPORT           ;sampling is done, so finish up

;restore INJPRD0 and SAMDLY0

          MOV SAMPRD0,0001H

          JMP FREQ             ;go to frequency count routine

DOWNSAMPRD:
          DEC SAMPRD

;Actual frequency measurement step start here**********************

;make initial output level for TC toggle mode set (HI) for counter 5
;command code 1110 1101 (EDH)
;set toggle output (11101), counter 5 (101)

FREQ:     MOV DX,BASADR
          INC DX               ;DX = BASADR +1
          MOV AX,00EDH
          CALL DELAY
          OUT DX, AL

;load and arm low order counter
;command code = 011X XXXX
;for load and arm the selected counter (low order)

          MOV AX, 1
          MOV CX, CTER1
```

```
          DEC CX
          SHL AX, CL
          OR AX,60H
          CALL DELAY
          OUT DX,AL           ;low order counter

;load and arm hi order counter
;command code= 011X XXXX
;for load and arm the selected counter (HI order)

          MOV AX, 1
          MOV CX, CTER2
          DEC CX
          SHL AX, CL
          OR AX,60H
          CALL DELAY
          OUT DX,AL           ;counters waiting

;working counters are counting
;load & arm timebase counter 5
;command code = 0111 0000(70H)

          MOV AX,0070H        ;command byte
          CALL DELAY
          OUT DX,AL           ;timebase counter running

;Wait for gate to low

GETLOW:   CALL DELAY
          IN AL, DX
          TEST AL,20H         ;test out5 bit of status register
          JNZ GETLOW          ;if set, continue to count

;Transfer accumulated count to hold registers (low order counters)
;00A3 = 0000 0000 101X XXXX (save counters in Hold registers)
;008X = 0000 0000 100X XXXX --- disarm and save counters

          MOV AX,3H           ;set up offset for counters
          MOV CX, CTER1
          DEC CX
          SHL AX, CL
          OR AX,0080H
          CALL DELAY
          OUT DX,AL           ;save in hold register

;point to hold register of low order counter
;command code = 0001 0XXX

          MOV AX, CTER1
          OR AX,0010H
          CALL DELAY
          OUT DX,AL           ;set up pointer

;procedure for transferring the counted value to memory locations
```

```
          PUSH ES              ;save ES onto stack
          MOV AX,MEMSEG
          MOV ES,AX
          MOV AX,POINTER       ;AX =0 for the first time
          SHL AX, 1
          SHL AX, 1
          MOV DI,AX            ;di values are 0,4,8,... for low order
                               ;counter

;read hold register and transfer to memory locations

          DEC DX
          CALL DELAY
          IN AL,DX             ;read low byte
          MOV BL, AL
          CALL DELAY
          IN AL,DX             ;read high byte
          MOV BH,AL            ;BX = data
          MOV ES:[DI],BX       ;transfer to memory locations
          XOR BX,BX

;point to hold register of high order counter
;command code = 0001 0XXX

          INC DX
          MOV AX, CTER2
          OR AX,0010H
          CALL DELAY
          OUT DX,AL
          INC DI
          INC DI

;read hold register and transfer to DI%(X)

          DEC DX
          CALL DELAY
          IN AL, DX
          MOV BL, AL
          CALL DELAY
          IN AL, DX
          MOV BH, AL
          MOV ES:[DI],BX
          POP ES               ;restore ES

;wait for all the values to be stored

          INC POINTER
          MOV AX,DPOINT
          CMP POINTER,AX
          JGE FINISH

;check for the termination by pressing <F1> function key during
;measurement
```

```
          MOV DL,0FFH          ;poll for a key at the end of each
                               ;dpoint
          MOV AH,06H           ;read keyboard character (function 6)
          INT 21H
          CMP AL,3BH           ;<F1> pressed?
          JE FINISH            ;if pressed, terminate

          JMP begin

;*************************************************************************
;transfer memory in memseg to BASIC's array

FINISH:
          mov ax,00ffH         ;for reset injector and master reset
          MOV DX, basadr
          inc dx               ;dx = control port
          CALL DELAY
          out dx,al            ;issue master reset if finished

;make all the outputs of B PORT zero(0000 0000) before leaving

          MOV AX,00H
          CALL BPORT

;RETURN TO CALLER ROUTINES ***************************************

;procedure for returning to BASIC

          PUSH ES              ;prepare for block move
          MOV AX, BASEG
          MOV ES,AX            ;destination segment = BASIC's segment
          LEA DX,CTER1         ;source segment = current data segment
          MOV SI, DX
          MOV DI, DPTR
          CLI                  ;no interrupts during block move
          CLD                  ;increment SI/DI
          MOV CX,11            ;move 11 words (D0-11)
REP       MOVSW                ;block move
          STI                  ;re-enable interrupts
          POP ES               ;restore ES

          POP DS               ;restore BASIC's data segment

;restore other registers in order to return correctly

          POP SS               ;unload stack to start state
          POP BX
          POP ES
          POP BP
          sti

          RET 2                ;return for 1 argument
```

```
VAL00     PROC NEAR

VALVE:    MOV AX,03H          ;03H= 0000 0011
          MOV DX,303H
          CALL DELAY
          OUT DX, AL

;load counters in terms of data points

          INC NINJ            ;count up # of injection performed
          MOV AX,DI7          ;get injection interval
          MOV INJDLY, AX
          MOV AX,DI8          ;get sample injection period
          MOV INJPRD,AX
          MOV INJPRD0,00H
          MOV SAMDLY0,00H
          mov samprd0,00h
          RET
VAL00 ENDP

VAL01     PROC NEAR

BPORT:    MOV DX,303H
          CALL DELAY
          OUT DX, AL
          RET
VAL01 ENDP

DEL       PROC NEAR

DELAY:    JMP DELRET
DELRET:   RET

DEL ENDP

ctm05 ENDP

          CODE  ENDS          ;end of segment
          END                 ;end of program
```